STATIC AND DYNAMICAL FLUORESCENCE RESPONSE OF SOME MOLECULES IN ROOM TEMPERATURE IONIC LIQUIDS AND IN MEDIA CONTAINING PHASE TRANSFER CATALYSTS

A Thesis

Submitted for the Degree of

DOCTOR OF PHILOSOPHY

by

Rana Karmakar

School of Chemistry
University of Hyderabad
Hyderabad 500 046
India

May 2003

To my

Family members

Contents

DECLARATION

I hereby declare that the matter embodied in this Thesis is the results of investigation carried out by me in the School of Chemistry, University of Hyderabad, Hyderabad – 500 046, India under the supervision of **Prof. Anunay Samanta.**

In keeping with the general practice of reporting scientific observations, due acknowledgements have been made wherever the work described is based on the findings of other investigators. Any error or omission that might have occurred is solely regretted.

Rana Karmakar

Rana Karmakar

May 2003

SCHOOL OF CHEMISTRY
UNIVERSITY OF HYDERABAD
HYDERABAD-500 046, INDIA

Phone: +91-40-2301 1594 (office
+91-40-2301 0715 (home
Fax: +91-40-2301 2460
Email: assc@uohyd.ernet.in
anunay_s@yahoo.com

Anunay Samanta, F.A.Sc.
Professor

May 9, 2003

CERTIFICATE

Certified that the work embodied in the Thesis entitled ***"Static and Dynamical Fluorescence Response of Some Molecules in Room Temperature Ionic Liquids and in Media Containing Phase Transfer Catalysts"*** has been carried out by **Mr. Rana Karmakar** under my supervision and the same has not been submitted elsewhere for any degree.

Anunay Samanta
(Thesis Supervisor)

Dean
School of Chemistry

DEAN
School of Chemistry
University of Hyd.
Hyderabad-46.

Acknowledgements

It is my great privilege to convey respectful thanks to my supervisor, Prof. Anunay Samanta for his constant inspiration, guidance and suggestions from the very beginning of my research work.

I am deeply indebted to the past and present Dean, School of Chemistry for their moral support, all the faculty members and non-teaching staffs for their help and suggestions all over the time in different aspects. I am quite thankful to Prof. P. Natarajan and Dr. P. Ramamurthy, for the instrumental facility at National Center for Ultra fast Process, Chennai. Special thanks to Mrs. V. K. Indirapriyadarshini and Mr. C. Selvaraj for the help during decay measurement and further analysis.

A special note of thanks should also be a recorded in favor of all my friends, past and present laboratory mates Saroja, Ramachandram, Satyen, Sankaran, Sandip, Prasun, Moloy and Aniruddha for their constant co-operation and help at every step was more than a responsibility.

I would like to acknowledge Council of Scientific and Industrial Research (CSIR) for the financial assistance and Department of Science and Technology (DST), Government of India for their generous grants to support the present works.

Finally I want to convey my deep regards to my uncle and father, whom I lost on the way and my mother and wife, whose constant moral and mental support has helped to complete the thesis.

Rana Karmakar

List of Publications:

1. Fluorescence Signaling of Transition Metal Ions by Multi-Component Systems Comprising 4-Chloro-1,8-naphthalimide as Fluorophore.
   B. Ramachandram, N.B. Sankaran. R. Karmakar, S. Saha and A. Samanta, *Tetrahedron.* **2000**, *56*, 7041.

2. Phase Transfer Catalyst Induced Changes in the Absorption and Fluorescence Behavior of Some Electron Donor-Acceptor Molecules.
   Rana Karmakar and Anunay Samanta, *J. Am. Chem. Soc.* **2001**, *123*, 3809.

3. Solvation Dynamics of Coumarin-153 in a Room Temperature Ionic Liquid.
   Rana Karmakar and Anunay Samanta, *J. Phys. Chem. A.* **2002,** 106, 4447.

4. Steady State and Time–Resolved Fluorescence Behavior of C153 and PRODAN in Room Temperature Ionic Liquids.
   Rana Karmakar and Anunay Samanta, *J. Phys. Chem. A.* **2002,** 106, 6670.

5. Dynamics of Solvation of the Fluorescent State of Some Electron Donor-Acceptor Molecules in Room Temperature Ionic Liquids, [BMIM][$(CF_3SO_2)_2N$] and [EMIM][$(CF_3SO_2)_2N$].
   Rana Karmakar and Anunay Samanta, *Communicated for publication.*

6. Intramolecular Excimer Formation Kinetics in Room Temperature Ionic Liquids.
   Rana Karmakar and Anunay Samanta, *Communicated for publication.*

Introduction

This chapter provides the necessary background information on the phase transfer catalyst (PTC) and room temperature ionic liquid (RTIL) with which the present thesis is concerned. Also provided in this chapter is a brief introduction to some of the photophysical processes such as solvation dynamics and excited state complex formation that form the subject matter of the current investigation. The chapter is concluded describing the motivation of the present work and the layout of the thesis.

1.1. Phase transfer catalyst (PTC)

The reaction between an ionic species dissolved in aqueous phase with other reactant dissolved in organic solvents (and is immiscible with water) is expected to be quite slow or may not occur at all. Such reaction at the phase boundaries suffers from the limited interfacial area and low surface concentration of the reactants. Phase transfer catalysts (PTCs) are the simplest solution to this problem.[1-5] In a binary two-phase solution, a good phase transfer catalyst circulates between the two phases across the interface and transfers the necessary ions from the aqueous to the organic phase and enhances the reaction rate in the latter phase.

Although reactions involving the PTCs started in 1913,[1] the technique was first highlighted in a systematic way by Makosza and coworkers in 1965 using a different name 'catalytic two-phase reaction'.[6] The name 'phase transfer catalysis' was first introduced by Starks in his patents in 1968[7-9] and latter, in the paper published in 1971.[10] Liotta and coworkers introduced crown ether as PTC for the first time in both liquid-solid and liquid-liquid interface in 1974.[11] During the past three decades the PTCs have been exploited in innumerable number of synthetic, chemical and structural applications and a large number of publications and patents have come out of these efforts.[5,12-23] The use of PTCs as an essential component for the stabilization of nanoparticles in nonpolar medium have been reported recently.[24-28] So far the extensively used PTCs are the quaternary salts of tetraalkyl ammonium, phosphonium and arsonium ions with four identical alkyl groups ($R_4N^+X^-$, $R_4P^+X^-$, $R_4As^+X^-$) and crown ether (1),

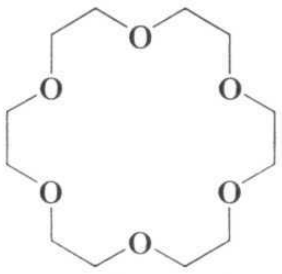

18-Crown-6

(1)

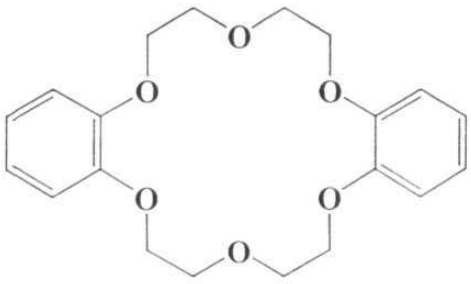

Dibenzo-18-Crown-6

(2)

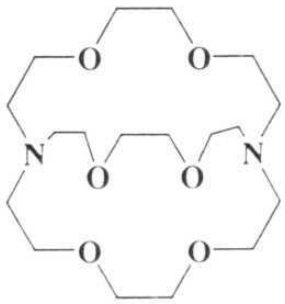

[2.2.2]Cryptate

(3)

dibenzocrown ether (2) and cryptate (3). Various other crowns or cryptates with different cavity sizes are also used for binding and transfer of specific ions.

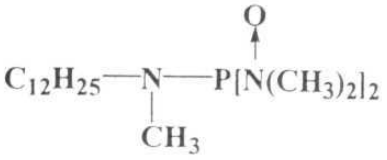

(4)

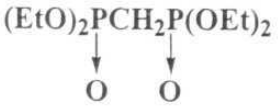

(5)

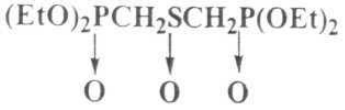

(6)

Apart from the substances mentioned above, N-dodecyl phosphoramides (4) is another excellent PTC for several displacement reactions and for $KMnO_4$ oxidation of stilbene. Methylene–bridged phosphorus and sulpher oxides (5, 6) are used as PTCs for the alkylation of phenylacetone with alkyl iodides (or bromides) and aqueous sodium hydroxides.[2]

The most popular model for ion initiation reaction in liquid-liquid bi-phasic system is the ion exchange mechanism proposed by Stark[10] and interfacial reaction mechanism by Makosza.[29] From electrochemical point of view, the distribution potential between the two immiscible phases spontaneously formed by partitioning of ionic PTC is the predominating driving force for its phase transfer activity.[30,31] The role of PTCs lie not merely in the transfer of ions from a polar to a nonpolar medium, but also in the transfer of free radical, a simple molecule and energy in chemical form.[2] The effectiveness of the PTCs depends on several factors including the solvent, structure of the salt, lipophilicity of both cation and anion present in the salt and presence of other influencing agents. The organic solvent should be aprotic and completely immiscible with water. It has

been observed that low boiling chlorinated hydrocarbon, such as dichloromethane or chloroform gives an effective extraction coefficient against aqueous media although these solvents create environmental hazards, when used in bulk. A higher hydrophobicity of the cationic counterpart improves the transfer capacity from aqueous to organic phase. The influence of the anionic part depends on several factors. However, it has been observed that a lipophilic anion can give a better extractability over a hydrophilic one. Among the halides, the general trend suggests a higher efficiency of the iodide ion relative to the bromide, which is again more efficient than the chloride ion.[1,2]

The quaternary ammonium salts are the most commonly used phase-transfer catalysts in chemical applications.[1-5,10,23,28,32-37] Quaternary ammonium salts with one or two large alkyl groups, such as cetyltrimethylammonium bromide, are known as surfactants, which when added to a two-phase aqueous-organic system, form micelles in the aqueous phase. On the other hand, quaternary ammonium salts with all four identical alkyl groups, such as tetrabutylammonium bromide, are good PTCs. The popularity of the quaternary salts as PTCs are primarily due to the ease of synthesis of these salts with various cation-anion combinations by simple alkylation of the tertiary amine.[38,39] Low cost, low reactivity, and high catalytic activity are some other reasons that contributed to the extensive usage of these salts as PTCs. It is also quite easy to make optically active quaternary salts by incorporating an optically active group in the structure.[40-43]

A simple halide replacement reaction in the presence of PTC, for example,

$$RX_{org} + Y_{aq}^{-} \xrightarrow{PTC} RY_{org} + X_{aq}^{-}$$

takes places in the following steps:

$$[Q^{+}X^{-}]_{org} + Y_{aq}^{-} \leftrightarrow [Q^{+}Y^{-}]_{org} + X_{aq}^{-}$$

$$[Q^{+}Y^{-}]_{org} + RX_{org} \rightarrow [Q^{+}X^{-}]_{org} + RY_{org}$$

where, Q^{+} stands for the quaternary cation. The first step involves the transfer of the anion (Y^{-}) from the aqueous to an organic phase, whereas the second one represents the displacement reaction in the organic phase. Therefore, the primary requirement for a good PTC is to have sufficient organic structure to become soluble in organic medium. It is generally found that methyl or ethyl group in cationic structure gives a poor phase transfer capability compared to its higher homologue due to lesser solubility in the nonpolar phase. The distribution coefficient of a quaternary salt between two immiscible phases is increased roughly by a factor of 2 for each addition of a single methylene group in a given homologous series.[2] In nonpolar media, the PTCs are known to exist as ion pairs. The quaternary cation with long hydrophobic chain entails the extraction of ionic or highly polar molecules into an organic solvent or their solubilization therein.

1.2. Inverse phase transfer catalyst (IPTC)

'Inverse phase transfer catalysis', a name coined by Mathias and Vaidya,[44] is a process in which an organic reactant (located in an organic medium) is converted to an ionic intermediate with the help of a catalyst, termed

as 'inverse phase transfer catalyst (IPTC) and then transferred to the aqueous phase for further reaction. The usage of inverse phase transfer catalysis, though less common than phase transfer catalysis, as a synthetic technique is increasingly becoming popular these days.[45-49] The commonly used IPTCs are water soluble α- or β-cyclodextrins,[50-52] tetramethyl or tetraethylammonium quaternary salts, substituted pyridines[47] and pyridinium oxides.[53]

1.3. High temperature molten salt

High temperature molten salts are expected to be ionic due to large electronegativity difference between the constituting ions. However, they show pronounced covalent effects in their dynamical properties.[54] This is true even for pure NaCl (m.p. 801 ^{0}C) or LiCl/KCl mixture (6:4, m.p. 352 ^{0}C). $ZnCl_2$ is one of the most extensively studied molten salts presumably for its low glass transition temperature and slow structural relaxation.[55-58] La Violette and coworkers[59] determined the structural properties of $ZnBr_2$ that melt at more than 650 ^{0}C. Recently, using Raman Spectroscopy, Papatheodorou and coworkers investigated the structural properties of molten binary mixtures of ZrF_4-KF,[60] $ZrCl_4$-ACl[61] and $ThCl_4$-ACl[62] (A = Li, Na, K, Cs) at high temperatures.

On the other hand, fused organic salts are rather low melting compared to the inorganic ones.[63,64] Gordon and Subba Rao prepared a series of straight chain isomers of tetra-n-pentylammonium salts with different combination of anions (9) and studied the various physical properties.[65] The binary phase diagram indicates a range of melting points starting from 47 to 205 ^{0}C depending

on the choice of the cation and anion. However, some of them, particularly those with a lower symmetry of the cation, remain liquid at room temperature once it melts. Table 1.1 shows melting point of some commonly used quaternary ammonium salts.

Table 1.1. ***Melting point of some common quaternary ammonium salts***[a]

Quaternary ammonium molten salt	Melting point (^{0}C)
Tetrabutylammonium iodide, Bu_4NI	146
Tetrapropylammonium hydrogen sulfate, Pr_4NHSO_4	160
Tetrabutylammonium tetrafluoroborate, Bu_4NBF_4	162
Tetrapropylammonium tetrafluoroborate, Pr_4NBF_4	248
Tetrabutylammonium hexafluorophosphate, Bu_4NPF_6	247
Tetrapropylammonium hexafluorophosphate, Pr_4NPF_6	237
Tetrabutylammonium tetraphenylboride, Bu_4NBPH_4	237
Tetrapropylammonium tetraphenylboride, Pr_4NBPH_4	206

a. from ref. [66]

Huppert and coworkers studied the steady sate and time-resolved fluorescence behavior of organic molecules in solid melts[67] as well as in molten salts[68-70] of quaternary ammonium perchlorate and hydrogen sulfate that melt at a temperature noticeably higher than the room temperature. The utility of these molten salts as a solvent could not be extended further due to their lower stability in the molten state. Also, the high melting temperature and corrosive nature of these salts enhance the decomposition of many organic and biological reactants therein.

1.4. Room temperature ionic liquid (RTIL)

Room temperature ionic liquids (RTILs) are also organic salts that in their pure state are liquids at ambient temperature. These are colorless and relatively low viscous liquids compared to the high temperature molten salts. The first example of this series is ethylammonium nitrate reported in 1914.[71,72] This salt has a melting point as low as 12 ^{0}C. However, it could not draw much attention for its excessive moisture sensitive nature (water content 200 - 600 ppm). The concept of real room temperature ionic liquid started after the invention of halogenoaluminate(III) ionic liquid. The first example of this class uses a mixture of aluminum(III) chloride with a proper percentage of 1-alkylpyridinium bromide.[73] In 1982, Wilkes and his group introduced imidazolium ion for the first time as a cationic component of the organic salt.[74] They used a mixture of 1-ethyl-3-methylimidazolium chloride ([EMIM]Cl) and aluminum(III) chloride ($AlCl_3$) that showed an improved liquid range and could be used as a solvent catalysts for Friedel Crafts acylations.[75]

Modifications in the alkyl chain length and cation-anion combination in these liquid salts led to the identification of a new class of versatile solvents.[76-86] A major point of attraction of these salts was the adjustable Lewis acidity and viscosity by simply changing the molar ratio of the two components. An equimolar mixture of [EMIM]Cl and $AlCl_3$ constitutes a neutral melt, whereas a lower proportion of $AlCl_3$ produces Cl^- and $AlCl_4^-$ as primary anions, resulting a basic melt. On the other hand, acidic melt can be prepared with an excess of AlCl where the primary constituting ions are $AlCl_4^-$ and $Al_2Cl_7^-$.[87] Eventhough it i

rather easy to prepare halogenoaluminate(III) ionic liquids, proper care is necessary in handling them. These liquids are extremely sensitive to atmospheric moisture and readily decompose in the presence of specific organic compounds. Moreover, these are corrosive to skin tissue and create environmental hazard when exposed to water producing toxic halogen hydracid. Complete miscibility with water makes them a poor choice in several separation techniques.[88]

The research employing the ionic liquids as the reaction media received a boost in 1992 after the invention of air and water stable ionic liquids based on 1-ethyl-3-methylimidazolium cation and tetrafluoroborate anion, $[EMIM][BF_4]$.[89] In the subsequent years the corresponding hexafluorophosphate, which is more stable towards hydrolysis and is hydrophobic in nature, has been synthesized.[90] Suarez and coworkers successfully used the butyl analogue, 1-butyl-3-methylimidazolium tetrafluoroborate, $[BMIM][BF_4]$ and 1-butyl-3-methylimidazolium hexafluorophosphate, $[BMIM][PF_6]$ in the two-phase catalytic hydrogenation of cyclohexane with rhodium complexes.[91] Bonhote et al. discovered a series of new ionic liquids based on 1,3-dialkylimidazolium cation and six different anions.[92] The most promising one is based on bis(trifluoromethanesulphonyl)imide anion. These are relatively low viscous liquids compared to corresponding hexafluorophosphate salts and are thermally stable up to 400 ^{0}C, optically more transparent and hydrophobic (water content is less than 2%).

The quest for 'green chemistry' has led to the identification of newer RTILs other than N-alkylpyridinium (7) and N,N'-dialkylimidazolium cations (8)

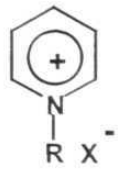
(7)

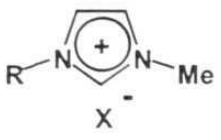
(8)

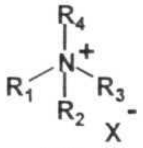
(9)

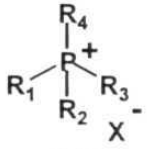
(10)

X = BF_4, PF_6, NO_3, $(CF_3SO_2)_2N$, CH_3COO, CF_3COO, $C_4F_9SO_3$, CF_3SO_3, SbF_6

R = alkyl group

and determining their role as a substitute of the conventional solvents. A wide variety of chemical reactions such as Friedel Craft reactions,[75] Heck reaction,[93-96] Diels-Alder reactions,[97,98] hydrogenation,[91,99-101] transition metal ion catalysis,[80,102] biocatalysis,[103-106] and polymerization[107,108] have been performed in RTILs. Some excellent review articles and interesting papers have appeared addressing the detailed physiochemical properties, synthetic and electrochemical application of RTILs.[88,102,108-135] Recently, different physical and structural properties of the RTILs have been examined theoretically using force-field liquid state simulation.[136] The various properties that make these ionic liquids, as environmentally benign solvents for carrying out chemical reactions are negligible vapor pressure, wide liquid range, high thermal stability, wide electrochemical window, high ionic conductivity and ability to dissolve a large variety of substances. Many RTILs are recyclable after use and hence, are comparatively least polluting solvents. The RTILs can also dissolve a number of gases[137] including supercritical CO_2.[138,139] The viscosity and melting point of these liquids are strongly influenced by the length of the alkyl chain attached to

the cation and also by the nature of anionic counterpart.[140] The lipophilicity of these salts can be tuned by replacement of the anionic component by subsequent simple metathesis reaction and increasing alkyl chain length in the cationic counterpart.[141,142]

Alkyl ammonium (9) or phosphonium ionic liquid (10) can be prepared by quarternisation of the appropriate amine or phosphine. The imidazolium based ionic liquids are synthesized from a corresponding common precursor, 1,3-alkylmidazolium halide, usually the chloride or bromide. This precursor could be prepared by alkylation of 1-methylimidazole.[74,115] In the second step, the parent halide ion is replaced either by stoichiometric metathesis reaction with the sodium or silver salt of the desired anion in water or acetone depending on the solubility of the final liquid salt.[92,127,143] Hexafluorophosphate salts are normally prepared by reaction of appropriate chloride salt with HPF_6 in water.[116,126] Acid-base neutralization reactions are preferred in the preparation of many nitrate salts.[72,144] Alkyl trifluoromethanesulfonate salt can be prepared in a single step by direct alkylation of 1-alkylimidazole dissolved in 1,1,1-trichloroethane under inert atmosphere.[92]

Purification of the RTILs depend on the nature of the impurity present in the salt. Since most of the RTILs are prepared from the corresponding halide salt, one needs to make sure that the salt is free from halides. If the RTIL forms a bi-phasic mixture with water, a repeated aqueous extraction is well enough to make it completely halide free. The same procedure can be followed to remove acid impurity also. For water miscible ionic liquids, the workup is not that

straightforward. First, the RTIL is dissolved in a suitable organic solvent like dichloromethane (DCM) to precipitate the metal halide, filtered and then the organic layer is washed with cold water. The organic solvent and the trace amount of water are finally removed under high vacuum. This cleaning up procedure of the water miscible RTILs are time consuming and it reduces the yield of final product to a large extent.

1.5. Photophysical processes in conventional solvents

1.5.1. Solvation dynamics

Solvation dynamics generally refers to the reorientation of the solvent molecules around a solute dipole instantly created in a polar solvent. In the fluorescence study the solute refers to the fluorescence probe molecules that are weekly polar or nonpolar in the ground state but become highly dipolar upon excitation. Some typical fluorophores normally used for the study of solvation dynamics are shown in Fig. 1.1. Instantaneous excitation of the probe molecule with an ultra-short laser pulse disturbs the equilibrium arrangement of solvent dipoles around the probe molecule. The solvent molecules reorient themselves around the newly created dipole and the time taken for the rearrangement of the solvent molecules to form a new equilibrium configuration around the excited probe molecule is referred to as the relaxation time of the solvent. This relaxation time obviously depends on the viscosity, the molecular structure of the solvent and the temperature of the medium. In conventional solvents at room temperature the excited state equilibrium is reached prior to emission because the solvent

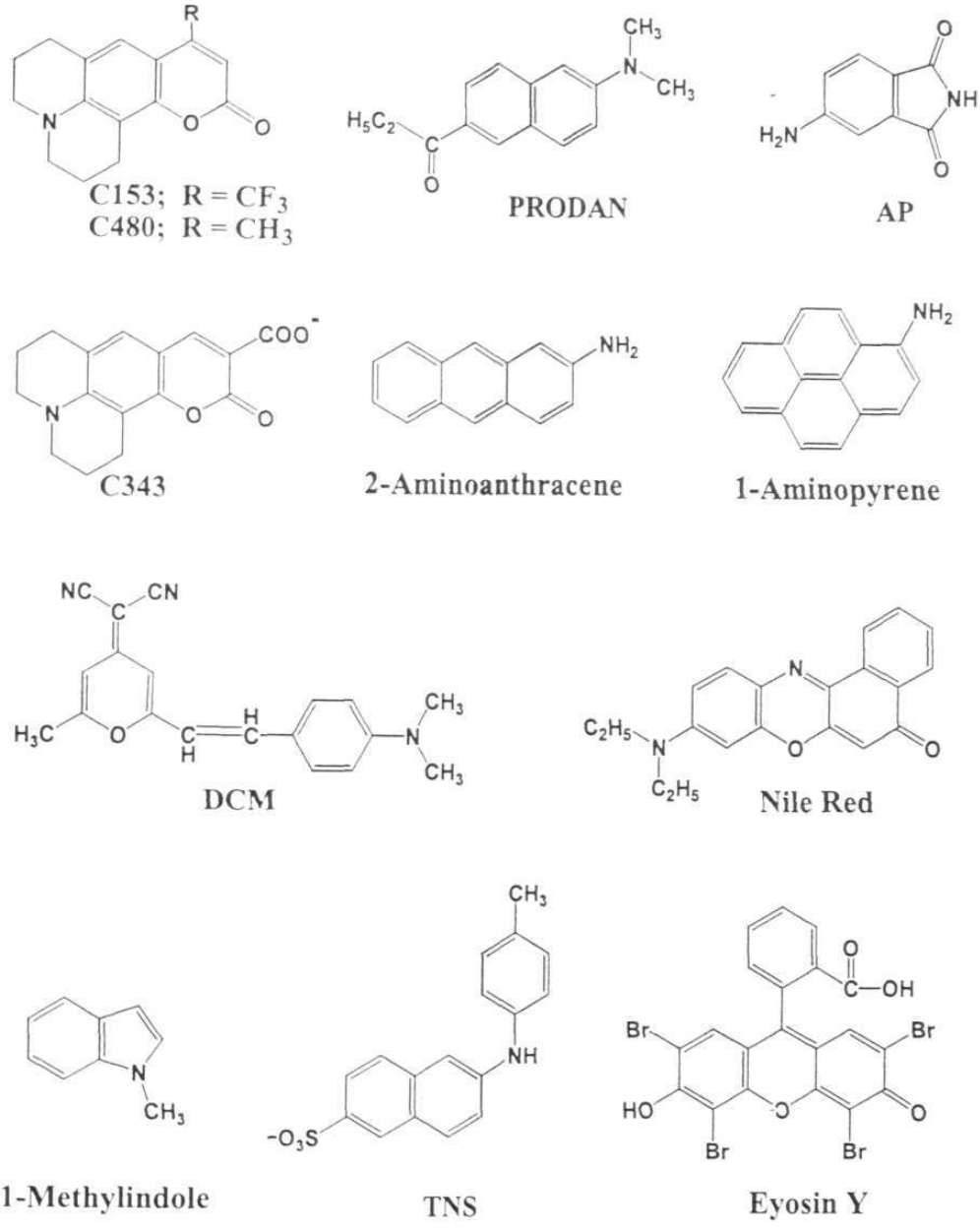

Fig. 1.1. ***Typical fluorescence probe molecules used for the study of solvation dynamics***

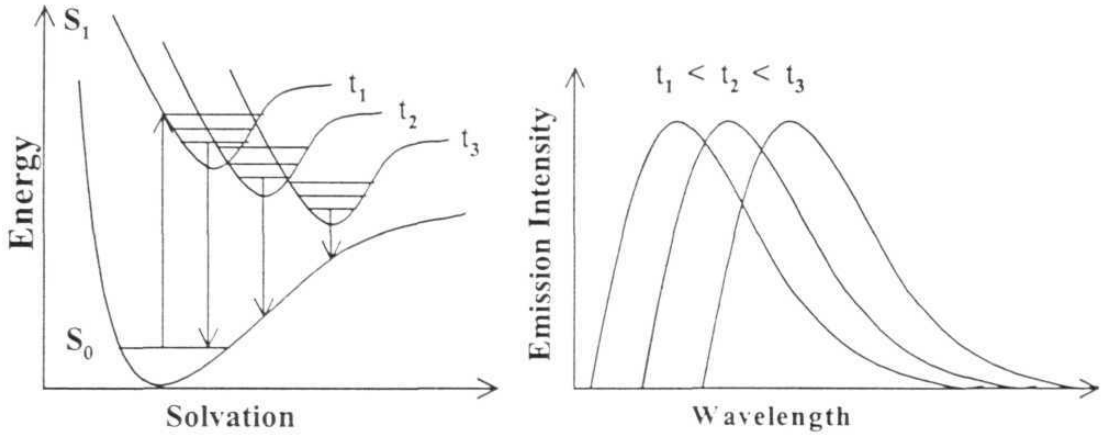

Fig. 1.2. ***Time-dependent Stokes shift***

relaxation times are typically less than 100 ps whereas the emission decay times are of the order of a few nanoseconds.[145] However, the relaxation times become much slower in a viscous solvent and in proteins[146,147] or in membranes.[148] In these cases, the emission occurs during the solvent relaxation and this results in a time-dependent shift in the emission spectra.[149-157] This phenomenon is pictorially shown in Fig.1.2.

Time-dependent Stokes shifts are measured from the time-resolved emission spectra (TRES), which are usually constructed by an indirect procedure starting with the measurement of a series of time-resolved decays monitoring 15 – 20 wavelengths across the entire steady state emission spectrum.[158,159] A wavelength dependent intensity decays are observed as a general case. The solvation dynamics is evaluated by monitoring the time dependence of the solvation correlation function, C(t), defined as[160,161]

$$C(t) = \frac{\bar{\nu}(t) - \bar{\nu}(\infty)}{\bar{\nu}(0) - \bar{\nu}(\infty)}$$

where, $\bar{\nu}(0)$, $\bar{\nu}(t)$ and $\bar{\nu}(\infty)$ are the peak frequencies of the TRES at time zero, at an intermediate time (t) and at infinite time after excitation respectively. The longitudinal relaxation time of the solvent, τ_L, is an exponential decay function of C(t) with time, so that $C(t) = \exp(-t/\tau_L)$. However, experimentally found C(t) functions are multi-exponential in nature and hence, an average solvation time $<\tau_L>$ is reported, where $< \tau_L > = \sum_{i=1}^{n} a_i \tau_i$. The simple continuum theory equates the longitudinal relaxation time, τ_L, with much slower Debye relaxation time, τ_D according to the following equation.[149-157,162-167]

$$\tau_L = \frac{2\varepsilon_\infty + \varepsilon_c}{2\varepsilon_0 + \varepsilon_c}\tau_D \cong \frac{2n^2 + 1}{2\varepsilon + 1}\tau_D \cong \frac{n^2}{\varepsilon}\tau_D$$

where, ε_∞ and ε_0 ($\varepsilon_\infty < \varepsilon_0$) are the infinite-frequency and low-frequency dielectric constant of the solvent. ε_c is the dielectric constant of the cavity containing the probe molecule. The equation is often simplified assuming $\varepsilon_\infty = n^2$, where n is the refractive index and replacing ε_0 by static dielectric constant, ε.

1.5.1.1. Relaxation processes in polar and nonpolar solvents

The relaxation processes in conventional solvents are usually faster due to very fast reorientation of the solvent molecules. Using ultrafast time resolution of the order of few femto-seconds and exact time zero calculation, Maroncelli and coworkers[156] showed that in major class of solvents where specific interaction

like hydrogen bonding is unimportant, the solvation times are in the sub picosecond time scale at room temperature. The result can be well explained using non-specific theories of solvation dynamics. The linear correlation between experimentally observed average relaxation time and longitudinal relaxation time, τ_L as predicted by simple continuum theory, depends primarily on the nature of solute-solvent interaction and temperature of the medium. Deviation from the above can be accounted for considering molecular nature of the solvent, translational contribution to the solvent relaxation and specific hydrogen bonding ability of the protic solvent.[168-174]

1.5.1.2. High pressure solvation dynamics

The effect of enhanced pressure on solvation dynamics of coumarin 153 in different alcohol has been studied by Hara and coworkers.[175] They observed a good correlation between the average solvation time and the longest longitudinal relaxation time of the alcohol used as the solvent. A similar observation was made by Huppert and coworkers while studying the solvation dynamics of coumarin 480 in ethanol at much higher pressure.[176] In atmospheric pressure ethanol shows usual monomeric relaxation process with a relaxation time of 35 ps. With gradual increase in pressure (> 0.5 Gpa) the solvation becomes biexponential in nature. A typical biphasic solvation time of 110 ps and 500 ps, with an average relaxation time of 410 ps was observed at a pressure of 1.55 Gpa. This slow dynamics has been explained on the basis of liquid-solid phase transition of ethanol in this high pressure. On the contrary, in solid phase, relaxation occurs at a relatively faster rate with an average time of 360 ps. The faster relaxation

process in solid crystalline alcohol is ascribed to rapid reorientation of the ethanol molecule in vicinity of the fluorescence probe.[176]

Hara and coworkers observed a faster solvation rate of C153 in aqueous Triton X-100 micelle with increase in pressure.[177] At enhanced pressure, a weakening of hydrogen bonding interaction at the Stern layer of the micelle is believed to result in an increased mobility of the water molecules, resulting a shorter relaxation time.

1.5.1.3. Solvation dynamics in confined environment

The relaxation in pure water is biexponential nature with an ultrafast relaxation time of 126 fs and a relatively slower one, 880 fs.[153] According to Fleming et al., the faster component arises due to intramolecular vibration of the water molecule and the slower one for the librational motion.[153] Interestingly, the presence of a slow component (of few nanoseconds) with significant amplitude has been reported by Bhattacharyya et al. for water present in a confined environment.[178,179] An extensive research by his group and others on solvation dynamics of water in micelles,[177,180-182] cyclodextrin,[183,184] nanoparticles,[185] polymer-surfactant aggregates,[186,187] protein[188,189] and DNA[190] gives a similar information. In all cases, two types of water molecules have been assigned, unbound or free and bound with the macromolecules by strong electrostatic interaction or hydrogen bonding. The former one is responsible for the faster component whereas the slow relaxation time arises due to the latter.

1.5.1.4. Solvation dynamics in ionic salt solution

Chapman and Maroncelli reported the static and dynamical nature of ionic solution using common solvatochromic probe molecules.[191] For this purpose they chose large number of metal perchlorate and halide salts and studied those in a number of non-aqueous solvents with different polarity. Their observations suggest an excitation wavelength dependent solvation rate. The solvent response functions could be extracted either by single exponential or biexponential decay function depending on the salt concentration. The ionic solvation is rather slow (few nanoseconds) when compared with that in conventional solvents. A profound effect of the solvent polarity and charge to size ratio of the cation has been observed. Considering the faster rotational rate of the probe molecule relative to spectral relaxation, a slow activated exchange between ions and solvent molecules in the first solvation shell of the probes is attributed to the slow dynamics in these media.

1.5.1.5. Solvation dynamics in high temperature molten salts

A slow solvation dynamics, similar to that in ionic salt solution, was observed by Huppert and coworkers in several solids[67] and in molten tetraalkylammonium salts[68-70] using different fluorescent probes. In all cases, the solvation process occurred in two different time scales (picosecond and nanosecond). The average relaxation time in molten salt was found relatively slower than that observed in pure solvent or electrolyte solutions. Unlike Chapman and Maroncelli,[191] this slow solvation was explained by Huppert and coworkers by taking into consideration the translational motion of the constituting

ions present in the media. According to Huppert et al., the fast component of the dynamics is due to the translational motion of the smaller species, the anion and the slower one is due to the larger cation. Both the solvation times were found to be dependent on the cation size and the chosen probe molecule.

1.5.2. Excited state complex

Excited state complexes are dimeric species formed either between two similar or dissimilar molecules that are stable only in the excited electronic state. The former is generally known as excimer and the latter, the exciplex.[192-194] The formation of aromatic excimer was first discovered by Förster and Kasper in 1954.[195] A new broad emission band that appeared in the longer wavelength side of the structured monomer emission in concentrated pyrene solution at room temperature was attributed to the excimer, formed by diffusive association of one photoexcited pyrene moiety in singlet excited state with another one in the ground state. It has been latter found that such phenomenon is rather common in several planar and nonplanar aromatic hydrocarbons other than pyrene in higher concentration.[192,196-198]

A similar broad red-shifted emission band has been observed for some specific organic molecules at low concentration where two planar aromatic hydrocarbon rings are attached by an alkyl chain or an ether linkage.[199-201] In these molecules, the long wavelength emission at low concentration is found to be due to the formation of excimer in an intramolecular fashion. Further research on this aspect has explored the optimum geometrical arrangement required for the formation of the intramolecular excimer, excimer formation kinetics and

thermodynamics in conventional polar and nonpolar solvents.[196-198,201-209] These results clearly indicate a correlation between the viscosity of the medium and the formation rate of the excimer.

1.6. Motivation of the present work

Even though the utility of the PTCs in various synthetic and chemical applications is well documented, the exact nature of the binding of these salts with polar organic molecules in a nonpolar medium has rarely been investigated spectroscopically. A few studies are reported, where other than its catalytic activity, the behavior of the PTC in the bulk phase has been monitored using spectroscopic techniques.[23,35,210,211] The interfacial behavior of a PTC associated with a phenoxide ion was studied by Uchiyama and coworkers in 1999, using a laser scattering method.[212] Thomas and Kamat[25] made use of a PTC to prepare and study the behavior of stable gold nano-particles in a nonpolar medium. Here, we attempt to find out whether the role of the PTCs lies merely in helping the solubilization of a polar system in nonpolar media to facilitate its reaction with a third substance in the organic medium. Specifically, we explore the exact nature of the interaction of the phase transfer catalysts with neutral polar organic systems and to what extent the PTCs change the photophysical properties of the solubilized systems.

In order to accomplish this objective, we have chosen basically two sets of fluorescent probe molecules (Fig. 1.3). Set-1 consists of 4-aminophthalimide (AP) and 4-aminonaphthalimide (ANP), two highly fluorescing electron donor-acceptor molecules that emit from intramolecular charge transfer (ICT) state with the

fluorescence parameters highly sensitive to the polarity of the media.[213-217] In Set-2, we have chosen three systems with a *fluorophore-spacer-receptor* architecture. In all these systems, the fluorophore moiety is derived from an

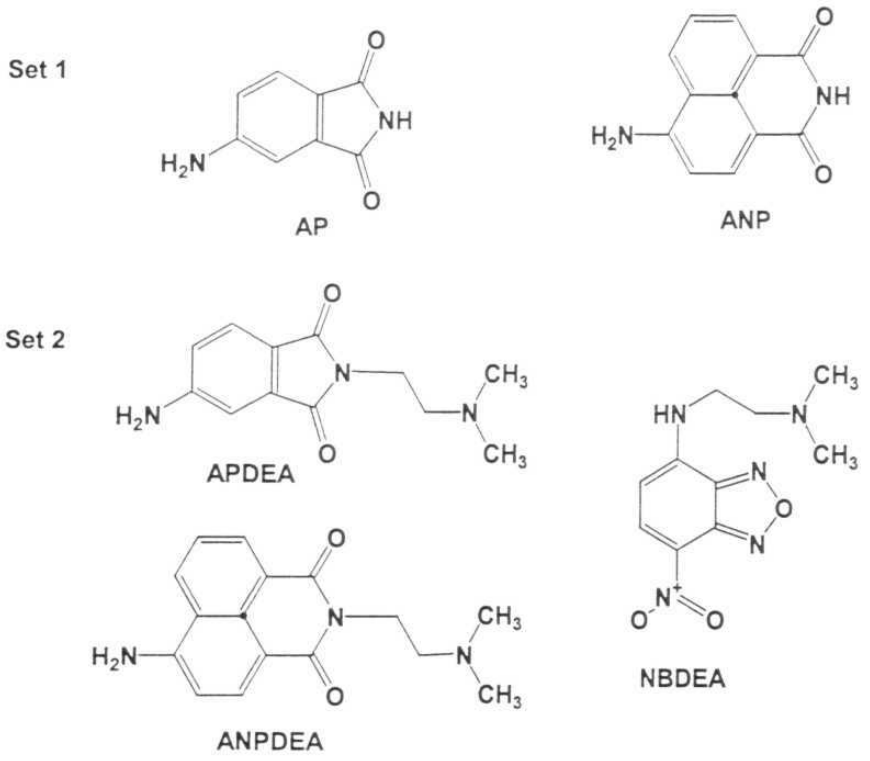

Fig. 1. 3

electron donor-acceptor molecule that emits from an ICT state. The spacer and the receptor moieties in these systems are a dimethylene and a dimethylamino moiety respectively. The photophysical behavior of these EDA molecules in the presence of the PTCs has been studied in details.

As evident from the discussion made earlier, room temperature ionic liquids (RTILs) are expected to be the reaction media for future. Until now, the

emphasis has been towards the characterization of various properties of these substances that make them better alternatives to the conventional solvents used in organic synthesis. Even though a large volume of data is already available on the suitability of these RTILs in carrying out various chemical reactions,[88,98,102,108-111,117,122,130,131,140,218,219] very few photophysical studies have been undertaken so far. Aki et al. have measured the polarity of a few RTILs by studying the steady state fluorescence behavior of two fluorescence probe molecules.[220] Using UV-visible absorption behavior of two solvatochromic dyes, Gordon and coworkers[221] have substantiated these data and indicated that the polarity of an ionic liquid is largely determined by the cationic component of the solvent. The feasibility of photoisomerization reaction of trans stilbene in RTIL has been investigated by Ozawa and Hamaguchi.[222] Photoinduced electron transfer[223] and hydrogen atom abstraction reactions[224] have also been studied. Taking note of the potential of the RTILs and the paucity of photophysical literature in these media, the present investigation on the photophysical behavior of some molecules has been undertaken. Since the ionic liquids are sufficiently polar and viscous liquids at ambient temperature, we have concentrated on photophysical processes that are dependent on these properties. Specifically, we have concentrated ourselves on the process of solvation of the fluorescent state of some dipolar molecules and on the formation of intramolecular excimer in RTILs.

In order to obtain an understanding of the solvation dynamics in these new liquids we have synthesized a series of RTILs based on 1-alkyl-3-methyl imidazolium salts (Fig. 1.4). The systems chosen are air and water stable and less viscous than those containing halide ions. [92]

RTILs

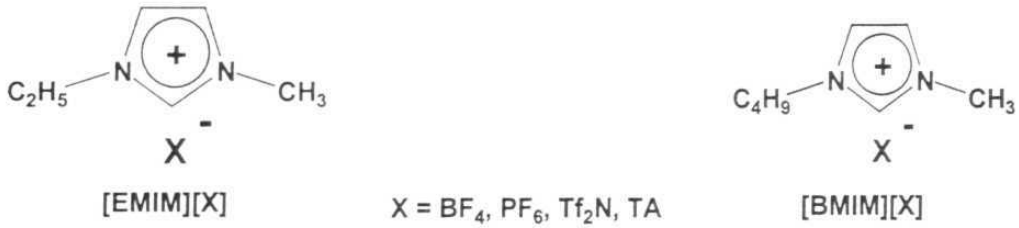

Fluorescence Probe

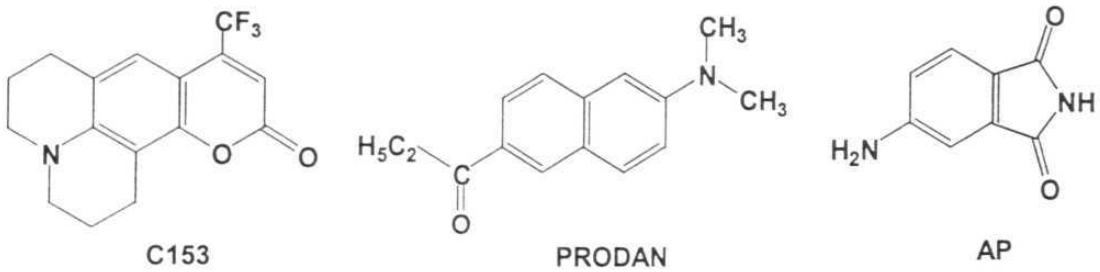

Fig. 1.4

In order to examine the process of solvation in RTILs we have chosen three different probe molecules, C153, PRODAN and AP, shown in Fig. 1.4. These fluorescence probe molecules have previously been utilized for the study of solvation dynamics in conventional solvents because of their high stability on high intense laser, instantaneous separation of charge on photo-excitation and

significant Stokes shift of the emission maximum as a function of the solvent polarity.[169,178,179,191]

In order to explore the utility of the room temperature ionic liquids in other photophysical studies, the formation of intramolecular excimer in 1,3-bis(1-pyrenyl)propane has been investigated by steady state and time-resolved fluorescence measurements. The molecule for this investigation is obviously chosen because the dynamics of intramolecular interaction in this system has been extensively studied in conventional media.[203,207,209]

1.7. Layout of the thesis

The thesis is divided into six chapters. The first chapter provides introductory background information on the phase transfer catalyst (PTC), room temperature ionic liquid (RTIL) and different photophysical processes with which the current investigation is concerned. In the second chapter, details of the preparation and purification of various RTILs, method of the treatment of the experimental data and the instrumentation used in the thesis have been described. Third chapter provides the absorption and emission behavior of the EDA molecules in the presence of the PTCs. The fourth chapter deals with relaxation of the fluorescent state of some probe molecules in a series of RTILs. The fifth chapter of the thesis is concerned with intramolecular excimer formation process of 1,3-bis(1-pyrenyl)propane in few RTILs. The last chapter summarizes the results of the present investigation and outlines the scope of further investigation that can be initiated based on the present findings.

1.8. References

(1) Dehmlow, E. V.; Dehmlow, S. S. *Phase Transfer Catalysis*; Verlag Chemie: Weinheim, 1983.

(2) Starks, C. M.; Liotta, C. *Phase Transfer Catalysis: Principles and Techniques*; Academic Press: New York, 1978.

(3) Halpern, M. E. *Phase-Transfer Catalysis, Mechanism and Syntheses*; American Chemical Society: Washington, DC, 1997.

(4) Sasson, Y.; Neumann, R. *Handbook of Phase Transfer Catalysis*; Blackie Academic and Professional: London, 1997.

(5) Weber, W. P.; Gokel, G. W. *Phase Transfer Catalysis in Organic Synthesis*; Springer-Verlag: Berlin, 1977.

(6) Makosza, M.; Serafinowa, B. *Rocz. Chem.* **1965**, *39*, 1223.

(7) Starks, C. M.; Napier, D. R. ; Aust. Pat. 439286:, 1968.

(8) Starks, C. M.; Napier, D. R. ; French Pat. 1573164:, 1969.

(9) Starks, C. M.; Napier, D. R. ; Brit. Pat. 1227144:, 1971.

(10) Starks, C. M. *J. Am. Chem. Soc.* **1971**, *93*, 195.

(11) Liotta, C. L.; Harris, H. P. *J. Am. Chem. Soc.* **1974**, *95*, 2250.

(12) Jonczyk, A.; Zomerfeld, T. *Tet. Lett.* **2003**, *44*, 2359.

(13) Kong, Y.-T.; Imabayashi, S.-I.; Kakiuchi, T. *J. Am. Chem. Soc.* **2000**, *122*, 8215.

(14) Campbell, C. J.; Rusling, J. F. *Langmuir* **1999**, *15*, 7416.

(15) Yadav, G. D.; Naik, S. S. *Org. Process Res. Dev.* **1999**, *3*, 83.

(16) Sirovski, F. S. *Org. Process Res. Dev.* **1999**, *3*, 437.

(17) Perrard, T.; Plaquevent, J.-C.; Desmurs, J.-R.; Hebrault, D. *Org. Lett.* **2000**, *2*, 2959.

(18) Wang, M.-L.; Huang, T.-H.; Wu, W.-T. *Ind. Eng. Chem. Res.* **2002**, *41*, 518.

(19) Albanese, D.; Landini, D.; Maia, A.; Penso, M. *Ind. Eng. Chem. Res.* **2001**, *40*, 2396.

(20) Ohtani, N.; Morimoto, Y.; Naitou, M.; Kasuga, Y.; Tsuchimoto, D. *Langmuir* **2001**, *17*, 3829.

(21) Kim, Y.-W.; Brueggemeier, R. W. *Tet. lett.* **2002**, *43*, 6113.

(22) Li, X.; Wang, J.; Mason, R.; Bu, X. R.; Harrison, J. *Tetrahedron* **2002**, *58*, 3747.

(23) Ma, G.; Freiser, H.; Muralidharan, S. *Anal. Chem.* **1997**, *69*, 2827.

(24) Brust, M.; Walker, M.; Bethell, D.; Schiffrin, D. J.; Whyman, R. *Chem. Commun.* **1994**, 801.

(25) Thomas, K. G.; Kamat, P. V. *J. Am. Chem. Soc.* **2000**, *122*, 2655.

(26) Chandrasekharan, N.; Kamat, P. V. *Nano Lett.* **2001**, *1*, 67.

(27) George, T. K.; Zajicek, J.; Kamat, P. V. *Langmuir* **2002**, *18*, 3722.

(28) Kamat, P. V. *J. Phys. Chem. B.* **2002**, *106*, 7729.

(29) Makosza, M. *Pure. Appl. Chem.* **1975**, *43*, 439.

(30) Cunnane, V.; Schiffrin, D. J.; Beltran, C.; Geblewicz, G.; Solomon, T. *J. Electroanal. Chem.* **1988**, *247*, 203.

(31) Tan, S. N.; Dryfe, R. A.; Girault, H. H. *Helv. Chim. Acta.* **1994**, *77*, 231.

(32) Jones, R. A. *Quaternary Ammonium Salts, Their Use in Phase-Transfer Catalyzed Reactions*; Academic Press: New York, 2001.

(33) Annunziata, R.; Benaglia, M.; Cinquini, M.; Cozzi, F.; Tocco, G. *Org. Lett.* **2000**, *2*, 1737.

(34) Wang, M.-L.; Tseng, Y.-H. *J. Mol. Cat. A: Chem.* **2002**, *188*, 51.

(35) Asai, S.; Nakamura, H.; Tanabe, M.; Sakamoto, K. *Ind. Eng. Chem. Res.* **1994**, *33*, 1687.

(36) Wu, H. S.; Meng, S. S. *J. Chem. Eng. Jpn.* **1996**, *29*, 1007.

(37) Lizawa, A.; Yamada, Y.; Ogura, Y.; Sato, Y. *Polym. Phase Transfer Catal.* **1994**, 2057.

(38) Goerdeler, J. *Methoden Org. Chem. (Houben-Weyl), 4th Ed.* **1958**, *11-Part 2*, 591-640.

(39) Henderson, W. A.; Buckler, S. A. *J. Am. Chem. Soc.* **1960**, *82*, 5794.

(40) Kim, D. Y.; Park, E. J. *Org. Lett.* **2002**, *4*, 545.

(41) Kim, D. Y.; Huh, S. C. *Tetrahedron* **2001**, *57*, 8933.

(42) Kim, D. Y.; Huh, S. C.; Kim, S. M. *Tet. Lett.* **2001**, *42*, 6299.

(43) Arai, S.; Tsuji, R.; Nishida, A. *Tet. Lett.* **2002**, *43*, 9535.

(44) Mathias, L. T.; Vaidya, R. A. *J. Am. Chem. Soc.* **1986**, *108*, 1093.

(45) Yadav, G. D.; Jadhav, Y. B. *J. Mol. Cat. A: Chem.* **2002**, *184*, 151.

(46) Boyer, B.; Hambardzoumian, A.; Roque, J.-P.; Beylerian, N. *J. Chem. Soc., Perkin Trans. 2.* **2002**, 1689.

(47) Lu, Y. L.; Jwo, J.-J. *J. Mol. Cat. A: Chem.* **2001**, *170*, 57.

(48) Boyer, B.; Hambardzoumian, A.; Roque, J.-P.; Beylerian, N. *Tetrahedron* **2000**, *56*, 303.

(49) Monflier, E.; Tilloy, S.; Fremy, G.; Castanet, Y.; Mortreux, A. *Tet. Lett.* **1995**, *36*, 9481.

(50) Barak, G.; Sasson, Y. *Bull. Soc. Chim. Fr.* **1988**, *3*, 584.

(51) Ganeshpure, P. A.; Satish, S. *J. Chem. Soc. Chem. Commun.* **1988**, *14*, 981.

(52) Shimiju, S.; Sasaki, Y.; Hirai, C. *Bull. Chem. Soc. Jpn.* **1990**, *63*, 176.

(53) Zeldin, M. ; Indiana university Foundation, US Pat. 4855433:, 1988.

(54) Madden, P. A.; Wilson, M. *J. Phys.: Condens. Matter* **2000**, *12*, 95.

(55) Doermus, R. H. *Glass Science*; 2nd ed.; Wiley: New York, 1994.

(56) Aliotta, F.; Maisano, G.; Migliardo, P.; Vasi, C.; Wanderlingh, F.; Pedro-Smith, G.; Triolo, R. *J. Chem. Phys.* **1981**, *75*, 613.

(57) Soltwish, M.; Sukmanowski, J.; Quitmann, D. *J. Chem. Phys.* **1987**, *86*, 3207.

(58) Ribeiro, M. C. C.; Wilson, M.; Madden, P. A. *J. Chem. Phys.* **1999**, *110*, 4803.

(59) La Violette, R. A.; Budzien, J. L.; Stillinger, F. H. *J. Chem. Phys.* **2000**, *112*, 8072.

(60) Dracopoulos, V.; Vagelatos, J.; Papatheodorou, G. N. *J. Chem. Soc., Dalton Trans.* **2001**, 1117.

(61) Photiadis, G. M.; Papatheodorou, G. N. *J. Chem. Soc., Dalton Trans.* **1998**, 981.

(62) Photiadis, G. M.; Papatheodorou, G. N. *J. Chem. Soc., Dalton Trans.* **1999**, 3541.

(63) Gordon, J. E. *J. Am. Chem. Soc.* **1964**, *86*, 4492.

(64) Gordon, J. E. *J. Org. Chem.* **1965**, *30*, 2760.

(65) Gordon, J. E.; SubbaRao, G. N. *J. Am. Chem. Soc.* **1978**, *100*, 7445.

(66) Lind, J. E., Jr.; Abdel-Rehim, H. A. A.; Rudich, S. W. *J. Phys. Chem.* **1966**, *70*, 3610.

(67) Bart, E.; Meltsin, A.; Huppert, D. *J. Phys. Chem.* **1995**, *99*, 9253.

(68) Bart, E.; Meltsin, A.; Huppert, D. *J. Phys. Chem.* **1994**, *98*, 3295.

(69) Bart, E.; Meltsin, A.; Huppert, D. *J. Phys. Chem.* **1994**, *98*, 10819.

(70) Bart, E.; Meltsin, A.; Huppert, D. *Chem. Phys. Lett.* **1992**, *200*, 592.

(71) Walden, P. *Bull. Acad. Imper. Sci. (St. Petersburg)* **1914**, 1800.

(72) Sugden, S.; Wilkins, H. *J. Chem. Soc.* **1929**, 1291.

(73) Hurley, F. H.; Weir, T. P. *J. Electrochem. Soc.* **1951**, *98*, 203.

(74) Wilkes, J. S.; Levisky, J. A.; Wilson, R. A.; Hussey, C. L. *Inorg. Chem.* **1982**, *21*, 1263.

(75) Boon, J. A.; Levinsky, J. A.; Pflug, J. L.; Wilkes, J. S. *J. Org. Chem.* **1986**, *51*, 480.

(76) Hussey, C. L. *Adv. Molten Salt Chem.* **1983**, *5*, 185.

(77) Fannin, A. A.; Floreani, D. A.; King, L. A.; Landers, J. S.; Piersma, B. J.; Stech, D. J.; Vaughn, R. L.; Wilkes, J. S.; Williams, J. L. *J. Phys. Chem.* **1984**, *88*, 2614.

(78) Sanders, J. R.; Ward, E. H.; Hussey, C. L. *J. Electrochem. Soc.* **1986**, *133*, 325.

(79) Zawodzinski, T. A., Jr.; Carlin, R. T.; Osteryoung, R. A. *Anal. Chem.* **1987**, *59*, 2639.

(80) Hussey, C. L. *Pure & Appl. Chem.* **1988**, *60*, 1763.

(81) Abdul-Sada, A. K.; Al-Juaid, S.; Greenway, A. M.; Hitchcock, P. B.; Howells, M. J.; Seddon, K. R.; Welton, T. *Struct. Chem.* **1990**, *1*, 391.

(82) Elaiwi, A.; Hitchcock, P. B.; Seddon, K. R.; Srinivasan, N.; Tan, Y.-M.; Welton, T.; Zora, J. A. *J. Chem. Soc. Dalton Trans.* **1995**, 3467.

(83) Trulove, P. C.; Osteryoung, R. A. *Inorg. Chem.* **1992**, *31*, 3980.

(84) Campbell, J. L. E.; Johnson, K. E. *J. Am. Chem. Soc.* **1995**, *117*, 7791.

(85) Mantz, R. A.; Trulove, P. C.; Carlin, R. T.; Theim, T. L.; Osteryoung, R. A. *Inorg. Chem.* **1997**, *36*, 1227.

(86) Dyson, P. J.; Grossel, M. C.; Srinivasan, N.; Vine, T.; Welton, T.; Williams, D. J.; White, J. P.; Zigras, T. *J. Chem. Soc., Dalton Trans.* **1997**, 3465.

(87) Schreiter, E. R.; Stevens, J. E.; Ortwerth, M. F.; Freeman, R. G. *Inorg. Chem.* **1999**, *38*, 3935.

(88) Welton, T. *Chem. Rev.* **1999**, *99*, 2071.

(89) Wilkes, J. S.; Zaworotko, M. J. *J. Chem. Soc. Chem. Commun.* **1992**, 965.

(90) Fuller, J.; Carlin, R. T.; De Long, H. C.; Haworth, D. *J. Chem. Soc., Chem. Commun.* **1994**, 299.

(91) Suarez, P. A. Z.; Dullius, J. E. L.; Einloft, S.; De Souza, R. F.; Dupont, J. *Polyhedron* **1996**, *15*, 1217.

(92) Bonhote, P.; Dias, A. P.; Papageorgiou, N.; Kalyanasundaram, K.; Gratzel, M. *Inorg. Chem.* **1996**, *35*, 1168.

(93) Kaufmann, D. E.; NourooZian, M.; Henze, H. *Synlett.* **1996**, 1091.

(94) Carmichael, A. J.; Earle, M. J.; Holbrey, J. D.; McCormac, P. B.; Seddon, K. R. *Org. Lett.* **1999**, *1*, 997.

(95) Xu, L.; Chen, W.; Xiao, J. *Organometallics* **2000**, *19*, 1123.

(96) Xu, L.; Chen, W.; Ross, J.; Xiao, J. *Org. Lett.* **2001**, *3*, 295.

(97) Fischer, T.; Sethi, A.; Welton, T.; Woolf, J. *Tetrahedron Lett.* **1999**, *40*, 793.

(98) Song, C. E.; Shim, W. H.; Roh, E. J.; Lee, S. G.; Choi, J. H. *Chem. Commun.* **2001**, 1122.

(99) Chauvin, Y.; Mussmann, L.; Olivier, H. *Angew. Chem. Int. Ed. Engl.* **1995**, *34*, 2698.

(100) Liu, F.; Abrams, M. B.; Baker, R. T.; Tumas, W. *Chem. Commun.* **2001**, 433.

(101) Brown, R. A.; Pollet, P.; McKoon, E.; Eckert, C. A.; Liotta, C. L.; Jessop, P. G. *J. Am. Chem. Soc.* **2001**, *123*, 1254.

(102) Wasserscheid, P.; Keim, W. *Angew. Chem., Int. Ed. Engl.* **2000**, *39*, 3772.

(103) Lau, R. M.; van Rantwijk, F.; Seddon, K. R.; Sheldon, R. A. *Org. Lett.* **2000**, *2*, 4189.

(104) Schofer, S. H.; Kaftzik, N.; Wasserscheid, P.; Kragl, U. *Chem. Commun.* **2001**, 425.

(105) Itoh, T.; Akasaki, E.; Kudo, K.; Shirakami, S. *Chem. Lett.* **2001**, 262.

(106) Kim, K. W.; Song, B.; Choi, M. Y.; Kim, M. J. *Org. Lett.* **2001**, *3*, 1507.

(107) Carlin, R. T.; Osteryoung, R. A.; Wilkes, J. S.; Rovang, J. *Inorg. Chem.* **1990**, *29*, 3003.

(108) Scott, M. P.; Brazel, C. S.; Benton, M. G.; Mays, J. W.; Holbrey, J. D.; Rogers, R. D. *Chem. Commun.* **2002**, 1370.

(109) Dupont, J.; de Souza, R. F.; Suarez, P. A. Z. *Chem. Rev.* **2002**, *102*, 3667.

(110) Zhao, D.; Wu, M.; Kou, Y.; Min, E. *Catal. Today.* **2002**, *74*, 157.

(111) Sheldon, R. *Chem. Commun.* **2001**, 2399.

(112) Holbrey, J. D.; Seddon, K. R. *Clean Products and Processes* **1999**, *1*, 223.

(113) Seddon, K. R. In *Molten Salt Forum: Proceedings of the 5th International Conference on Molten Salt Chemistry and Technology*; Wendt, H., Ed., 1998; Vol. 5-6.

(114) Appleby, D.; Hussey, C. L.; Seddon, K. R.; Turp, J. E. *Nature* **1986**, *323*, 614.

(115) Hasan, M.; Kozhevnikov, I. V.; Siddiqui, M. R. H.; Steiner, A.; Winterton, N. *Inorg. Chem.* **1999**, *38*, 5637.

(116) Gordon, C. M.; Holbrey, J. D.; Kennedy, A. R.; Seddon, K. R. *J. Mater. Chem.* **1998**, *8*, 2627.

(117) Freemantle, M. *Chem. Eng. News* **1998**, *76*, 32.

(118) Freemantle, M. *Chem. Eng. News* **1998**, *76*.

(119) Demberelnyamba, D.; Shin, B. K.; Lee, H. *Chem. Commun.* **2002**, 1538.

(120) Seddon, K. R. *J. Chem. Technol. Biotechnol.* **1997**, *68*, 351.

(121) Seddon, K. R. *Kinet. Catal.* **1996**, *37*, 693.

(122) Ranu, B. C.; Das, A.; Samanta, S. *J. Chem. Soc., Perkin Trans. 1* **2002**, 1520.

(123) Larsen, A. S.; Holbrey, J. D.; Tham, F. S.; Reed, C. A. *J. Am. Chem. Soc.* **2000**, *122*, 7264.

(124) Branco, L. C.; Crespo, J. G.; Afonso, C. A. M. *Angew. Chem. Int. Ed.* **2002**, *41*, 2771.

(125) Ishida, Y.; Miyauchi, H.; Saigo, K. *Chem. Commun.* **2002**, 2240.

(126) Huddleston, J. G.; Willauer, H. D.; Swatloski, R. P.; Visser, A. E.; Rogers, R. D. *Chem. Commun.* **1998**, 1765.

(127) Holbrey, J. D.; Seddon, K. R. *J. Chem. Soc., Dalton Trans.* **1999**, 2133.

(128) MacFarlane, D. R.; Golding, J.; Forsyth, S.; Forsyth, M.; Deacon, G. B. *Chem. Commun.* **2001**, 1430.

(129) Matsumoto, H.; Kageyama, H.; Miyazaki, Y. *Chem. Commun.* **2002**, 1726.

(130) Wheeler, C.; West, K. N.; Liotta, C. L.; Eckert, C. A. *Chem. Commun.* **2001**, 887.

(131) Varma, R. S.; Namboodiri, V. V. *Chem. Commun.* **2001**, 643.

(132) Noda, A.; Hayamizu, K.; Watanabe, M. *J. Phys. Chem. B* **2001**, *105*, 4603.

(133) Fuller, J.; Carlin, R. T.; Osteryoung, R. A. *J. Electrochem. Soc.* **1997**, *144*, 3881.

(134) Merrigan, T. L.; Bates, E. D.; Dorman, S. C.; Davis, J. H., Jr. *Chem. Commun.* **2000**, 2051.

(135) Gannon, T. J.; Law, G.; Watson, P. R. *Langmuir* **1999**, *15*, 8429.

(136) Andrade, J. D.; Boes, E. S.; Stassen, H. *J. Phys. Chem. B.* **2002**, *106*, 3546.

(137) Anthony, J. L.; Maginn, E. J.; Brennecke, J. F. *J. Phys. Chem. B.* **2002**, *106*, 7315.

(138) Blanchard, L. A.; Hancu, D.; Beckman, E. J.; Brennecke, J. F. *Nature* **1999**, *399*, 28.

(139) Blanchard, L. A.; Brennecke, J. F. *Ind. Eng. Chem. Res.* **2001**, *40*, 287.

(140) Seddon, K. R.; Stark, A.; Torres, M.-J. *Personal Communication* **2001**.

(141) Huddleston, J. G.; Visser, A. E.; Reichert, W. M.; Willauer, H. D.; Broker, G. A.; Rogers, R. D. *Green. Chem.* **2001**, *3*, 156.

(142) Dzyuba, S. V.; Bartsch, R. A. *Chem. Commun.* **2001**, 1466.

(143) Koch, V. R.; Nanjundiah, C.; Appetecchi, G. B.; Scrosati, B. *J. Electrochem. Soc.* **1995**, *142*, L116.

(144) Poole, C. F.; Kersten, B. R.; Ho, S. S. J.; Coddens, M. E.; Furton, K. G. *J. Chromatogr.* **1986**, *352*, 407.

(145) Lakowicz, J. R. *Principles of Fluorescence Spectroscopy*; Second ed.; Kluwer Academic/Plenum Publishers: New York, 1999.

(146) Demchenko, A. P.; Apel, H. J.; Sturmer, W.; Feddersen, B. *Biophys. Chem.* **1993**, *48*, 135.

(147) Wang, R.; Sun, S.; Bekos, E. J.; Bright, F. V. *Anal. Chem.* **1995**, *67*, 149.

(148) Hutterer, R.; Schneider, F. W.; Lanig, H.; Hof, M. *Biochim. Biophys. Acta* **1997**, *1323*, 195.

(149) Fleming, G. R.; Cho, M. *Ann. Rev. Phys. Chem.* **1996**, *47*, 109.

(150) Stratt, R. M. *Acc. Chem. Res.* **1995**, *28*, 201.

(151) Rossky, P. J.; Simon, J. D. *Nature* **1994**, *370*, 263.

(152) Hynes, J. T. In *Ultrafast Spectroscopy*; Simon, J. D., Ed.; Kluwer: Dordrecht, 1994.

(153) Jimenez, R.; Fleming, G. R.; Kumar, P. V.; Maroncelli, M. *Nature* **1994**, *369*, 471.

(154) Koti, A. S. R.; Krishna, M. M. G.; Periasamy, N. *J. Phys. Chem. A.* **2001**, *105*, 1767.

(155) Castner, E. W., Jr.; Maroncelli, M. *J. Mol. Liq.* **1998**, *77*, 1.

(156) Horng, M. L.; Gardecki, J. A.; Papazyan, A.; Maroncelli, M. *J. Phys. Chem.* **1995**, *99*, 17311.

(157) Horng, M. L.; Gardecki, J. A.; Maroncelli, M. *J. Phys. Chem. A.* **1997**, *101*, 1030.

(158) Easter, J. H.; DeToma, R. P.; Brand, L. *Biophys. J.* **1976**, *16*, 571.

(159) O'Connor, D. V.; Phillips, D. *Time-Correlated Single Photon Counting*; Academic Press: New York, 1984.

(160) Bagchi, B.; Oxtoby, D. W.; Flemming, G. R. *Chem. Phys.* **1984**, *86*, 257.

(161) van der Zwan, G.; Hynes, J. T. *J. Phys. Chem.* **1985**, *89*, 4181.

(162) Nandi, N.; Roy, S.; Bagchi, B. *J. Chem. Phys.* **1995**, *102*, 1390.

(163) Roy, S.; Bagchi, B. *J. Chem. Phys.* **1993**, *99*, 9938.

(164) Bagchi, B.; Chandra, A. *Adv. Chem. Phys.* **1991**, *80*, 1.

(165) Castner, E. W.; Fleming, G. R.; Bagchi, B.; Maroncelli, M. *J. Chem. Phys.* **1988**, *89*, 3519.

(166) Bushuk, B. A.; Rubinov, A. N. *Opt. Spectrosc.* **1997**, *82*, 530.

(167) Bagchi, B.; Biswas, R. *Acc. Chem. Res.* **1998**, *31*, 181.

(168) Castner, E. W., Jr.; Maroncelli, M.; Fleming, G. R. *J. Chem. Phys.* **1987**, *86*, 1090.

(169) Chapman, C. F.; Fee, R. S.; Maroncelli, M. *J. Phys. Chem.* **1995**, *99*, 4811.

(170) Chapman, C. F.; Fee, R. S.; Maroncelli, M. *J. Phys. Chem.* **1990**, *94*, 4929.

(171) Su, S. G.; Simon, J. D. *J. Phys. Chem.* **1987**, *91*, 2693.

(172) Kahlow, M. A.; Jarzeba, W.; Kang, T. J.; Barbara, P. F. *J. Chem. Phys.* **1989**, *90*, 151.

(173) Simon, J. D. *Acc. Chem. Res.* **1988**, *21*, 128.

(174) Su, S. G.; Simon, J. D. *J. Phys. Chem.* **1986**, *90*, 6475.

(175) Kometani, N.; Kajimoto, O.; Hara, K. *J. Phys. Chem. A.* **1997**, *101*, 4916.

(176) Molotsky, T.; Koifman, N.; Huppert, D. *J. Phys. Chem. A.* **2002**, *106*, 12185.

(177) Hara, K.; Kuwabara, H.; Kajimoto, O. *J. Phys. Chem. A.* **2001**, *105*, 7174.

(178) Bhattacharyya, K.; Bagchi, B. *J. Phys. Chem. A* **2000**, *104*, 10603.

(179) Bhattacharyya, K. *Acc. Chem. Res.* **2003**, *36*, 95.

(180) Sarkar, N.; Datta, A.; Das, S.; Bhattacharyya, K. *J. Phys. Chem.* **1996**, *100*, 15483.

(181) Pal, S. K.; Sukul, D.; Mandal, D.; Sen, S.; Bhattacharyya, K. *Chem. Phys. Lett.* **2000**, *327*, 91.

(182) Mandal, D.; Sen, S.; Bhattacharyya, K.; Tahara, T. *Chem. Phys. Lett.* **2002**, *359*, 77.

(183) Vajda, S.; Jimenez, R.; Rosenthal, S. J.; Fidler, V.; Fleming, G. R.; Castner, E. W. J. *J. Chem. Soc., Faraday Trans.* **1995**, *91*, 867.

(184) Sen, S.; Sukul, D.; Dutta, P.; Bhattacharyya, K. *J. Phys. Chem. A.* **2001**, *105*, 10635.

(185) Pant, D.; Levinger, N. E. *J. Phys. Chem. B.* **1999**, *103*, 7846.

(186) Sen, S.; Sukul, D.; Dutta, P.; Bhattacharyya, K. *J. Phys. Chem. B.* **2002**, *106*, 3763.

(187) Sen, S.; Dutta, P.; Sukul, D.; Bhattacharyya, K. *J. Phys. Chem. A.* **2002**, *106*, 6017.

(188) Pal, S. K.; Peon, J.; Zewail, A. H. *Proc. Natl. Acad. Sci., USA* **2002**, *99*, 1763.

(189) Pierce, D. W.; Boxer, S. G. *J. Phys. Chem.* **1992**, *95*, 5560.

(190) Brauns, E. B.; Madaras, M. L.; Coleman, R. S.; Murphy, C. J.; Berg, M. A. *Phys. Rev. Lett.* **2002**, *88*, 158101-1.

(191) Chapman, C. F.; Maroncelli, M. *J. Phys. Chem.* **1991**, *95*, 9095.

(192) Stevens, B. *Adv. Photochem.* **1971**, *8*, 161.

(193) Birks, J. B. *Rep. Prog. Phys.* **1975**, *38*, 903.

(194) *The Exciplex*; Gordon, M.; Ware, W. R., Eds.; Academic Press Inc.: New York, 1975.

(195) Forster, T.; Kasper, K. *Z. Phys. Chem. (Munich)* **1954**, *1*, 275.

(196) Hirayama, F. *J. Chem. Phys.* **1965**, *42*, 3163.

(197) Zachariasse, K. A.; Kuhnle, W.; Weller, A. *Chem. Phys. Lett.* **1978**, *59*, 375.

(198) Birks, J. B. In *"Photophysics of Aromatic Molecules"*; Wiley: New York, 1970.

(199) Hirayama, F. *J. Chem. Phys.* **1965**, *42*, 3163.

(200) Chandross, E. A.; Dempster, C. J. *J. Am. Chem. Soc.* **1970**, *92*, 3586.

(201) Todesco, R.; Gelan, J.; Martens, H.; Put, J.; De Schryver, F. C. *J. Am. Chem. Soc.* **1981**, *103*, 7304.

(202) Saigusa, H.; Lim, E. C. *Acc. Chem. Res.* **1996**, *29*, 171.

(203) Zachariasse, K. A.; Duveneck, G.; Busse, R. *J. Am. Chem. Soc.* **1984**, *106*, 1045.

(204) Van der Auweraer, M.; Gilbert, A.; De Schryver, F. C. *J. Am. Chem. Soc.* **1980**, *102*, 4008.

(205) Goldenberg, M.; Emert, J.; Morawetz, H. *J. Am. Chem. Soc.* **1978**, *100*, 7171.

(206) Zachariasse, K. A. *Trends. Photochem. Photobiol.* **1994**, *3*, 211.

(207) Snare, M. J.; Thistlethwaite, P. J.; Ghiggino, K. P. *J. Am. Chem. Soc.* **1983**, *105*, 3328.

(208) Nishizawa, S.; Kato, Y.; Teramac, N. *J. Am. Chem. Soc.* **1999**, *121*, 9463.

(209) Zachariasse, K. A.; Striker, G. *Chem. Phys. Lett.* **1988**, *145*, 251.

(210) Asai, S.; Nakamura, H.; Tanabe, M.; Sakamoto, K. *Ind. Eng. Chem. Res.* **1993**, *32*, 1438.

(211) Wang, M. L.; Ou, C. C. *Ind. Eng. Chem. Res.* **1994**, *33*, 2034.

(212) Uchiyama, Y.; Tsuyumoto, I.; Kitamori, T.; Sawada, T. *J. Phys. Chem. B.* **1999**, *103*, 4663.

(213) Saroja, G.; Samanta, A. *Chem. Phys. Lett.* **1995**, *246*, 506.

(214) Saroja, G.; Samanta, A. *J. Chem. Soc., Faraday Trans.* **1996**, *92*, 2697.

(215) Saroja, G.; Ramachandram, B.; Saha, S.; Samanta, A. *J. Phys. Chem. B.* **1999**, *103*, 2906.

(216) Ramachandram, B.; Samanta, A. *J. Chem. Soc., Chem. Commun.* **1997**, 1037.

(217) Saroja, G.; Soujanya, T.; Ramachandram, B.; Samanta, A. *J. Fluores.* **1998**, *8*, 405.

(218) Wasserscheid, P.; Gordon, C. M.; Hilgers, C.; Muldoon, M. J.; Dunkin, I. R. *Chem. Commun.* **2001**, 1186.

(219) Grodkowski, J.; Neta, P. *J. Phys. Chem. B.* **2002**, *106*, 11130.

(220) Aki, S. N. V. K.; Brennecke, J. F.; Samanta, A. *Chem. Commun.* **2001**, 413.

(221) Muldoon, M. J.; Gordon, C. M.; Dunkin, I. R. *J. Chem. Soc., Perkin Trans. 2* **2001**, *2001*, 433.

(222) Ozawa, R.; Hamaguchi, H. *Chem. Lett.* **2001**, 736.

(223) Gordon, C. M.; Mclean, A. J. *Chem. Commun.* **2000**, *15*, 1395.

(224) Muldoon, M. J.; Mclean, A. J.; Gordon, C. M.; Dunkin, I. R. *Chem. Commun.* **2001**, 2364.

Chapter 2

Experimental methodologies

The present chapter provides the details of the experimental procedures followed in different parts of this thesis. This includes the methods of the preparation of the various ionic liquids and the purification of various chemicals including some conventional solvents. Picosecond and nanosecond time-resolved single photon counting setup and laser system are described in details along with the data analysis technique and method of extracting time-resolved emission spectra (TRES) from a series of time-resolved decays. The methodologies adopted for the theoretical calculations to obtain the optimized geometry and ground state dipole moment of some molecules are also discussed in brief.

2.1. Experimental

2.1.1. Materials and purification

AP was obtained from TCI and recrystallized twice from ethanol in the presence of activated charcoal. The purity of the yellow crystalline sample was confirmed by TLC using 50% ethylacetate:hexane mixture as an eluant. ANP, purchased from Aldrich, was recrystallized twice from absolute ethanol before performing spectroscopic measurements. APDEA, ANPDEA, NBDEA, NP, MNP and NPDEA were received from Dr. B. Ramachandram and the column-purified

compounds were further recrystallized from ethanol if necessary. The detailed procedure of the synthesis of these compounds has been described elsewhere.[1]

C153 (laser grade) from Eastman Kodak, PRODAN and py(3)py from Molecular Probes were used as obtained. Pyrene and DMABN, obtained from Aldrich, were recrystallized twice from ethanol before the experiment.

Five different phase transfer catalysts, namely tetrabutylammoniumbromide (TBAB), tetrabutylammoniumchloride (TBAC), tetraoctylammoniumbromide (TOAB), tetrabutylammoniumiodide (TBAI), tetrabutylammoniumperchlorate (TBAP), were procured from Aldrich and used without any purification.

Silica gel and neutral alumina for column chromatography were obtained from Acme Scientific Chemicals, India. The various drying agents, CaH_2, $MgSO_4$, KOH, NaOH, P_2O_5, CaO and Mg turnings used at different stages of the purification procedure were purchased from locally available firms.

1-methylimidazole (99%), sodium tetrafluoroborate ($NaBF_4$) (97%), sodium trifluoroacetate (CF_3COONa) (98%) and hexafluorophosphoric acid (HPF_6) (65% solution in water) required for the synthesis of the RTILs were procured from Lancaster, whereas the lithium salt of bistrifluoromethanesulfonimide (puriss) was obtained from Fluka. 1-chlorobutane (HPLC grade), 1,1,1-trichloroethane (99%) were obtained from Aldrich. Bromoethane (extra pure) was purchased from locally available grade. Both 1-chlorobutane and bromoethane were distilled from P_2O_5 and 1-methylimidazole was vacuum distilled from KOH prior to synthesis.

The deuteriated solvents, $CDCl_3$ (Isotec, Inc), methanol-d_4 (Acros Organic) and D_2O (Merck, India) used for NMR analysis were used as received.

2.1.2. Synthesis and purification of ionic liquids

All the desired butyl salts were prepared from their chloro analogue, [BMIM]Cl, whereas the ethyl salts from the corresponding bromide salt, [EMIM]Br in dry nitrogen atmosphere. The synthetic procedure adopted for the preparation of different room temperature ionic liquids is illustrated schematically in Fig. 2.1. The halide salts used for the reactions were prepared by methods described elsewhere[2,3] and were washed several times with hot dry ethylacetate until the washing was free from unreacted 1-methylimidazole. This was ensured by the absence of strong absorption peak at around 275 nm in the UV-absorption spectrum in ethylacetate washing.

The halides were then recrystallized from ethylacetate:acetonitrile mixture before proceeding to the next reaction step. The final desired products were washed with conductivity water for hydrophobic ionic liquids like [BMIM][PF_6] to ensure complete removal of the parent halide as well as the acids present with it. For other water insoluble and partly soluble ionic liquids, the crude final products were dissolved in dichloromethane (DCM) and the organic layer was washed several times with conductivity water until they were found free from the halide impurity. This was ensured by the absence of any precipitation of silver halide when either the ionic liquids or the water washings were treated with aqueous $AgNO_3$ solution. On the other hand, water-soluble ionic liquids like, [EMIM][BF_4] and [EMIM][CF_3COO] were dissolved in large excess of DCM and

passed through a medium-sized dry silica gel packed column and neutral alumina column successively to remove the halide and other impurities. This procedure works quite satisfactorily for tetrafluoroborate salts but found not so effective for the most hygroscopic trifluoroacetate ionic liquid, [EMIM][CF_3COO]. Specially, the poor partition coefficient of this particular salt between DCM and water makes it really difficult to separate fully from its parent halide.

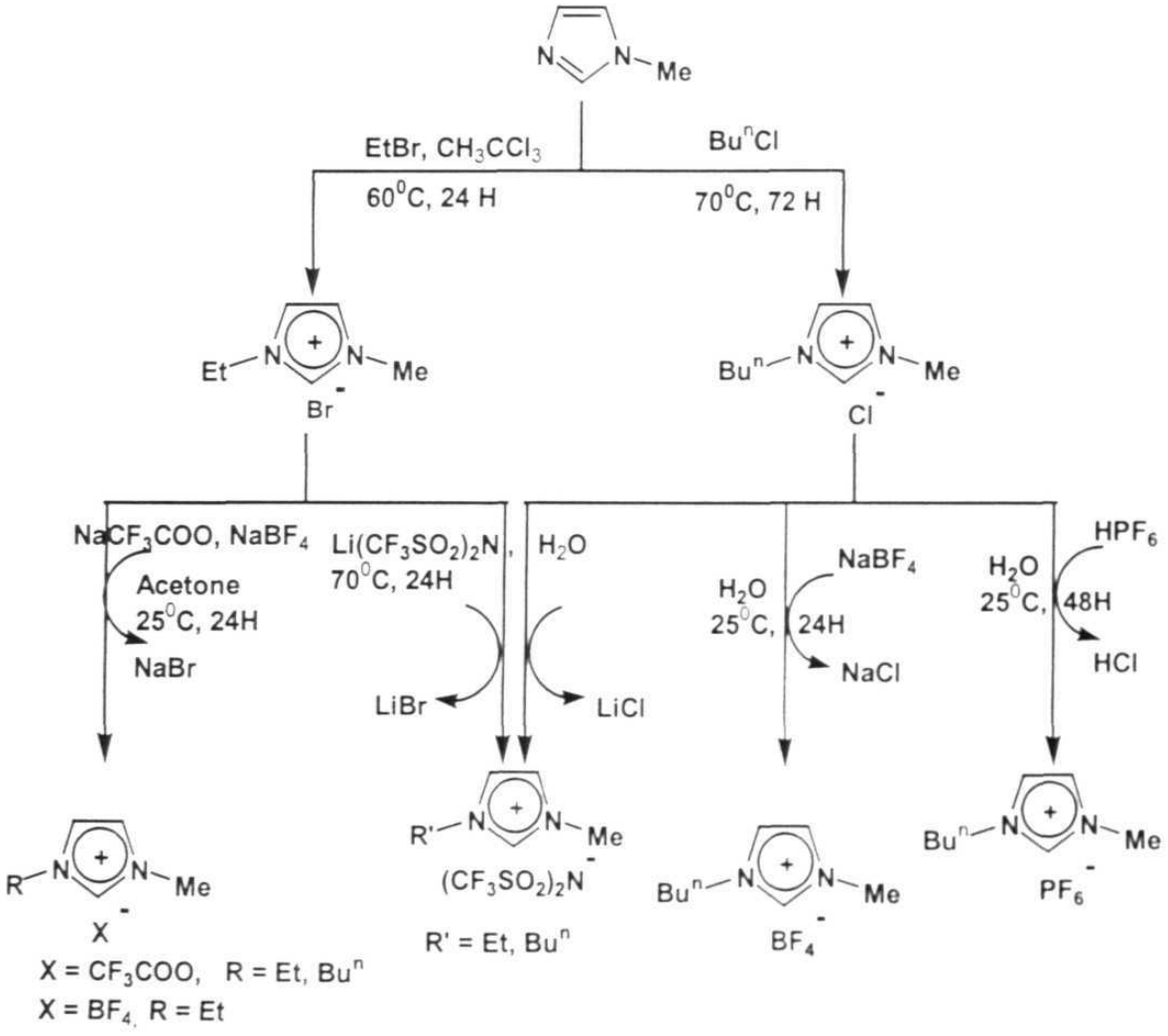

Fig. 2.1. *A schematic diagram for synthesis of different ionic liquids*

To obtain the spectroscopic purity, all the ionic liquids were further diluted with DCM or acetonitrile and then treated with activated charcoal for at least 48 hours and filtered a couple of times by passing through a medium size silica gel packed column. The liquids were then transferred in clean and dry reagent bottles and kept under vacuum (Hindhivac, Model: ED-3, with maximum partial pressure 1×10^{-3} mbar) for 7–10 hours at 50-60 °C temperature. This completely removed the previously used organic solvent and maximum amount of water from it. These liquids were then stored in a desiccator under dry nitrogen. The purity of the liquid salts was assessed successively by IR, NMR and UV measurements and comparing the data with the standard data on the samples.[2-5]

2.1.2.1. 1-butyl-3-methylimidazolium chloride, [BMIM]Cl

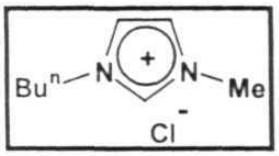

[BMIM]Cl was prepared from 1-methylimidazole (distilled from KOH in high vacuum) with two-fold excess of 1-chlorobutane (freshly distilled from P_2O_5) in dry nitrogen atmosphere by refluxing the mixture at 70 °C for minimum 72 hours.[2] The highly viscous oily salt so obtained was cooled and purified according to the procedure described above.

2.1.2.2. 1-ethyl-3-methylimidazolium bromide, [EMIM]Br

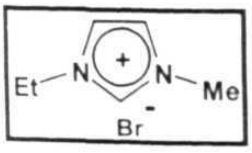

Freshly distilled bromoethane, (3 mol) was added drop wise over 1 hour under constant stirring to a solution of 1-methylimidazole (1 mol) in 160 ml of 1,1,1-trichloroethane. The turbid reaction mixture was refluxed in nitrogen atmosphere at 70 °C for 24

hours. Heating was extended for longer time than that recommended (2 hours) by Bonhote and coworkers,[3] to reduce the amount of unreacted 1-methylimidazole in the halide salt. The halide salt was obtained as white solid after cooling the reaction mixture in ice bath. It was then separated from the mother liquor and treated with hot ethylacetate–acetonitrile mixture for further purification.

2.1.2.3. 1-butyl-3-methylimidazolium tetrafluoroborate, [BMIM][BF$_4$]

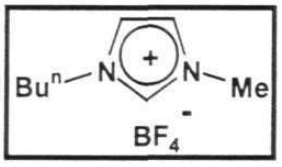

[BMIM][BF_4] was prepared by the metathesis of 1-butyl-3-methylimidazolium chloride [BMIM]Cl (1 mol) with $NaBF_4$ (1 mol) in water at room temperature.[4] The minimum volume of water was used to dissolve both salts before mixing. The mixture was stirred for 24 hours for the completion of the reaction. The liquid salt was then cooled and preferentially extracted with excess DCM at low temperature (0-5 ^{0}C). The organic layer was then washed twice with ice-cold water to remove trace quantity of parent halide that may come in the previous extraction. The crude tetrafluoroborate salt was obtained by evaporating the DCM layer in vacuum.

2.1.2.4. 1-ethyl-3-methylimidazolium tetrafluoroborate, [EMIM][BF$_4$]

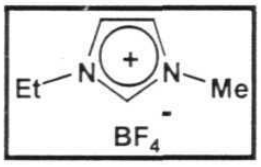

[EMIM][BF_4] was prepared by the metathesis of 1-ethyl-3-methylimidazolium bromide, [EMIM]Br (1 mol) with $NaBF_4$ (1 mol) in acetone at room temperature. This method is actually similar to the procedure adopted for the preparation of [BMIM][BF_4] by Suarez et al.[5] It is to be noted here that we have avoided preparing [EMIM][BF_4] using

conventional silver method[4] as we found that even trace quantity of silver was enough to destroy the fluorescence probe molecules within a short time.

2.1.2.5. 1-butyl-3-methylimidazolium trifluoroacetate, [BMIM][CF_3COO]

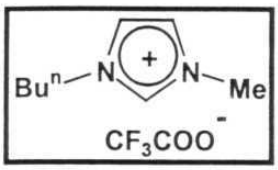

18.3 g (105 mmol) [BMIM]Cl was first dissolved in 100 ml acetone and 14.3 g (105 mmol) CF_3COONa was slowly mixed to it. The mixture was stirred for 72 hours at room temperature in nitrogen atmosphere. The liquid layer was collected after filtering out solid NaCl and concentrated to get crude [BMIM][CF_3COO].

2.1.2.6. 1-ethyl-3-methylimidazolium trifluoroacetate, [EMIM][CF_3COO]

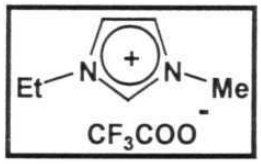

The procedure adopted for the preparation of this salt was similar to that used for [BMIM][CF_3COO]. The liquid salt was prepared from 40.6 g (213 mmol) [EMIM]Br and 29 g (213 mmol) CF_3COONa in 150 ml acetone at room temperature.

2.1.2.7. 1-butyl-3-methylimidazolium hexafluorophospate, [BMIM][PF_6]

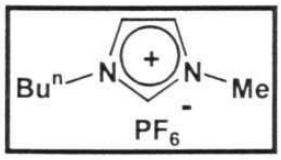

77 ml (343 mmol) of ice cooled HPF_6 (65% solution in water) was added drop wise (over ~ 45 minutes) to a dilute solution of [BMIM]Cl (50 g, 286 mmol) in 250 ml of cold water with constant stirring. This slow addition prevented rise of the temperature of the system. The reaction mixture was stirred for 24 hours at room temperature and after decanting the upper acidic layer, the lower viscous ionic liquid portion was washed with excess water until it was free from acid.[6]

2.1.2.8. 1-butyl-3-methyl imidazoliumbis(trifluoromethanesulphonyl) imide, [BMIM][$(CF_3SO_2)_2N$]

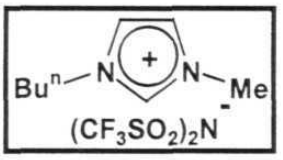

For the preparation of [BMIM][$(CF_3SO_2)_2N$], 20.20 g (116 mmol) of [BMIM]Cl was mixed with 33.22 g (116 mmol) of $Li(CF_3SO_2)_2N$ in 150 ml of water and the mixture was refluxed at 70 °C for at least 15 hours. The water insoluble [BMIM][$(CF_3SO_2)_2N$] so obtained was extracted by DCM.[3]

2.1.2.9. 1-ethyl-3-methyl imidazolium bis(trifluoromethanesulphonyl) imide, [EMIM][$(CF_3SO_2)_2N$]

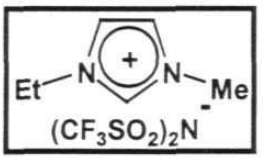

13.53 g (70 mmol) of [EMIM]Br and 20.35 g (70 mmol) of $Li(CF_3SO_2)_2N$ were mixed in 100 ml of water taken in 500 ml round-bottomed flask attached with a water condenser and the mixture ware refluxed at 60-70 °C in an oil bath for 15 hours. The hydrophobic $(CF_3SO_2)_2N$ salt forms a bi-phasic mixture with water.[3]

2.1.3. Purification of conventional solvents

All the solvents used for spectroscopic measurements were rigorously purified by following standard literature procedures.[7] The extent of dryness of each solvent was checked by measuring the $E_T(30)$ value of the solvent and comparing this value with the literature value. The $E_T(30)$ scale of solvent polarity was proposed by Dimorth and Reichardt.[8,9] The $E_T(30)$ value of a solvent is the

energy (in kcal/mol) corresponding to the lowest energy absorption maximum (at 25 ^{0}C and 1 atm pressure) of the betaine dye, shown in Fig. 2.2, in that solvent. This suggests that the $E_T(30)$ value is related to the wavelength of lowest energy absorption maximum of the dye as,[9]

$$E_T(30)\ (\text{kcal/mol}) = 28591/\ \lambda_{max}\ (\text{nm}) \qquad (2.1)$$

where, λ_{max} is the wavelength of the longest absorption maximum in nanometer. The calculated $E_T(30)$ value from the absorption spectrum was then compared with the literature value of the respective solvent.[9] The betaine dye was received as a generous gift from Prof. C. Reichardt of Philips University and used without further purification. All the dried solvents were found to be optically transparent in the wavelength range (250 nm – 700 nm) of our interest.

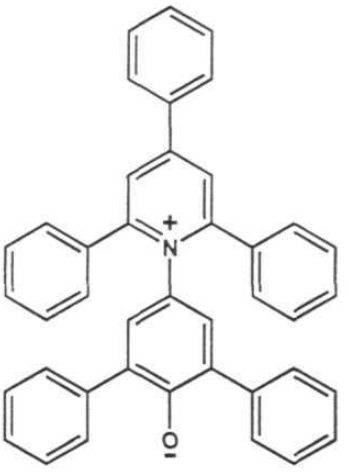

Fig. 2.2

Acetonitrile (AN): Maximum water was eliminated by adding coarse blue silica gel in the solvent with occasional shaking in nitrogen atmosphere for at least 3 hours. Finally the solvent was fractionally distilled out over dry CaH_2.

Ethanol (EtOH): Absolute (99.5%) ethanol was prepared by refluxing with freshly ignited CaO (250 g/l.) for at least 6 hours, standing overnight and distilled cautiously to exclude moisture. For further dehydration of absolute ethanol magnesium ethoxide was used. This was prepared by 5 g of clean dry magnesium turnings and 0.5 g of iodine in a round-bottomed flask, followed by 50-75 ml of

absolute ethanol, and warming the mixture until a vigorous reaction occurs. The heating was continued until all the magnesium was converted to the ethoxide, after that the remaining alcohol was added slowly and refluxed for an hour and distilled to collect the final dry ethanol.

Hexane, cyclohexane, toluene, 1,4-dioxane: Dried by refluxing with metallic sodium and benzophenone until the solution became deep blue due to formation of disodium benzophenone complex during reflux and its persistence on cooling. Finally the dry solvent was fractionally distilled and collected in a dry reagent bottle, sealed immediately with parafilm and kept in desiccator.

Water: Deionized water, collected from an ion exchange resin column, was first treated with sodium hydroxide and little potassium permanganate and distilled to get conductivity water. The same was freshly distilled once again to get the water used for the study.

2.1.4. Sample preparation for spectral measurements

In conventional solvents, dilute solutions of the probe molecules were used for both absorption and fluorescence measurements. The optical densities of the solutions employed for all measurements were maintained between 0.1 and 0.2 at the longest wavelength absorption maxima. This corresponded to a probe concentration between 20 to 80 μM. In the case of experiment involving py(3)py, the concentration was maintained at 20 μM. A measured amount of solid tetraalkylammonium salts was added directly to a 2.5 ml solution of the sample

solution taken in a cuvette for studying the salt effect. The samples were deoxygenated by bubbling a stream of dry nitrogen gas directly into the cuvette for 15–20 minutes especially before performing the time-resolved studies.

The sample preparation in ionic liquids was not so straightforward. Each time before performing any experiment the required ionic liquids were kept in high vacuum at 50-60 ^{0}C for at least 5 hours to remove any moisture trapped in these media. Such treated liquids were slowly allowed to cool down to room temperature under vacuum prior to the addition of the probe molecule. 2.5 ml of ionic liquid at room temperature was used to prepare the sample solution in each case and the quartz cuvette was sealed immediately with septum and parafilm. Precaution was taken in every step to avoid water contamination from atmosphere. The sample cuvette was kept in sealed condition at least for 24 hours with occasional shaking to overcome the slow solubility of the probe in ionic liquids. Each sample was then deoxygenated by bubbling dry nitrogen gas for a period of minimum 30 minutes prior to any experimental measurement. The sealed sample solutions were found to be stable for months under dark condition.

2.2. Instrumentation

The NMR and IR spectra of the liquid samples were recorded on Bruker ACF-200 NMR Spectrometer and Fourier transform Infrared Spectrometer (Shimadzu, Model no. FTIR-8300) respectively. The absorption spectra were recorded on UV-Vis-NIR scanning spectrophotometer (Shimadzu, Model no. UV-3101PC). The steady state fluorescence spectra at room temperature were recorded either on Jasco FP-777 (for the study involving the phase transfer

catalysts) or SPEX FluoroMax–3 spectrofluorometer. The fluorescence spectra were corrected for the instrumental response.

2.2.1. Picosecond time correlated single photon counting setup

The picosecond time-resolved fluorescence measurements were performed using a picosecond laser as the excitation source, a microchannel plate (MCP) photomultiplier tube as detector and a single photon counting setup.[10,11] A diode-pumped Millennia (5 W) CW laser (Spectra Physics) output at 532 nm was used to pump the Titanium–Sapphire rod in Tsunnami picosecond mode-locked laser system (Spectra Physics, Model no. 4960 M3S). The Titanium–Sapphire rod was oriented at Brewster's angle to the laser beam. The wavelength tuning range afforded by this laser system was 720-850 nm. The pulse repetition rate was 82 MHz and the full width at half maxima (FWHM) was less than 2 ps. Scanning auto correlator (AC, Model 409-08, Spectra Physics) was used to monitor the shape and pulse-width of the pulse from Tsunnami. The pulse was displayed on an oscilloscope for real time viewing. The laser pulse was next focussed onto the pulse picker (Model 3980, Spectra Physics), which selected the pulse from 82 MHz train at a maximum pulse selection rate of 4 MHz. The output from the pulse picker was frequency-doubled using a flexible harmonic generator (FHG–23, Spectra Physics). The frequency-doubled 375 nm output was used to excite the sample.

IBH 5000U fluorescence spectrophotometer was used for picosecond excitation and detection system attached with MCP photomultiplier tube (160 – 850 nm), NIM timing electronics and MCA utility software (Fig. 2.3). The

emission monochromator (MC) was in Seya–Namioka configuration with 10 cm focal length and f/3 aperture. The wavelength selection in the monochromator was achieved automatically via the personal computer. The emission was detected at right angle to the excitation beam using a Hamamatsu 323P MCP photomultiplier. The emission was collected at magic angle polarization (54.7°) to avoid bias due to polarization effect for all viewing angles. The instrument response time was ~ 50 ps.

A part of the incident picosecond pulse train selected from a quartz plate via a neutral density filter (NDF) was focused on a photodiode (PD). The PD signal was fed into a constant fraction discriminator (CFD, ORTEC) to discriminate the background noise and to generate the precise timing pulse. The output of the CFD *normally* serves as the START pulse of the time-to-amplitude converter (TAC). However, the experiment was carried out in "reverse" mode in order to minimize the data collection time. The photodiode signal was used as STOP signal for the TAC. Detection of the first emitted photon by the MCP photomultiplier generated a pulse, which was fed into the CFD. This served as a START signal (in the "reverse" mode) for the TAC. The MCP output was directly read on a rate meter. The time difference between the START and STOP pulse was due to the time taken by the pulses to travel through the cables/electronics and for the excited state to relax and emit a photon. The TAC converts this time difference to a voltage, which was then fed into the computer via a MCP card (using Data station software by Oxford Corporation, UK). Repetitive laser pulsing and emitted photon collection produce a histogram of counts versus time channel. This provided the time profile of the fluorescence

signal. The fluorescence decay of the sample was further analyzed using IBH data analysis software for windows (version 6.1.36).

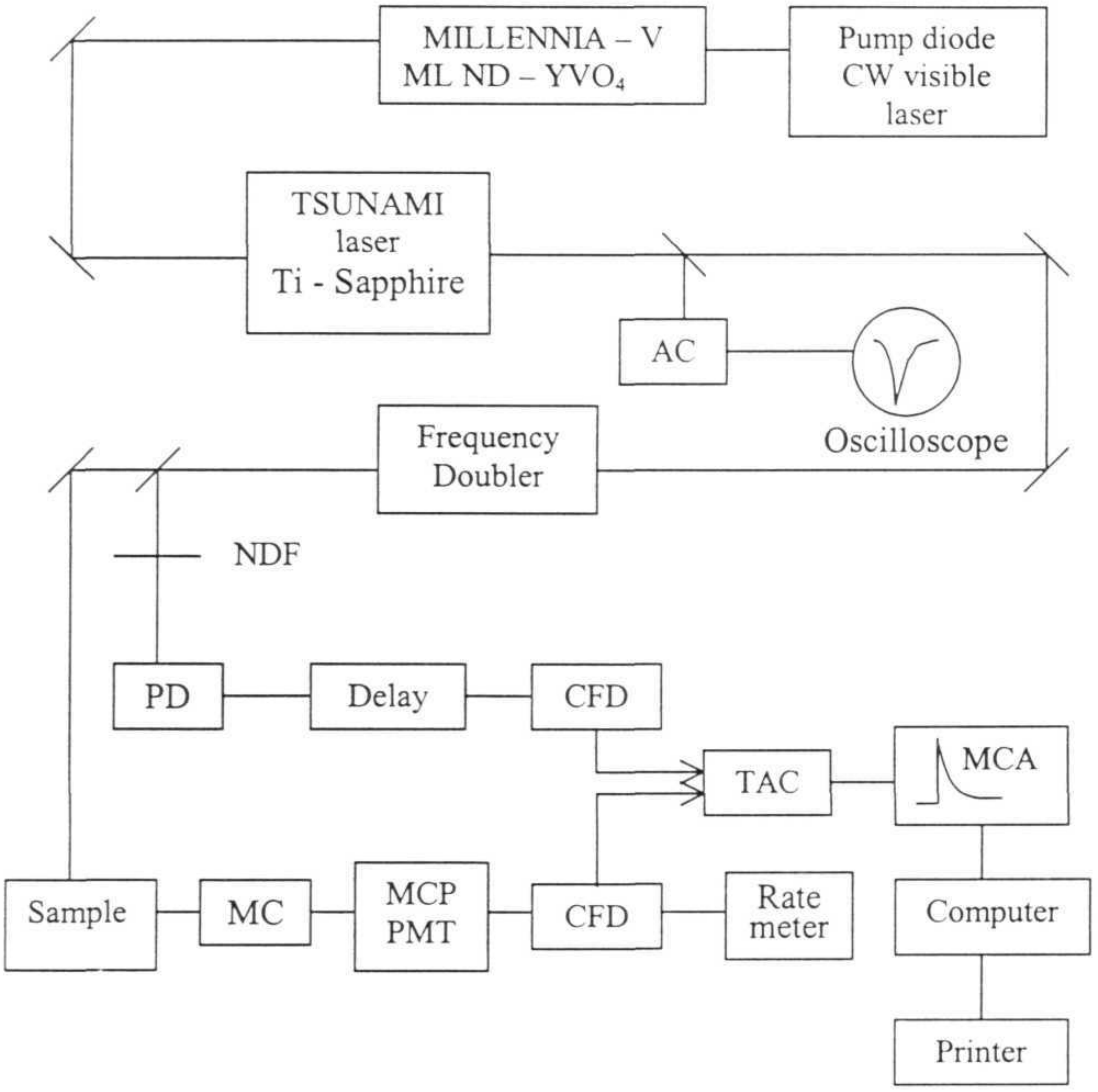

Fig. 2.3. ***Block diagram of picosecond single photon counting setup***

2.2.2. Nanosecond time correlated single photon counting setup

This system consisted of IBH 5000 single photon counting spectrophotometer, along with PMT (Hamamatsu 3235) with a spectral range of 190-650 nm. The instrument was operated with a thyratron-gated flash lamp filled with hydrogen at a pressure of 0.5 atm. The lamp frequency was tuned to 40 kHz and the pulse-width of the lamp under the operating condition was ~ 1.4 ns. Unlike the previous setup, here the output of CFD served as the START pulse for TAC (Tennelec, Model TC 863) and the fluorescence photon recorded by the emission photomultiplier, as determined by CFD (ORTEC, Model 584), generated a pulse that served as the STOP signal for TAC. The same software provided by IBH was used here also for further analysis of data. The instrumental response was measured using very dilute solution of Ludox in a quartz cuvette, served as a scattering solution.

2.2.3. Data analysis

The lifetimes were estimated from the measured fluorescence decay curves and the instrumental profiles using a nonlinear least-squares iterative fitting procedure (IBH Decay analysis software, version 6.1.36). This program uses a reconvolution method for the analysis of the experimental data.[12] When the decay time is long compared to the decay time of the excitation pulse, the excitation may be described as a δ-function. However, when the lifetime is short, distortion of the experimental data occurs by the finite decay time of the instrumental pulse and response time of the photomultiplier and associated electronics. Since the measured decay function is convolution of the true

fluorescence decay and the instrumental pulse, it is necessary to deconvolute the measured data from the later in order to get the actual fluorescence lifetime. The mathematical expression of this procedure is given by the equation,

$$D(t) = \int_0^t P(t')G(t-t')dt' \qquad (2.2)$$

where, D(t) is the fluorescence intensity at any time t. P(t′) is the intensity of the exciting light at time t′. G(t-t′) is the response function of the experimental system. The experimental data D(t) and P(t′) from the MCA are fed into a personal computer to determine the lifetime. The deconvolution has been achieved by mixing the instrumental profile and a projected decay to form a new reconvoluted set. The data is compared with the experimental set and the difference between the data points summed that produced χ^2 function for fitting. The deconvolution proceeds through a series of such iteration until an insignificant change of χ^2 occurs between two successive iterations. The goodness of the fit was evaluated from the reduced χ^2 values and the plot of the weighted residuals.

2.3. Method for calculating TRES

The time-resolved emission spectra (TRES) were constructed indirectly by measuring a series of fluorescence decay profiles at every 10 nm wavelength intervals across the entire steady state emission spectrum of the probe molecule in a particular solvent. Each intensity decay curve was then fitted to a triexponential decay function to obtain a χ^2 value between 1 and 1.2. This procedure

deconvoluted the measured decay from its instrumental response and increased the effective time-resolution of the experiments to ~25 ps. The impulse response function I (λ, t) was calculated from those best-fitted curve. To make the time-integrated intensity at each wavelength equal to the steady state intensity at that wavelength, a set of H (λ) values were calculated using,

$$H(\lambda) = \frac{I_{ss}(\lambda)}{\sum_i \alpha_i(\lambda)\tau_i(\lambda)} \qquad (2.3)$$

where I_{ss} (λ) is the steady state intensity , α_i (λ) is the preexponential coefficient and τ_i (λ) is the decay time at that wavelength with $\sum \alpha_i$ (λ) = 1. The time-resolved emission spectra at different time were calculated from the appropriately normalized intensity decay function I′ (λ, t) for different wavelength at different time, where I′ (λ, t) = H (λ) × I (λ, t). The emission maximum at each time $\bar{\nu}$ (t) was obtained by fitting the spectra to lognormal line shape function known for its better representation of the emission spectrum in polar solvents. The lognormal function[13,14] can be expressed as,

$$\begin{aligned} F(\bar{\nu},t) &= h\exp\left\{-\ln(2)[\ln(1+\alpha)/\gamma]^2\right\}, \quad for \quad \alpha > -1 \\ &= 0, \qquad\qquad\qquad\qquad\quad for \quad \alpha \le -1 \end{aligned} \qquad (2.4)$$

where, $\alpha \equiv \frac{2\gamma\,[\bar{\nu} - \bar{\nu}_p]}{\Delta}$, h is the peak height, $\bar{\nu}_p$ is the peak frequency, γ is the asymmetry parameter and Δ is the width of the curve. While fitting our spectral data all the above four parameters were allowed to vary freely and a nonlinear

least square fitting was used to extract the best-fitted curve until successive iterations gave the identical χ^2 value.

Apart from using $\bar{\nu}_p$, obtained directly from the lognormal fits, several authors have been used the average frequency (first moment) of the spectrum, the average of the half-height points or the high-frequency half-height points.[14-18] The solvation dynamics described by the normalized Stokes shift correlation function C(t) defined as,[19,20]

$$C(t) = \frac{\bar{\nu}(t) - \bar{\nu}(\infty)}{\bar{\nu}(0) - \bar{\nu}(\infty)} \qquad (2.5)$$

was calculated using the peak frequency of the time-resolved emission spectra, where, $\bar{\nu}(0)$, $\bar{\nu}(t)$ and $\bar{\nu}(\infty)$ are the peak frequencies instantly after excitation, at an intermediate time (t) and at infinite time after excitation (when the spectrum does not show any time dependent Stokes shift) respectively. The method of determination of $\bar{\nu}(0)$ from the time-resolved data is dependent on the finite time-resolution of the instrumental setup.[21-23] Hence, the initial response of the solvent that occurs within the first ~25 ps (time-resolution of the picosecond single photon count setup, after deconvolution of the fitted decay curves) would not be included in the so obtained C(t) function. The procedure developed by Fee and Maroncelli[21] to estimate the fast initial solvation time beyond the time-resolution of the pico-second setup has not been followed in our calculation for technical difficulties.

In all the cases, the obtained C(t) functions can be fitted well with a simple biexponential decay function, $C(t) = a_1 \exp^{-t/\tau 1} + a_2 \exp^{-t/\tau 2}$ where τ_1 and τ_2 are the

two relaxation times having amplitudes of a_1 and a_2 respectively. Research groups of Barbara and Huppert have used a stretched factor β in order to improve their biexponential fitting parameters.[24-27] However, in our case, no significant improvement to the quality of the fit has been noticed by varying the β value from 0.4 to 0.9. As the time dependence of C(t) consists of more than one components, the relaxation time is generally expressed as an average. The average relaxation time, $\langle\tau\rangle$ is defined as, $\langle\tau\rangle = a_1\tau_1 + a_2\tau_2$, where a_1, a_2 are the corresponding amplitudes of the relaxation time, τ_1, τ_2 respectively and $(a_1 + a_2) = 1$.

2.4. Estimation of polarity in E_T(30) and E_T^N Scale

The wavenumber corresponding to the fluorescence maximum, $\bar{\nu}_{max}^{flu}$, of each probe molecule in various conventional solvents was experimentally measured from its steady state emission spectra at room temperature. The values were then plotted against known E_T(30) values of the solvent[9] to obtain the linear relationship between the two quantities. Using this relationship and the measured $\bar{\nu}_{max}^{flu}$ value of the probe in RTIL, the E_T(30) value of the RTIL was estimated.

The normalized microscopic solvent polarity parameter, E_T^N value of each RTIL was calculated from the following relation, using the estimated E_T(30) value of RTIL and the same of tetramethylsilane (TMS) and water as a reference solvent.[9]

$$E_T^N = [E_T(\text{RTIL}) - E_T(\text{TMS})] / [E_T(\text{water}) - E_T(\text{TMS})] \qquad (2.6)$$

2.5. Standard error limits

The estimated error limits in different measurements are:

λ_{max} (fluo/abs)	± 1 nm
τ (higher than 1ns)	± 5 %
τ (lower than 1ns)	± 15 - 20 %
Binding constants	± 10 %
Polarity of ionic liquids in $E_T(30)$ scale	± 10 %
Relaxation time	± 10 %

2.6. Theoretical calculation

The molecular structure of different fluorophores in gas phase and their dipole moments were calculated using quantum mechanical calculation based on semiemperical AM1 (Austin Model 1) method.[28,29] The calculations were performed in a personal computer using Hyper Chem package (Release 5.0) for Windows obtained from Hypercube, Inc. The unrestricted geometry optimization of the molecular structure was done by AM1 method in view of its superiority over other semiemperical methods.[28-30] This was achieved using conjugate gradient (Polak-Ribiere) type of algorithm with root-mean-square (rms) gradient as the convergence criterion. The rms gradient was kept below 0.001 kcal/(Åmol) in all the cases. The ground state dipole moments were calculated from single point calculation on the optimized geometry.

2.7. References

(1) Ramachandram, B., Ph. D. Thesis, University of Hyderabad, Hyderabad, India, **1999**.

(2) Hasan, M.; Kozhevnikov, I. V.; Siddiqui, M. R. H.; Steiner, A.; Winterton, N. *Inorg. Chem.* **1999**, *38*, 5637.

(3) Bonhote, P.; Dias, A. P.; Papageorgiou, N.; Kalyanasundaram, K.; Gratzel, M. *Inorg. Chem.* **1996**, *35*, 1168.

(4) Holbrey, J. D.; Seddon, K. R. *J. Chem. Soc., Dalton Trans.* **1999**, 2133.

(5) Suarez, P. A. Z.; Dullius, J. E. L.; Einloft, S.; De Souza, R. F.; Dupont, J. *Polyhedron* **1996**, *15*, 1217.

(6) Huddleston, J. G.; Willauer, H. D.; Swatloski, R. P.; Visser, A. E.; Rogers, R. D. *Chem. Commun.* **1998**, 1765.

(7) Perrin, D. D.; Armarego, W. L. F.; Perrin, D. R. *Purification of Laboratory Chemicals*; II ed.; Pergamon Press: New York, 1980.

(8) Dimroth, K.; Reichardt, C. *Fortschr. Orgn. Forsch.* **1968**, *11*, 1.

(9) Reichardt, C. *Solvents and Solvent Effects in Organic Chemistry*; VCH: Weinheim, 1988.

(10) O'Connor, D. V.; Phillips, D. *Time-Correlated Single Photon Counting*; Academic Press: London, 1984.

(11) Lakowicz, J. R. *Principles of Fluorescence Spectroscopy*; Second ed.; Kluwer Academic/Plenum Publishers: New York, 1999.

(12) Bevington, P. R. *Data Reduction and Error Analysis for the Physical Sciences*; McGraw-Hill: New York, 1969.

(13) Fraser, R. D. B.; Suzuki, E. In *Spectral Analysis*; Blackburn, J. A., Ed.; Marcel Dekker: New York, 1970.

(14) Horng, M. L.; Gardecki, J. A.; Papazyan, A.; Maroncelli, M. *J. Phys. Chem.* **1995**, *99*, 17311.

(15) Maroncelli, M.; Fleming, G. R. *J. Chem. Phys.* **1988**, *89*, 875.

(16) Maroncelli, M.; Fleming, G. R. *J. Chem. Phys.* **1988**, *89*, 5044.

(17) Maroncelli, M.; Fleming, G. R. *J. Chem. Phys.* **1990**, *92*, 3251.

(18) Siano, D. B.; Metzler, D. E. *J. Chem. Phys.* **1969**, *51*, 1856.

(19) Bagchi, B.; Oxtoby, D. W.; Flemming, G. R. *Chem. Phys.* **1984**, *86*, 257.

(20) van der Zwan, G.; Hynes, J. T. *J. Phys. Chem.* **1985**, *89*, 4181.

(21) Fee, R.; Maroncelli, M. *Chem. Phys.* **1994**, *183*, 235.

(22) Chapman, C. F.; Fee, R. S.; Maroncelli, M. *J. Phys. Chem.* **1995**, *99*, 4811.

(23) Fee, R. S.; Milsom, J. A.; Maroncelli, M. *J. Phys. Chem.* **1991**, *95*, 5170.

(24) Bart, E.; Meltsin, A.; Huppert, D. *J. Phys. Chem.* **1994**, *98*, 3295.

(25) Bart, E.; Meltsin, A.; Huppert, D. *J. Phys. Chem.* **1995**, *99*, 9253.

(26) Bart, E.; Meltsin, A.; Huppert, D. *Chem. Phys. Lett.* **1992**, *200*, 592.

(27) Bart, E.; Meltsin, A.; Huppert, D. *J. Phys. Chem.* **1994**, *98*, 10819.

(28) Dewar, M. J. S.; Zoebisch, E. G.; Healy, E. F.; Stewart, J. J. P. *J. Am. Chem. Soc.* **1985**, *107*, 3902.

(29) Dewar, M. J. S.; Dieter, K. M. *J. Am. Chem. Soc.* **1986**, *108*, 8075.

(30) Dewar, M. J. S.; Thiel, W. *J. Am. Chem. Soc.* **1977**, *99*, 4899.

Chapter 3

Influence of phase transfer catalysts on the photophysical properties of electron donor-acceptor molecules

The steady state and time-resolved fluorescence behavior of several electron donor acceptor (EDA) molecules in nonpolar media containing tetraalkylammonium salts, which are used extensively in chemical applications as phase transfer catalysts (PTCs),[1-10] are described in this chapter.

3.1. Introduction

Tetraalkylammonium halides with one or two large alkyl groups, such as cetyltrimethyl ammonium bromide (CTAB), are known as good surfactants. These substances when added to a two-phase aqueous-organic system normally produce micelles in aqueous medium.[11-13] On the other hand, small quaternary salts (e.g. tetrabutylammonium halides) or large ones (e.g. tetraoctylammonium halides) with all four identical alkyl groups are poor surfactants, but good phase transfer catalysts. These salts are used to bring closer two otherwise insoluble reactants in proper concentration to get a faster reaction rate. In a binary two-phase solution, a good phase transfer catalyst circulates between the two phases across the interface instead of staying in a single phase like micelles. These PTCs are generally less stable in aqueous medium. In nonpolar media, these are highly

soluble and known to exist as ion pairs.[1,2] Interestingly, even though the utility of the phase transfer catalysts in synthetic chemistry is rather well documented,[1,3-5] not much attention has been paid to understand the exact nature of the binding of these salts with polar organic molecules in a nonpolar medium. Recently PTCs have been effectively used to stabilize nanoparticles in a nonpolar medium.[14-16] Here we address ourselves to a fundamental question of finding out whether the role of the phase transfer catalysts lies merely helping the solubilization of a polar system in nonpolar media so as to facilitate its reaction with a third substance in an organic medium. Specifically, we attempt to find out the exact nature of the interaction of the phase transfer catalysts with neutral polar organic systems and to what extent the phase transfer catalysts change the original properties of the solubilized systems. In order to achieve this objective, we have selected several fluorescent electron donor-acceptor (EDA) systems as the probe molecules. Since the absorption and fluorescence behavior of these systems is mainly controlled by a low-lying intramolecular charge transfer (ICT) state, whose location is extremely sensitive to the surrounding medium, it is expected that the changes in the absorption and fluorescence properties induced by the PTCs will provide information on how the ion pairs interact with the probe molecules. The chosen EDA molecules can be categorized in two sets (Fig. 3.1). Set 1 consists of 4-aminophthalimide (AP) and 4-aminonaphthalimide (ANP), both known as highly fluorescing EDA molecules especially in nonpolar media. Both the molecules exhibit a broad emission band that originates from an ICT state, with the fluorescence parameters strongly dependent on the polarity of the media.[17-23] In Set 2, three multi-component systems, APDEA, ANPDEA and NBDEA with a

Set 1

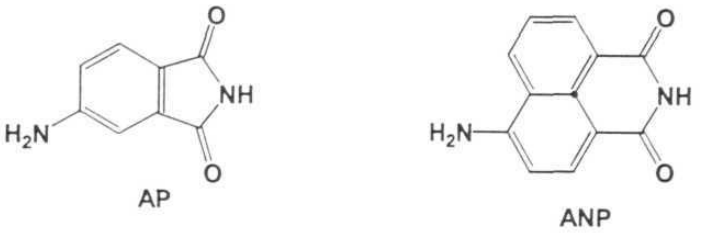

Set 2

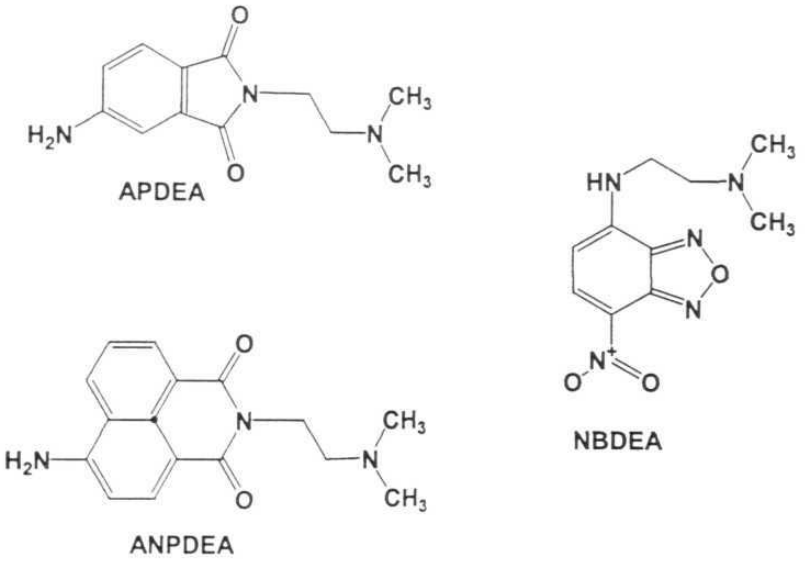

Fig. 3.1

fluorophore-spacer-receptor architecture have been chosen. The first two systems, APDEA and ANPDEA contain AP and ANP as the fluorophore linked with a dimethylamino group (as receptor for cations) via a dimethylene spacer.[21] NBDEA is another similar system containing a dimethylamino-nitrobenzoxadiazole (NBD) moiety, a popular fluorescence probe in biological

studies, as the fluorophore.[24,25] The solvent sensitive fluorescence properties of the NBD derivatives[26] and the ability of NBDEA in sensing various metal ions are well documented.[27,28] The fundamental difference in the photophysical properties of the parent systems (shown in set 1) and the multi-component systems (set 2) is that the former set of molecules are highly fluorescent (at least in the nonpolar media) while the latter are not. The low fluorescence quantum yields of the three-component systems are due to *through-space* photoinduced intramolecular electron transfer (PIET) between the receptor and fluorophore moieties.[17,21,27,28] PIET leads to 'switching off' of the fluorescence. However, in the presence of a guest capable of tying up the lone pair of electrons of the receptor, PIET communication between the receptor and the fluorophore gets cut-

Set 3

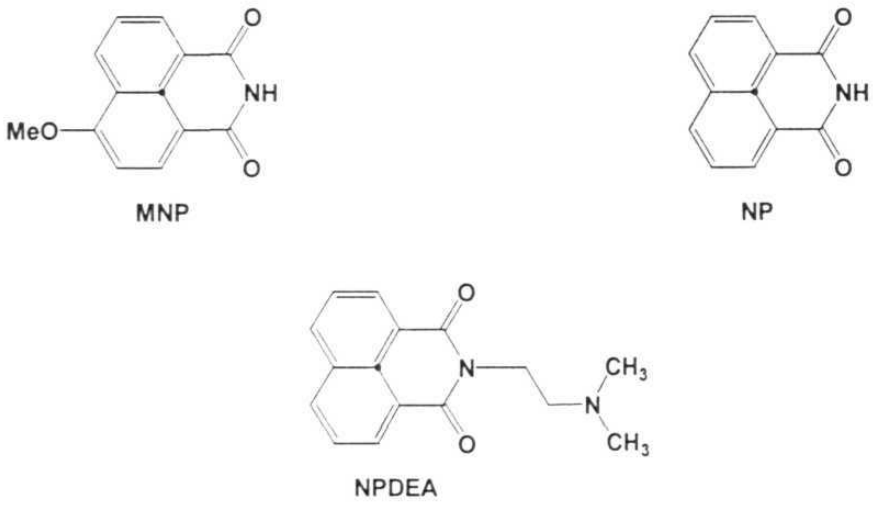

Fig. 3.2

off and the fluorescence of the system is 'switched on'.[17,21,27,28] We have also examined the effect of tetraalkylammonium salts on a few other systems (MNP and NP) that do not contain the strong electron donating amino group at the 4-position and NPDEA, which comprises NP as the fluorophore but contains an additional site for the cation binding. These systems are shown as Set 3 in Fig. 3.2. We thought that a study of the effect of the PTCs on the photophysical behavior of these systems would help understanding the exact role of the PTCs and in obtaining an answer to the question raised above.

3.2. Spectral properties

3.2.1. Absorption spectra

The effect of TOAB on the UV-visible absorption spectrum of AP is illustrated in Fig. 3.3 (a). With progressive addition of TOAB the long-wavelength charge transfer band of AP, which shows a maximum at around 350 nm in toluene, shifts towards red with a gain in intensity in the longer wavelength region. The presence of an isosbestic point at around 350 nm clearly suggests 1:1 complexation between AP and TOAB. In the presence of 4.4 mM TOAB the observed red shift in the absorption maximum of AP is ~ 20 nm. A similar observation has been made in the presence of TBAB and TBAC, where the observed spectral shift are ~12 nm and ~30 nm respectively in toluene.

The three-component system, APDEA, which contains AP as the fluorophore moiety with an additional cation-binding site, shows a very similar behavior [Fig. 3.3 (b)]. The spectral data of this system in the presence and in absence of various phase transfer catalysts are given in Table 3.1.

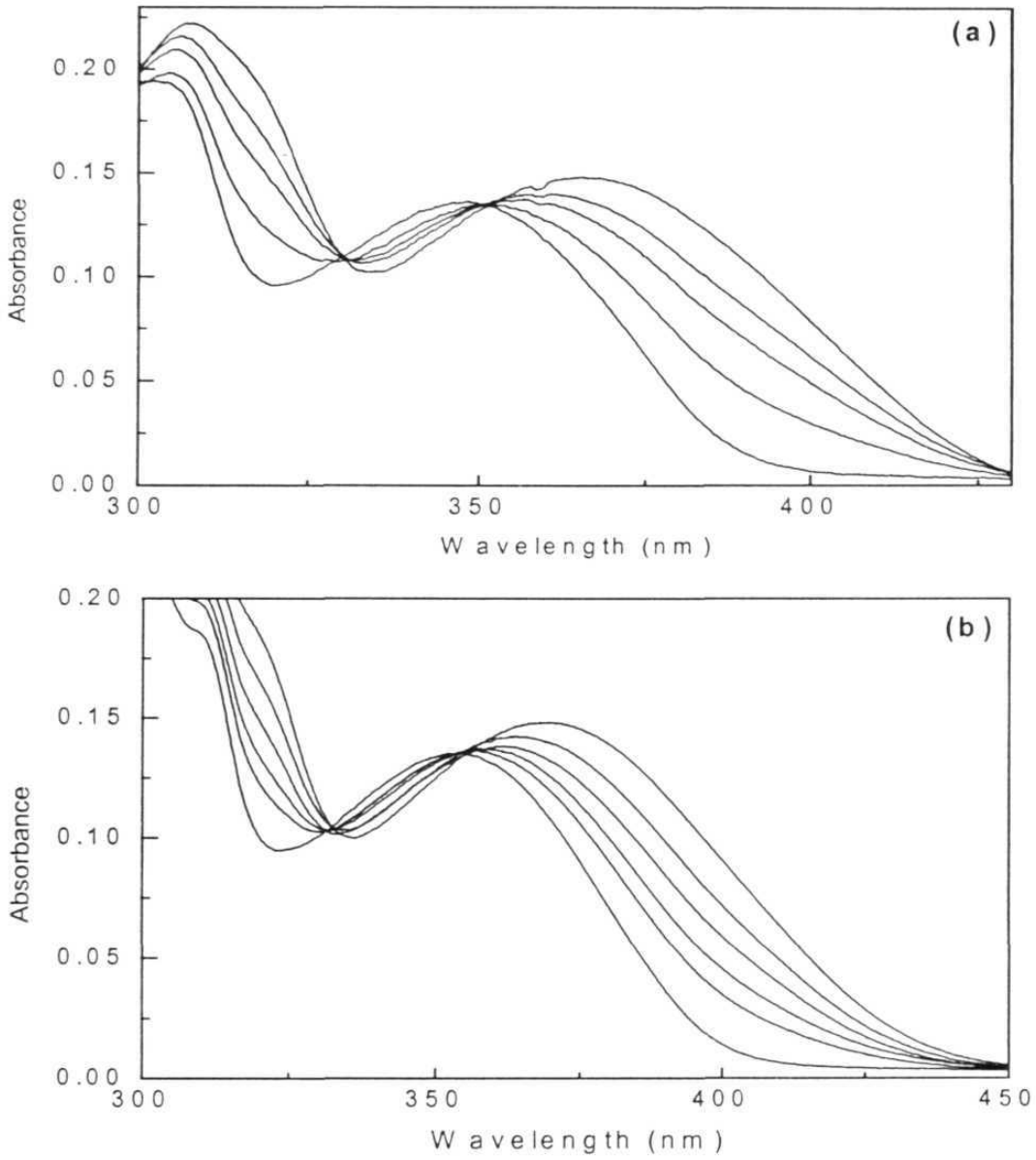

Fig. 3.3. *Effect of TOAB on the UV-visible absorption behavior of (a) AP and (b) APDEA in toluene. The concentrations of TOAB in increasing order of the absorbance at the longest wavelength maxima were 0, 0.66, 1.46, 2.19 and 4.39 mM in (a) and 0, 0.37, 0.66, 1.39, 2.27 and 4.54 mM in (b) respectively*

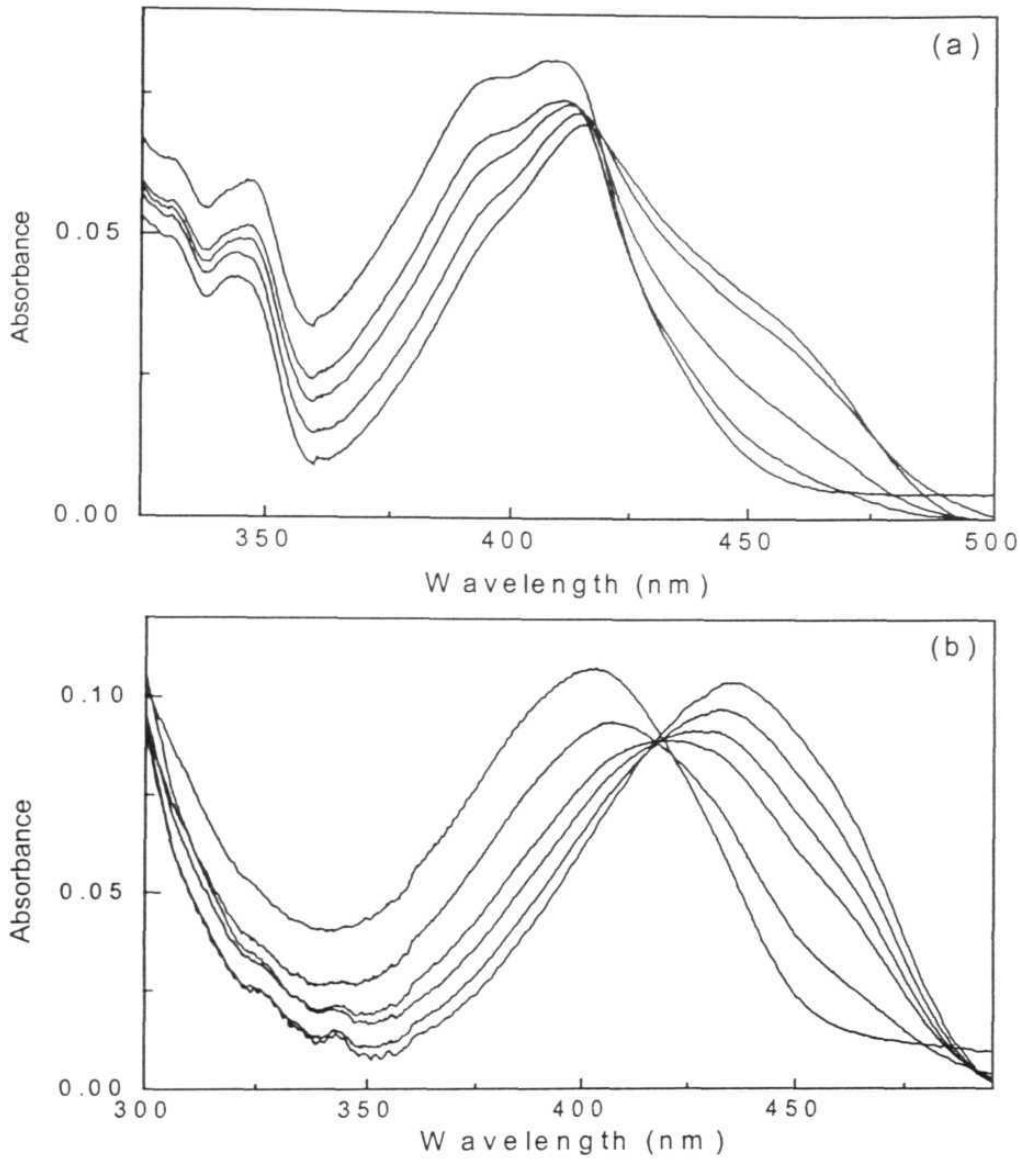

Fig. 3.4. *Effect of TOAB on the UV-visible absorption behavior of (a) ANP and (b) ANPDEA in toluene. The salt concentrations in increasing order of the absorbance at the longest wavelength maxima were 0, 0.15, 0.44, 0.88 and 1.54 mM in (a) and 0, 0.29, 0.88, 1.09, 1.83 and 3.73 mM in (b) respectively*

It is quite important to note in this context that in the presence of TBAI and TBAP no significant change in the absorption behavior of AP or APDEA has been observed. The absorption behavior of ANP and ANPDEA in the presence of the TOAB (depicted in Fig. 3.4) also indicates 1:1 complexation between these systems and TOAB. The spectral data for these systems in the presence of other phase transfer catalysts are also represented in Table 3.1.

Table 3.1. *Absorption and fluorescence spectral maxima observed for various systems in toluene in the presence of different tetraalkylammonium salts.*[a]

System	None		TOAB		TBAB		TBAC	
	λ_{max}^{abs} (nm)	λ_{max}^{flu} (nm)	λ_{max}^{abs} (nm)	λ_{max}^{flu} (nm)	λ_{max}^{abs} (nm)	λ_{max}^{flu} (nm)	λ_{max}^{abs} (nm)	λ_{max}^{flu} (nm)
AP	350	430	370	467	362	503	379	520
APDEA	353	430	379	502	380	504	380	515
ANP	403	469	420	520	434	522	424	533
ANPDEA	403	470	436	522	427	521	445	540
NBDEA	445	517	455	525	471	533	470	540
NPDEA	345, 332	370, 397	345, 332	370	345, 331	370	345, 332	370

[a]~2×10^{-5} M solution of the compounds in toluene was used at room temperature; the concentration of the PTCs was ~ 1.7 mM in the case of TBAC and 4.4 mM for the other salts; λ_{ex} = 350 nm for AP, APDEA, 305 nm for NPDEA, 380 nm for ANP, ANPDEA and 415 nm for NBDEA.

NBDEA too exhibits a Stokes shift of the absorption maximum in the presence of the tetraalkylammonium salts and the magnitude of the shift lies between 12 - 25 nm (vide Table 3.1). In this case, even though 1:1 complexation is indicated for lower concentration of TOAB, higher order complexes could be observed (as evident from the loss of isosbestic point) at higher concentration of the salt.

The other observations can be summarized as follows: Even though spectral changes similar to what have been described above could be observed for all the systems shown in Fig. 3.1 in other nonpolar solvents such as cyclohexane, no noticeable spectral change could be observed for these systems in polar solvents such as acetonitrile, ethanol or water. In 1,4-dioxane ($E_T(30)$ = 36.0),[29] which is slightly more polar than toluene ($E_T(30)$ of 33.9),[29] the complexation could be observed though not as prominently as in the case of toluene. This is illustrated in Fig. 3.5. Moreover, in this solvent, very often the initial isosbestic point could not be seen for higher concentration of the salts. Secondly, none of the systems exhibit any significant changes in the spectral behavior (even in nonpolar media) with PTCs such as TBAI or TBAP. Thirdly, for systems such as NP, MNP, which do not contain the amino group at the 4-position of the naphthalimide ring, no spectral changes could be observed with the tetraalkylammonium salts employed in this study. Moreover, it was found that NPDEA, which contains a cation-binding site but is devoid of the amino group at the 4-position of the ring, does not exhibit any shift of its absorption maximum in the presence of the phase transfer catalysts in nonpolar media.

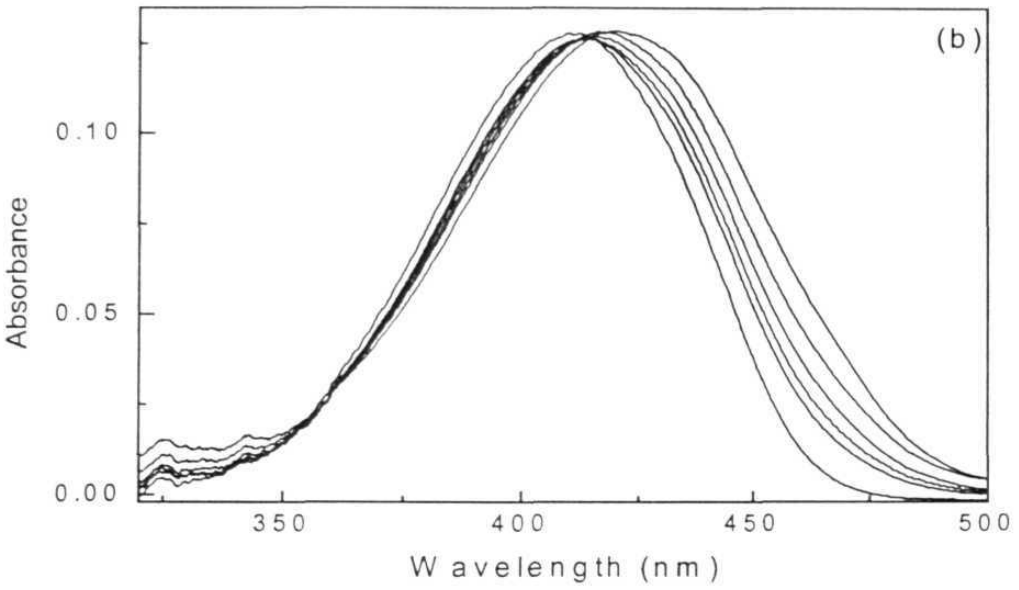

Fig. 3.5. *Effect of TOAB on the UV-visivle absorption behavior of ANPDEA in 1,4-dioxane. The salt concentrations in increasing order of the absorbance at the longest wavelength maxima were 0, 0.88, 1.2, 1.8, 2.6, and 4.5 mM respectively.*

3.2.2. Fluorescence spectra

In toluene, AP exhibits a broad structureless fluorescence band with a maximum at around 430 nm. In the presence of PTCs, this fluorescence gets quench and a relatively weak new emission band appears at a longer wavelength (Fig. 3.6). The existence of an isosbestic point confirms 1:1 complexation between the fluorescence probe molecules and the phase transfer catalysts. The peak positions of the new emission in presence of ~1.7 mM TOAB, TBAB, and TBAC are observed at 475, 503, and 520 nm, respectively (vide Table 3.1). While a similar behavior is noticed in the case of ANP (Fig. 3.6), the multi-component systems (APDEA, ANPDEA and NBDEA) behave slightly differently.

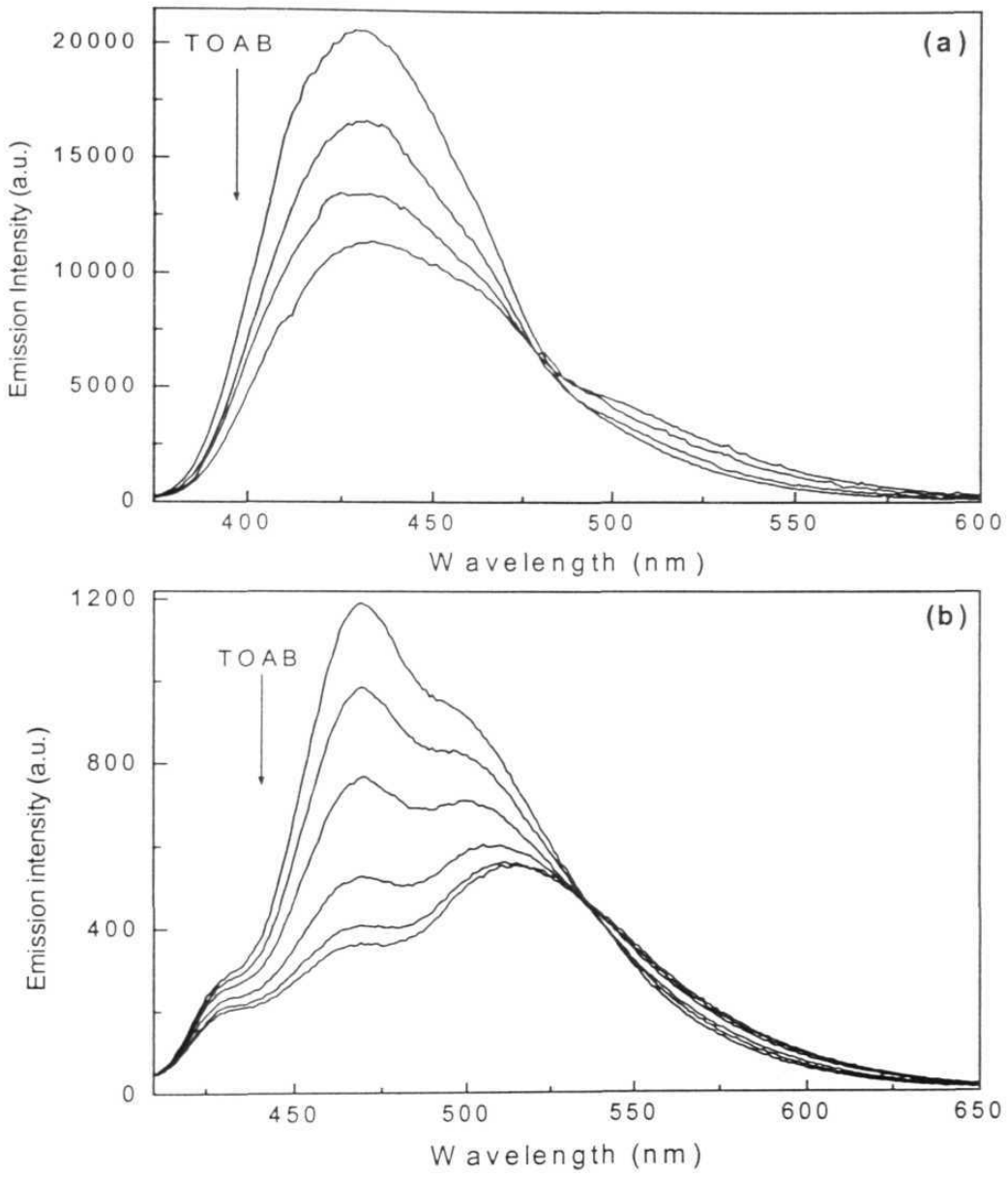

Fig. 3.6. *Effect of TOAB on the fluorescence behavior of (a) AP and (b) ANP in toluene. TOAB concentrations were 0, 0.51, 1.02 and 1.46 mM in (a) and 0, 0.15, 0.44, 0.88, 1.54 and 1.98 mM in (b) respectively. The excitation wavelength was 335 nm for AP and 380 nm for ANP.*

For the latter systems, in the presence of PTCs the original fluorescence gets quench and simultaneously a new emission band comes up at longer wavelength region. The new fluorescence band is found to be drastically Stokes-shifted relative to the original fluorescence maximum (Fig.3.7). The degree of enhancement of the fluorescence intensity relative to the original fluorescence band is found to be as large as 25-fold in case of APDEA. The changes in the fluorescence behavior of the molecules (set 1 and 2 in Fig. 3.1) as stated above could also be observed in other nonpolar solvents such as cyclohexane ($E_T(30)$ = 30.9).[29] In 1,4-dioxane ($E_T(30)$ = 36.0),[29]which is slightly more polar, the new emission is found to be much weaker compared to that observed in toluene ($E_T(30)$ = 33.9).[29] The spectral data of the systems in 1,4-dioxane in the presence of TOAB are given in Table 3.2. Fig. 3.8 shows the influence of TOAB on the fluorescence behavior of ANPDEA in 1,4-dioxane. However, in polar media, no noticeable changes in the fluorescence behavior could be observed in the presence of the tetraalkylammonium salts.

In the case of NP, MNP and NPDEA, no significant change in the fluorescence behavior of these systems has been observed even in nonpolar environment. TBAI and TBAP are found to have no significant influence on the fluorescence behavior of these systems even in the nonpolar media.

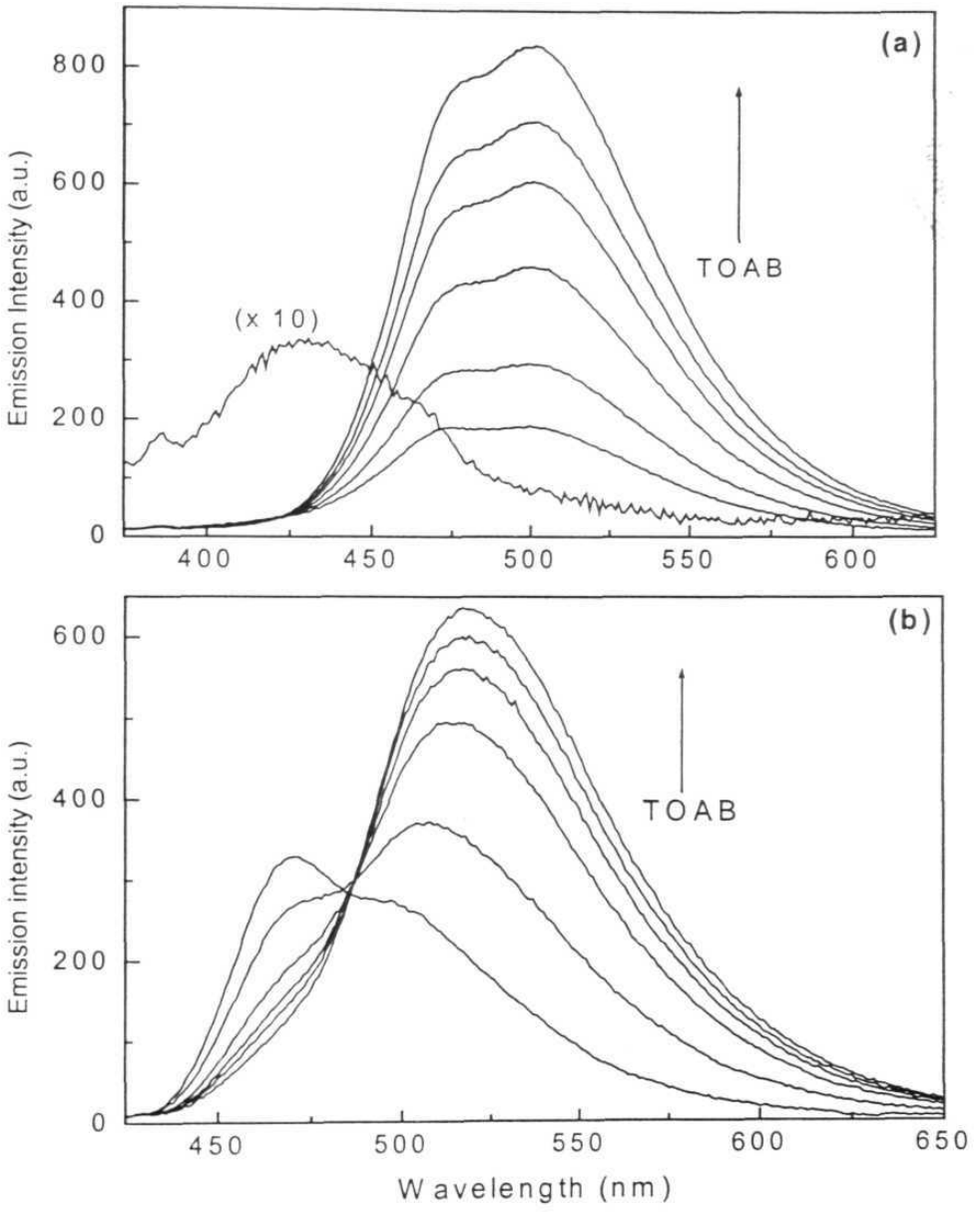

Fig. 3.7. *Effect of TOAB on the fluorescence behavior of (a) APDEA and (b) ANPDEA in toluene. TOAB concentrations were 0, 0.37, 0.66, 1.39, 2.27, 3.07 and 4.54 mM in (a) and 0, 0.29, 0.88, 1.09, 1.46 and 1.83 mM in (b). APDEA and ANPDEA were excited at 345 nm and 380 nm respectively.*

Table 3.2. *Absorption and fluorescence spectral maxima observed for various systems in 1,4-dioxane in the presence of tetraoctylammonium bromide (TOAB).*[a]

Systems	None		TOAB	
	λ_{max}^{abs} (nm)	λ_{max}^{flu} (nm)	λ_{max}^{abs} (nm)	λ_{max}^{flu} (nm)
AP	355	437	360	450
APDEA	360	449	365	474
ANP	409	503	424	514
ANPDEA	410	477, 503	425	518
NBDEA	450	528	460	543

[a]~2 × 10^{-5} M solution of the compounds in 1,4-dioxane was used at room temperature; Concentration of the TOAB was ~7.5 mM for NBDEA and ~ 6.7 mM for others; λ_{ex} = 370 nm for AP, 355 nm APDEA, 410 nm for ANP, 415 nm for ANPDEA and 460 nm for NBDEA.

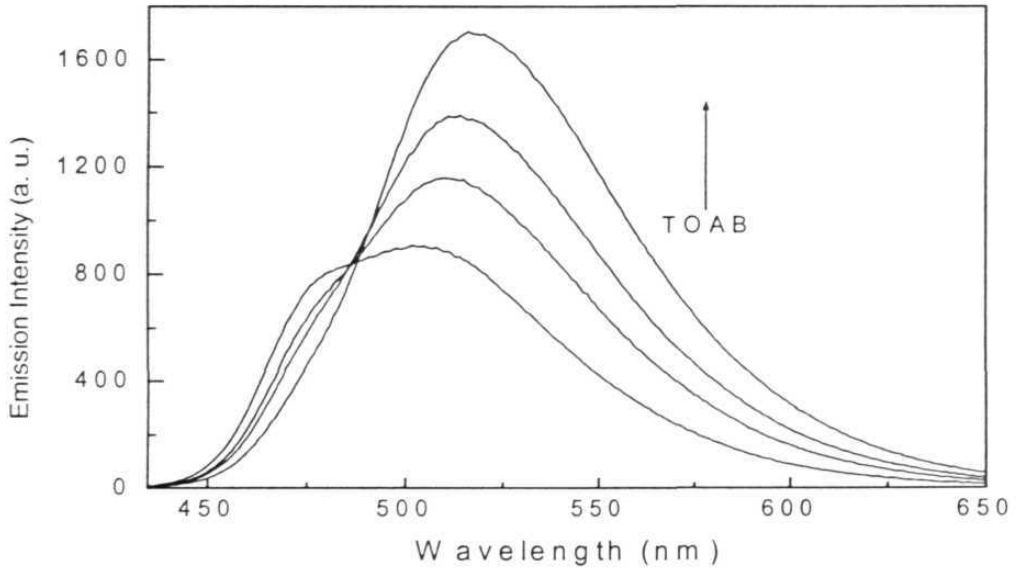

Fig. 3.8. *Effect of TOAB on the fluorescence behavior of ANPDEA in 1,4-dioxane. TOAB concentration was 0, 1.2, 2.6 and 6.9 mM respectively. The sample was excited at 415 nm.*

3.2.3. Fluorescence excitation spectra

In order to identify the origin of the new fluorescence emission we have measured fluorescence excitation spectra for all the systems monitoring the original fluorescence as well as the Stokes-shifted fluorescence band. A typical fluorescence excitation spectrum of AP in toluene is shown in Fig. 3.9. The excitation maximum obtained on monitoring the longer wavelength fluorescence band is found to be distinctly Stokes-shifted relative to that obtained on monitoring the original fluorescence band.

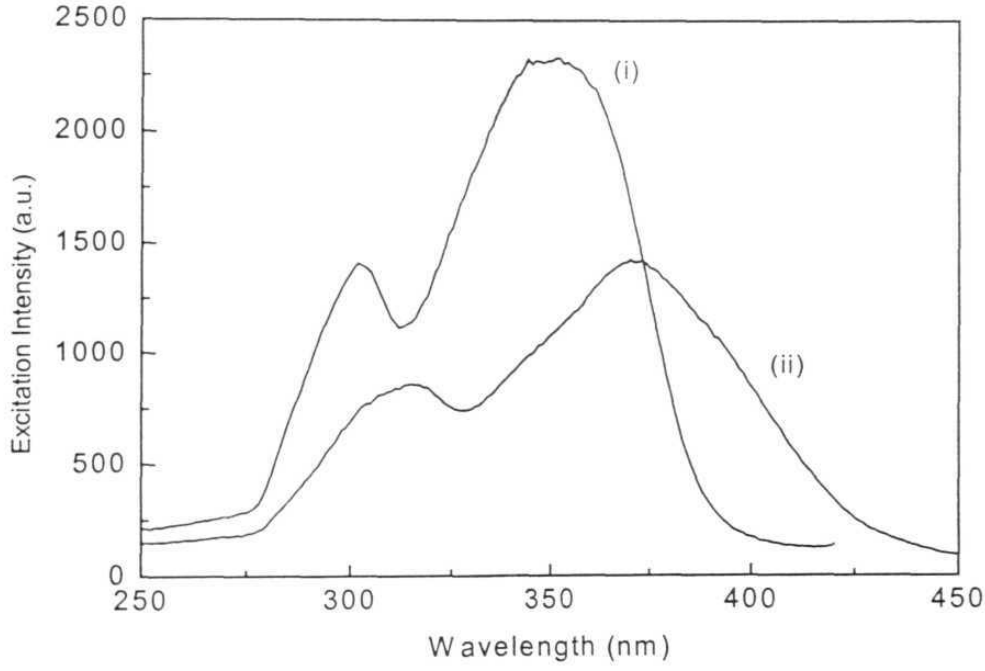

Fig. 3.9. *Effect of TOAB on the fluorescence excitation spectra of AP in toluene. TOAB concentration was 0 in (i) and 4.39 mM in (ii). The monitoring wavelengths were 430 and 467 nm respectively.*

However, the excitation maximum corresponding to the longer wavelength fluorescence band resembles very closely the absorption peak of the system in the presence of the quaternary ammonium salts. This suggests that the new emission originates from the ground state complex formed between the salts and the probe molecules.

3.2.4. Fluorescence decay behavior

With a view to obtaining further details on the nature of the interaction between the PTCs and fluorophores, we have also investigated the fluorescence decay behavior of the present systems in the absence and presence of the salts. In the presence of PTCs, we have measured the decay curves by monitoring the original fluorescence as well as the new fluorescence band. The decay parameters obtained for various systems in toluene and 1,4-dioxane are collected in Table 3.3. Some representative decay profiles depicting the influence of PTC along with the best fit to the decay are shown in Fig. 3.10. and Fig. 3.11. The main features of the decay behavior can be summarized as follows:

The major component of AP has a lifetime between 13 - 17 ns in toluene and 1,4-dioxane. In the presence of 4.4 mM TOAB, the τ values are reduced marginally to 11-12 ns. A similar behavior could be observed in the case of ANP, whose lifetimes (8.8 and 11.1 ns in toluene and 1,4-dioxane respectively) are lowered to 8.3 and 9.0 ns.

Table 3.3. *Fluorescence decay parameters[a] for the systems studied in the absence and in presence of TOAB (~4 mM) in toluene and 1,4-dioxane.*

Fluorophore	Solvent	Lifetimes/ns without TOAB	Lifetimes/ns in presence of TOAB	
			at short w.l.[b]	at long w.l.[b]
AP	toluene	3.9 (0.03)	2.7 (0.06)	3.2 (0.03)
		13.4 (0.08)	11.2 (0.06)	12.2 (0.09)
	1,4-dioxane	16.9 (0.07)	1.5 (0.03)	13.5 (0.08)
			12.2 (0.07)	
APDEA	toluene	0.1 (5.75)	0.5 (0.35)	2.9 (0.07)
		13.3 (0.01)	9.4 (0.02)	12.8 (0.05)
	1,4-dioxane	0.2 (1.84)	0.7 (0.22)	2.7 (0.08)
		17.5 (0.004)	12.0 (0.04)	13.1 (0.04)
ANP	toluene	1.6 (0.06)	1.9 (0.13)	8.5 (0.11)
		8.8 (0.08)	8.3 (0.03)	
	1,4-dioxane	11.1 (0.11)	9.0 (0.11)	9.9 (0.11)
ANPDEA	toluene	2.1 (0.17)	1.9 (0.17)	1.9 (0.07)
			4.4 (0.01)	8.1 (0.06)
	1,4-dioxane	3.3 (0.12)	2.3 (0.09)	3.1 (0.06)
		5.3 (0.03)	7.1 (0.05)	8.6 (0.08)
NBDEA	toluene	0.3 (0.91)	0.3 (0.79)	0.3 (0.61)
		6.4 (0.01)	6.7 (0.01)	7.1 (0.01)
	1,4-dioxane	0.2 (1.56)	0.6 (0.36)	1.2 (0.19)
		10.2 (0.03)	5.3 (0.01)	14.7 (0.02)

[a]Decay curves were fitted to a single or biexponential function depending on the quality of the plot of the residuals and the χ^2 values; preexponential factors were shown within the brackets; [b]short wavelength corresponds to 400, 450, and 495 nm for AP, ANP and NBD derivatives and long wavelength corresponds to 480, 540 and 555 nm respectively.

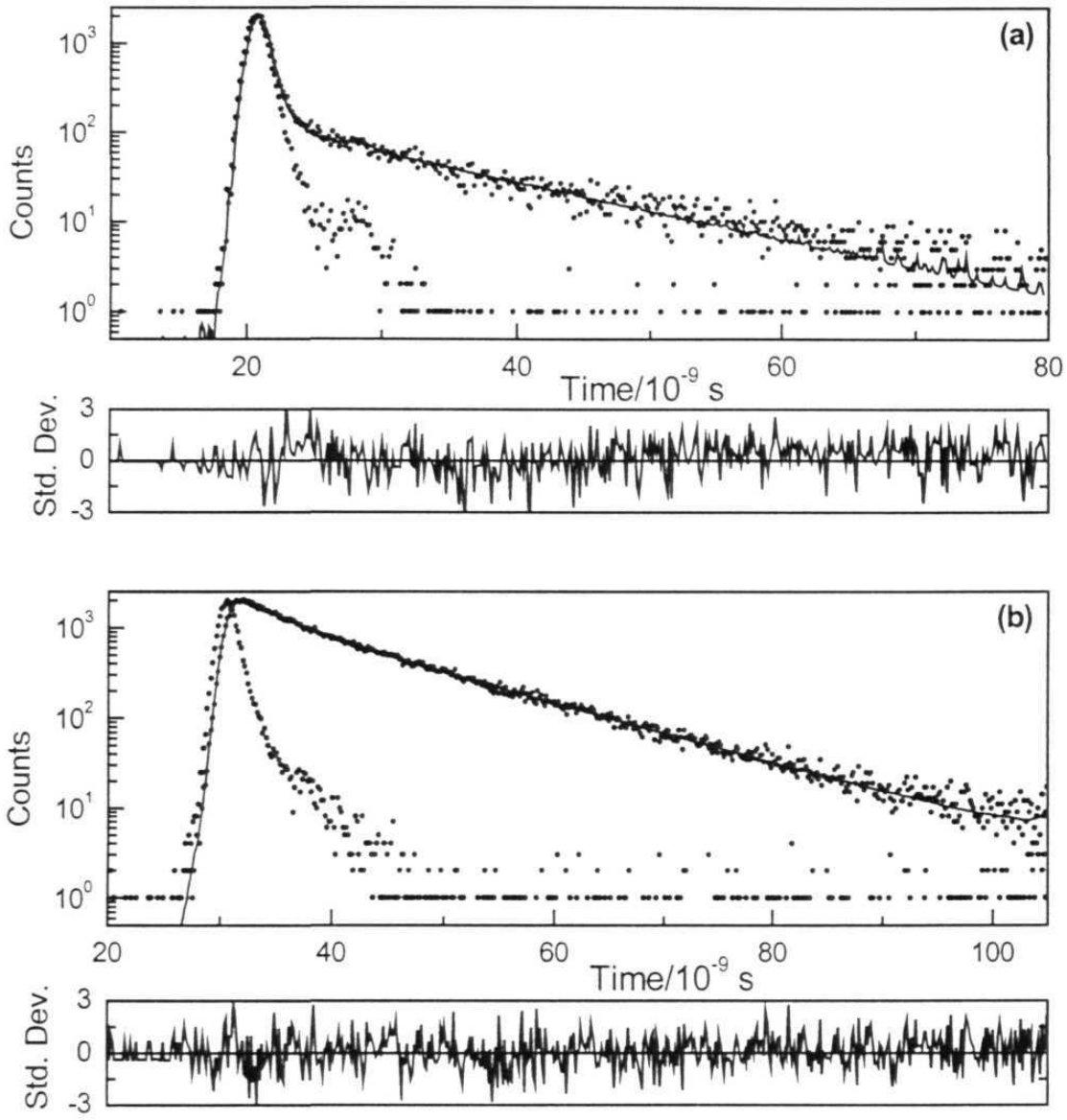

Fig. 3.10. *Effect of TOAB on the fluorescence decay behavior of APDEA in toluene (a) in the absence and (b) in the presence of TOAB. The monitoring wavelength was 430 nm and 525 nm for (a) and (b) respectively.* λ_{ex} *was 340 nm in both cases.*

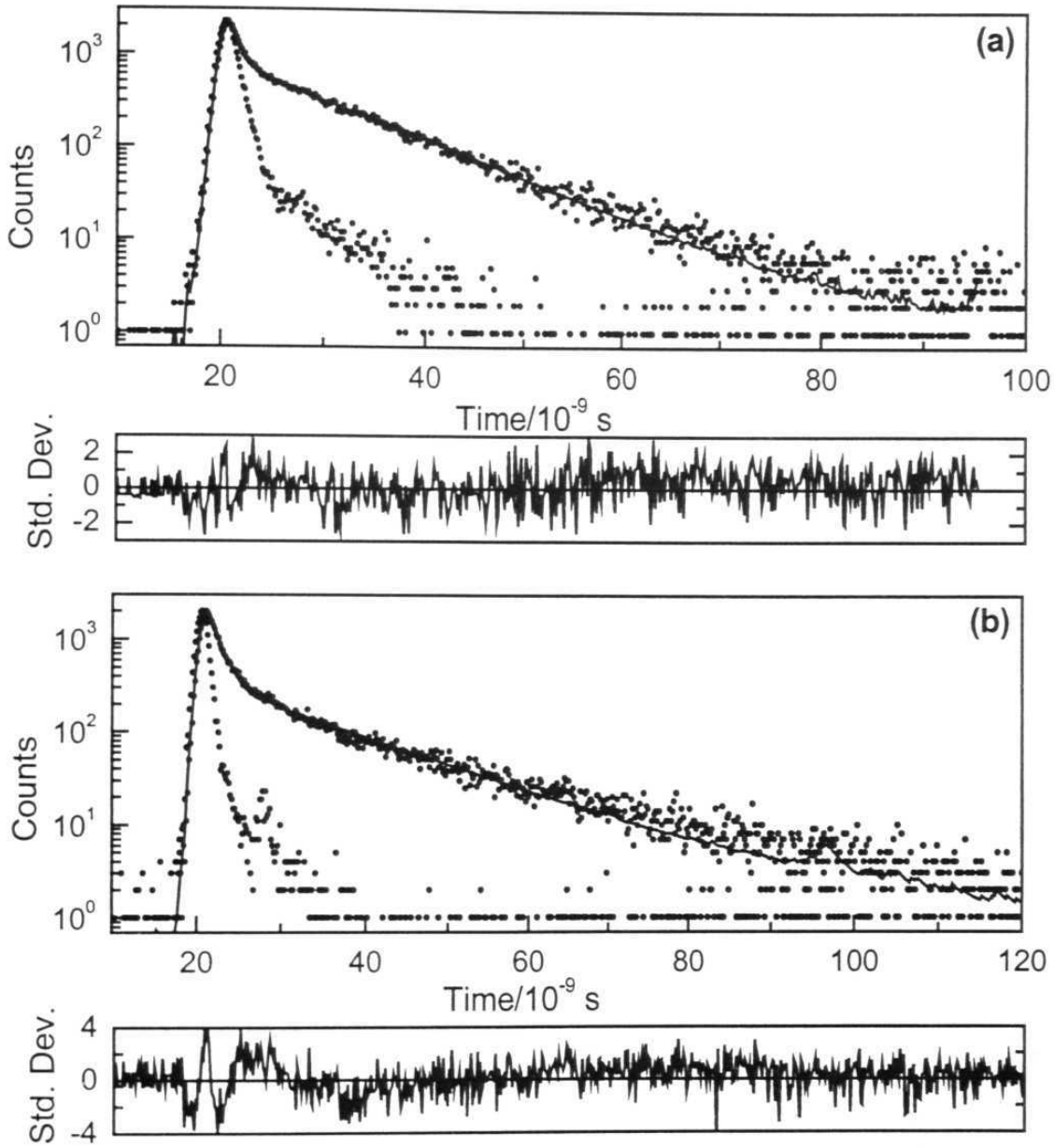

Fig. 3.11. *Effect of TOAB on the fluorescence decay behavior of NBDEA in 1,4-dioxane (a) in the absence and (b) in the presence of TOAB. The monitoring wavelength was 530 nm and 550 nm for (a) and (b) respectively. λ_{ex} was 450 nm in both cases.*

In contrast to AP, the major component of the decay in the case of the 3-component system, APDEA is a very short-lived species.[21] This is due to the photoinduced intramolecular electron transfer (PIET) quenching of the fluorescence. On addition of TOAB, an increase in the τ values of the short-lived component could be observed. Since in the case of ANPDEA, PIET is not very significant,[21] the major component has a comparatively longer lifetime and the influence of TOAB on this value is rather small. In the case of NBDEA, the influence of TOAB on the τ values of the major component of the decay is not very significant, as can be seen from Fig. 3.11.

3.3. Discussion

3.3.1. Formation constant (K) of the complexes

The phase transfer catalysts induced changes in the absorption behavior of the systems indicate the formation of a 1:1 complex in the ground state in nonpolar media. The formation constants of the complexes have been evaluated from the absorption data using the equation 3.1 (derivation of the equation is given in appendix 1). Considering 1:1 complexation between the probe molecule, A and the phase transfer catalyst, B, the complexation process can be simply written as

$$A + B <=> C$$

where, C stands for the complex. The final expression used for estimation of the binding constant is as follows:

$$\frac{OD_A}{OD_t - OD_A} = \frac{1}{[B]_t}\left(\frac{1}{K}\frac{\varepsilon_A}{\varepsilon_k}\right) + \frac{\varepsilon_A}{\varepsilon_k} \qquad (3.1)$$

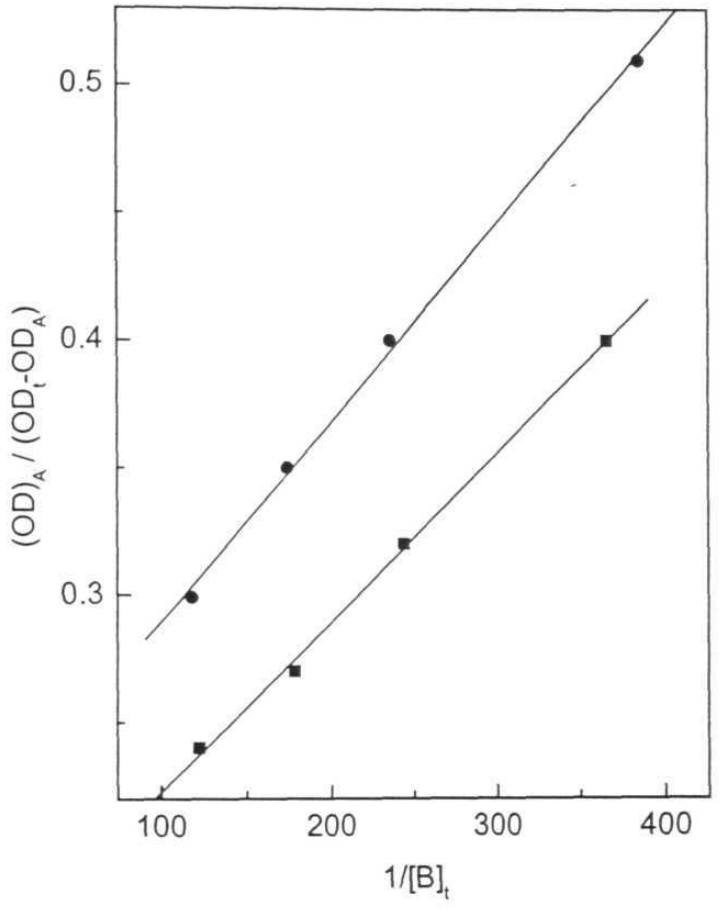

Fig. 3.12. *A plot of (OD_A) / $(OD_t - OD_A)$ vs $1/[B]_t$ based on equation 3.1. The data points denote for AP (■) and APDEA (●) respectively and the straight line represent the best fit to the data.*

where, OD_A stands for the initial optical density of A at given wavelength (λ), (OD_t) is the total absorbance at the same λ in the presence of PTC at a concentration of $[B]_t$. According to equation 3.1, a plot of $OD_A/(OD_t - OD_A)$ vs $1/[B]_t$ should yield a straight line whose intercept is given by ($\varepsilon_A/\varepsilon_k$) and the slope ($\varepsilon_A/\varepsilon_k K$). K values were estimated from the slope and the intercept of these plots. Some representative plots based on these

equations are shown in Fig. 3.12 and the calculated binding constant values have been collected in Table 3.4.

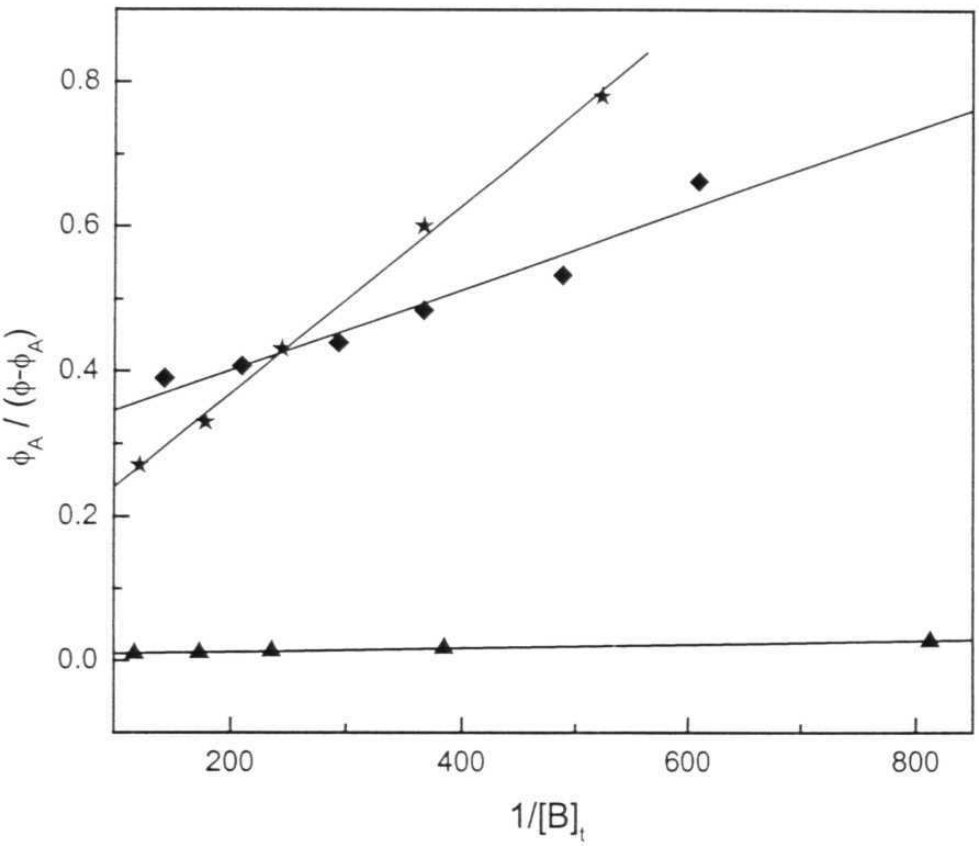

Fig. 3.13 *Representative plot of $\phi_A / (\phi-\phi_A)$ vs $1/[B]_t$ based on equation 3.2. The data points denote for AP* (H), *APDEA* (σ) *and ANPDEA* (υ) *in toluene respectively and the straight line represent the best fit to the data.*

We have further estimated the binding constant from steady state fluorescence intensity data according to equation 3.2 (derivation of this equation is provided in appendix 1).[30]

$$\frac{\phi_A}{\phi-\phi_A} = \left[\left(\frac{\phi_A}{\phi_C-\phi_A}\right)\frac{1}{K}\right]\frac{1}{[B]_t} + \frac{\phi_A}{\phi_C-\phi_A} \qquad (3.2)$$

In this equation, ϕ and ϕ_A are the emission intensities in presence and absence of PTC at a particular wavelength where the effect of complexation is prominent. In Fig. 3.13, the linear fits to the data points of AP, APDEA and ANPDEA in toluene, obtained using equation 3.2 are shown. The calculated binding constant values using equation 3.2 are given in Table 3.4.

Table 3.4. *Binding constant of TOAB with various probe molecules in toluene and 1,4-dioxane estimated from the absorption and the fluorescence data.*

System	Binding constant[a]/ M^{-1}			
	from absorption		from fluorescence	
	toluene	1,4-dioxane	toluene	1,4-dioxane
AP	175	40	85	105
APDEA	270	90	260	80
ANP	430	110	490	190
ANPDEA	580	230	530	230
NBDEA	110	140	[b]	180

[a] ± 10 %; [b] could not be calculated due to the poor quality of the data.

The data presented in Table 3.4 can be rationalized as follows: Barring a few scatter, the K values are generally higher in toluene compared to the respective values in 1,4-dioxane. This, coupled with the fact that no spectral changes could be observed for these systems in more polar solvents such as acetonitrile or methanol (indicating the instability of the complex), suggests that the complex is charge transfer in nature. Tetraalkylammonium salts exist

predominantly as ion-pair in nonpolar environment and can readily form charge transfer complex through electrostatic forces with the dipolar fluorophores. However, in the polar media they exist predominantly as solvated ions and the electrostatic interaction between the solvated cations and the dipolar fluorescent systems is expected to be rather low. Hence, based on these observations, a charge transfer nature of the 1:1 complex is concluded.

Between AP and ANP, the K values are relatively higher for the latter indicating a stronger binding of TOAB with ANP compared to AP. A similar trend is also noticed in case of APDEA and ANPDEA. Moreover, it should be noted that the dipolar systems (shown in set 3 Fig 3.2) do not display any significant changes in the spectral behavior even in the nonpolar media. Obviously, the dipolar nature of the fluorophore is one of the most important factors that determine the magnitude of the interaction between the fluorophore and the phase transfer catalyst. A comparatively higher K value for ANP is perhaps understandable as the AM1 (Austin model 1) calculated dipole moments of AP and ANP are 5.3 and 7.5 D respectively. However, since the interaction between the dipolar fluorophore and the phase transfer catalyst is governed by electrostatic forces, the absolute values of the charge at the positive and the negative end of the fluorophore and the distance separating them are more important than their product, dipole moment. When the distance separating the charges is too different for the two fluorophores, one obtains an incorrect assessment of the strength of the interaction from the dipole moment values alone. In order to avoid this, the mean distance between the 4-amino nitrogen atom and the carbonyl oxygen atom of the fluorophores has been calculated by AM1

method. The estimated distance is 6.1 and 6.8 Å for AP and ANP respectively. From the values of the dipole moment and the distance, the magnitude of charge localized at the 4-amino nitrogen atom is estimated as 0.18 and 0.23 esu for AP and ANP respectively. Since the absolute values of the charge (at the positive or negative end of the molecule) are higher for ANP, one can expect a stronger binding compared to AP.

3.3.2. Origin of the new emission

The fact that the Stokes-shifted new emission band originates from a charge transfer complex formed between the fluorophore and the phase transfer catalyst is clearly evident when a comparison is made between the excitation spectra of the systems in the presence and in absence of tetraalkylammonium salts. Interestingly, the emission maximum of this complex in the presence of tetraalkylammonium salts appears at a longer wavelength, very close to those observed for AP and ANP in a highly polar solvent such as alcohol or water.[30] As the fluorescence band position of the fluorophores is sensitive to the polarity of the medium, it may possible that the tetraalkylammonium salts, especially the chloride, being highly hygroscopic create a highly polar microenvironment around the fluorophore, which may lead to a Stokes shift of the fluorescence maxima. The fact that a preferential solvation of the fluorophores by the water molecules (associated with the catalysts) is not responsible for the Stokes-shifted new emission band of the systems is evident from the following observations. First, the fluorescence band position observed for the systems in the presence of TBAC are not very different from that observed in the presence of much less

hygroscopic salt, TBOB. Second, we have not observed any change in the absorption/fluorescence maximum of the systems on addition of few drops of water to the toluene solution of AP and ANP. Third, the fluorescence lifetimes of the fluorophores in aqueous or alcoholic solution of the systems are known to be much lower[30] than those observed in the presence of the tetraalkylammonium salts. All these observations clearly rule out the possibility of a change in polarity of the microenvironment around the dipolar probe molecules in the presence of PTCs.

3.3.3. Role of anion and cation

Our spectroscopic data indicate a highest efficiency of the chloride ion in inducing the spectral changes compared to other anions. The ability to form the charge transfer complex under an identical condition is slightly less for the bromide ions. On the other hand, Iodide and perchlorate ions are found to be rather ineffective in such a complex formation process. This observation, coupled with the fact that only the dipolar fluorophores show changes in the absorption and fluorescence behavior, allows us to understand the exact role of the cationic and the anionic components of the phase transfer catalyst. In AP and ANP, the positive charge is mainly centered at the 4-amino nitrogen atom and the negative charges are localized on the two carbonyl oxygen atoms. An ion-pair, the form in which the phase transfer catalysts exist in nonpolar media, is most likely to interact with a dipolar system with an anti-parallel orientation to form the 1:1 complex. One can therefore propose a structure of the complex as is depicted in Fig. 3.14.

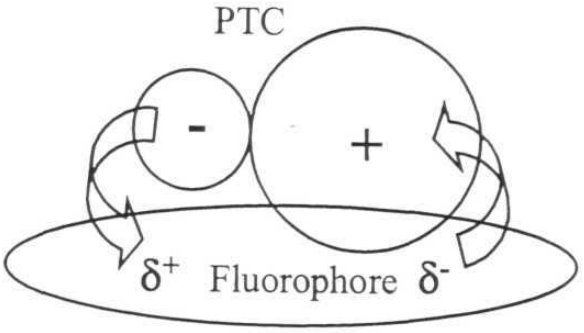

Fig. 3.14. *A schematic diagram of the complex indicating enhancement of the charge separation process in the fluorophore induced by the phase transfer catalyst (PTC).*

It is to be noted that a Stokes shift of the absorption or fluorescence peak of these dipolar fluorophores can arise due to two factors: a change in the polarity of the immediate environment of the fluorophore and a change in the extent of separation of charge within the fluorophore. The possibility that a change in the polarity of the environment is induced by the phase transfer catalysts has already been ruled out. This leaves us with only the other choice, an increased separation of charge in the fluorophore. It can be seen that the best way to enhance the charge separation between the 4-amino nitrogen atom and the carbonyl oxygen atoms is when the dipolar fluorophore and the phase transfer catalyst interact as suggested in Fig. 3.14. The halide ions essentially act as an additional source of electronic charge to the amino nitrogen atom of the fluorophore and the quaternary ammonium cation, by virtue of its location, can help the carbonyl oxygen atoms to withdraw more negative charge through the π-conjugated network of the fluorophore. This is how the charge separation in the dipolar

fluorophores is enhanced by the quaternary salts. The enhancement of the charge separation in the EDA fluorophores by the phase transfer catalyst as proposed here can be considered to some extent similar to that observed in presence of the metal salts.[31,32] However, unlike in the previous reports, where the charge separation was primarily controlled by the metal ions, in the present case, the anionic component plays a more important role. That is evident from the spectral data presented in Table 3.1. Clearly, chloride salts are more effective in enhancing the charge separation in the fluorophore compared to the bromide salts. The fact that iodide and perchlorate salts are rather ineffective in this regard can be explained when one can considers their size. A large size of these anions implies a low charge to volume ratio and less effectiveness in stabilizing a positive centre.

The results suggest that the cationic component of the phase transfer catalyst does not play any significant role in influencing the charge separation process. However, the difference in the fluorescence behavior of the AP and APDEA in the presence of a given PTC can be accounted for taking into consideration the role of the cation. It has been stated earlier that the intensity of the new Stokes shifted emission band is significantly higher in the case of APDEA. This shows that the cationic component of the ion-pair indeed interacts with the dimethylamino moiety of the three-component system, APDEA, thereby decreasing the through-space photoinduced electron transfer prevalent in the system and increasing the fluorescence intensity of this Stokes-shifted emission. An increase in the fluorescence lifetime of the short-lived species of APDEA in the presence of TOAB corroborates this conclusion.

3.3.4. Excited state interaction

The complexation between the phase transfer catalysts and the fluorophores has been shown to be a ground state phenomenon. However, it is a matter of interest whether there is an interaction between the two complexing partners in the excited state also. Had there been only a ground state interaction between the two, the fluorescence lifetime would have remained unaffected. However, the fluorescence lifetime data presented in Table 3.3 show that the lifetime of both AP and ANP is shortened in the presence of TOAB. For example, the fluorescence lifetime of AP in toluene is 13.4 ns in the absence of TOAB. In the presence of 4.4 mM TOAB, the lifetime is lowered to 11.2 ns. Using the Stern-Volmer equation for dynamic quenching,

$$\tau_0/\tau = 1 + k_q\tau_0[\text{TOAB}] \qquad (3.3)$$

where, τ_0 and τ are the fluorescence lifetimes in the absence and presence of TOAB, k_q is the rate constant for the excited state interaction between the fluorophore and the PTC and [TOAB] indicates the concentration of TOAB. We obtained a k_q value of 3.3×10^9 $M^{-1}s^{-1}$. Even though the fluorophore and TOAB interact in the excited state also, one might expect some contribution of this excited state interaction to the new fluorescence band observed. However, the absence of any growth (negative preexponential factor) in the decay profile of the long wavelength fluorescence band rules out this possibility.

3.4. Conclusion

In this chapter from a detailed steady state and time resolved studies on several dipolar probe molecules, we have shown that the quaternary ammonium

salts, which are frequently used as phase transfer catalysts, not only merely solubilize a polar system in a nonpolar medium (thereby enhance the reaction rate) but in the process, they can affect the properties of the solubilized systems quite significantly. The results of this investigation clearly demonstrate that a phase transfer catalyst employed in any investigation can not be taken as an innocuous reagent that just helps solubilization of a third substance, as is thought commonly. Specifically, from a detailed spectral and time-resolved study on a series of EDA molecules we have shown how a phase transfer catalyst binds to a dipolar system in nonpolar media and how this binding changes the photophysical behavior of the systems. It is shown that the influence of a phase transfer catalyst in modifying the properties of a system depends to a large extent on the dipolar nature of the fluorescent systems. Moreover, the anionic part of the ion-pair, the form in which the phase transfer catalysts exist in nonpolar media, seems to influence the photophysical properties of the EDA systems much more than the cationic counterpart.

3.5. References

(1) Dehmlow, E. V.; Dehmlow, S. S. *Phase Transfer Catalysis*; Verlag Chemie: Weinheim, 1983.

(2) Starks, C. M.; Liotta, C. *Phase Transfer Catalysis: Principles and Techniques*; Academic Press: New York, 1978.

(3) Sasson, Y.; Neumann, R. *Handbook of Phase Transfer Catalysis*; Blackie Academic and Professional: London, 1997.

(4) Weber, W. P.; Gokel, G. W. *Phase Transfer Catalysis in Organic Synthesis*; Springer-Verlag: Berlin, 1977.

(5) Halpern, M. E. *Phase-Transfer Catalysis, Mechanism and Syntheses*; American Chemical Society: Washington, DC, 1997.

(6) Arai, S.; Tsuji, R.; Nishida, A. *Tet. Lett.* **2002**, *43*, 9535.

(7) Yadav, G. D.; Jadhav, Y. B.; Sengupta, S. *J. Mol. Cat. A: Chem.* **2003**, in press.

(8) Wang, M.-L.; Tseng, Y.-H. *J. Mol. Cat. A: Chem.* **2002**, *188*, 51.

(9) Kim, D. Y.; Park, E. J. *Org. Lett.* **2002**, *4*, 545.

(10) Jones, R. A. *Quaternary Ammonium Salts, Their Use in Phase-Transfer Catalyzed Reactions*; Academic Press: New York, 2001.

(11) Kalyanasundaram, K. *Photochemistry in Microheterogeneous Systems*; Academic Press: New York, 1987.

(12) *Photochemistry in Organised and Constrained Media*; Ramamurthy, V., Ed.; VCH: New York, 1991.

(13) Lakowicz, J. R. *Principles of Fluorescence Spectroscopy*; Second ed.; Kluwer Academic/Plenum Publishers: New York, 1999.

(14) Brust, M.; Walker, M.; Bethell, D.; Schiffrin, D. J.; Whyman, R. *Chem. Commun.* **1994**, 801.

(15) Kamat, P. V. *J. Phys. Chem. B.* **2002**, *106*, 7729.

(16) Thomas, K. G.; Kamat, P. V. *J. Am. Chem. Soc.* **2000**, *122*, 2655.

(17) Ramachandram, B.; Saroja, G.; Sankaran, N. B.; Samanta, A. *J. Phys. Chem. B.* **2000**, *104*, 11824.

(18) Saroja, G.; Samanta, A. *Chem. Phys. Lett.* **1995**, *246*, 506.

(19) Saroja, G.; Samanta, A. *J. Chem. Soc., Faraday Trans.* **1996**, *92*, 2697.

(20) Saroja, G.; Ramachandram, B.; Saha, S.; Samanta, A. *J. Phys. Chem. B.* **1999**, *103*, 2906.

(21) Ramachandram, B.; Samanta, A. *J. Chem. Soc., Chem. Commun.* **1997**, 1037.

(22) Saroja, G.; Soujanya, T.; Ramachandram, B.; Samanta, A. *J. Fluores.* **1998**, *8*, 405.

(23) Soujanya, T.; Fessenden, R. W.; Samanta, A. *J. Phys. Chem.* **1996**, *100*, 3507.

(24) Chattopadhyay, A. *Chem. Phys. Lipids.* **1990**, *53*, 1.

(25) Hinterding, K.; Alonso-Diaz, D.; Waldmann, H. *Angew. Chem. Int. Ed.* **1998**, *37*, 688.

(26) Saha, S.; Samanta, A. *J. Phys. Chem. A.* **1998**, *102*, 7903.

(27) Ramachandram, B.; Samanta, A. *J. Phys. Chem. A.* **1998**, *102*, 10579.

(28) Ramachandram, B.; Samanta, A. *Chem. Phys. Lett.* **1998**, *290*, 9.

(29) Reichardt, C. *Solvents and Solvent Effects in Organic Chemistry*; VCH: Weinheim, 1988.

(30) Samanta, A.; Soujanya, T.; Krishna, T. S. R. *J. Phys. Chem.* **1992**, *96*, 8544.

(31) Mathevet, R.; Jonusauskas, G.; Rulliere, C.; Letard, J. F.; Lapouyade, R. *J. Phys. Chem.* **1995**, *99*, 15709.

(32) Delmond, S.; Letard, J. F.; Lapouyade, R.; Mathevet, R.; Jonusauskas, G.; Rulliere, C. *New. J. Chem.* **1996**, *20*, 861.

Chapter 4

Solvation dynamics in room temperature ionic liquids

The present chapter provides steady state and time-dependent fluorescence behavior of three probe molecules, C153, PRODAN and AP in several room temperature ionic liquids (RTILs). The polarity of these liquid salts in $E_T(30)$ and E_T^N scale has been estimated from the steady state fluorescence spectral data. The solvation dynamics has been studied from the temporal behavior of fluorescence. The observed dynamics in RTILs have been found to occur on two different time scales. The result has been attributed to the translational motion of the ion and ion-pair present in the system.

4.1. Introduction

Study of the time-dependent response of the solvent molecules to a newly created charge distribution in a dissolved solute has been an attractive topic of investigation for several years.[1-8] Experimentally, the time-dependent shift of the fluorescence spectrum of a probe molecule in polar media is quantitatively measured following excitation by an ultra-short laser pulse to obtain information on the solvation dynamics. So far the interest was confined to various conventional solvents[9-25] and organized assemblies in water.[3,26-33] A bi-phasic solvation dynamics with relatively slow relaxation time has been reported in molten salt at high temperature[34-37] and ionic salt solutions.[38,39]

We have studied the solvation dynamics in several RTILs that are moderate to highly viscous liquids at ambient temperature.[40-42] To the best of our knowledge, these are the first studies of this kind in RTILs. These studies are motivated by the fact that the RTILs are sufficiently polar and the polarity of these liquids can be tuned to some extent using different combinations of the constituting anion and cation of the salts. .[43-46] Moreover, it is possible to have RTILs with a range of viscosity values by simply adjusting the alkyl chain length attached to the cationic component and using different anions in the salts.[47,48] All the RTILs selected in our studies are optically clean in the area of interest. We have synthesized 1-butyl-3-methylimidazolium [BMIM] and 1-ethyl-3-methylimidazolium [EMIM] cation based RTILs with four fluorinated anions, $[BF_4]$, $[CF_3COO]$, $[(CF_3SO_2)_2N]$ and $[PF_6]$ for their wide liquid range, air and water stability at ambient temperature (Fig. 4.1).[†] Table 4.1 summarizes some of the physical properties of the prepared RTILs.

It is evident from Table 4.1 that the present RTILs can be broadly categorized in three groups on the basis of their water miscibility. Both the $[CF_3COO]$ salts and $[EMIM][BF_4]$ are completely miscible in water whereas the $[(CF_3SO_2)_2N]$ and $[PF_6]$ salts are hydrophobic in nature. On the other hand, $[BMIM][BF_4]$ is water soluble above 5-6 ^{0}C but produces a bi-phasic mixture below this temperature.[49,50] Even though the $[CF_3COO]$ and $[BF_4]$ salts are much more hygroscopic compared to those based on $[PF_6]$ and $[(CF_3SO_2)_2N]$, all of them are highly stable and less corrosive in nature.[47,51]

[†] $[EMIM][PF_6]$ is a solid (mp = 60^{0}C), unsuitable for our studies at room temperature.

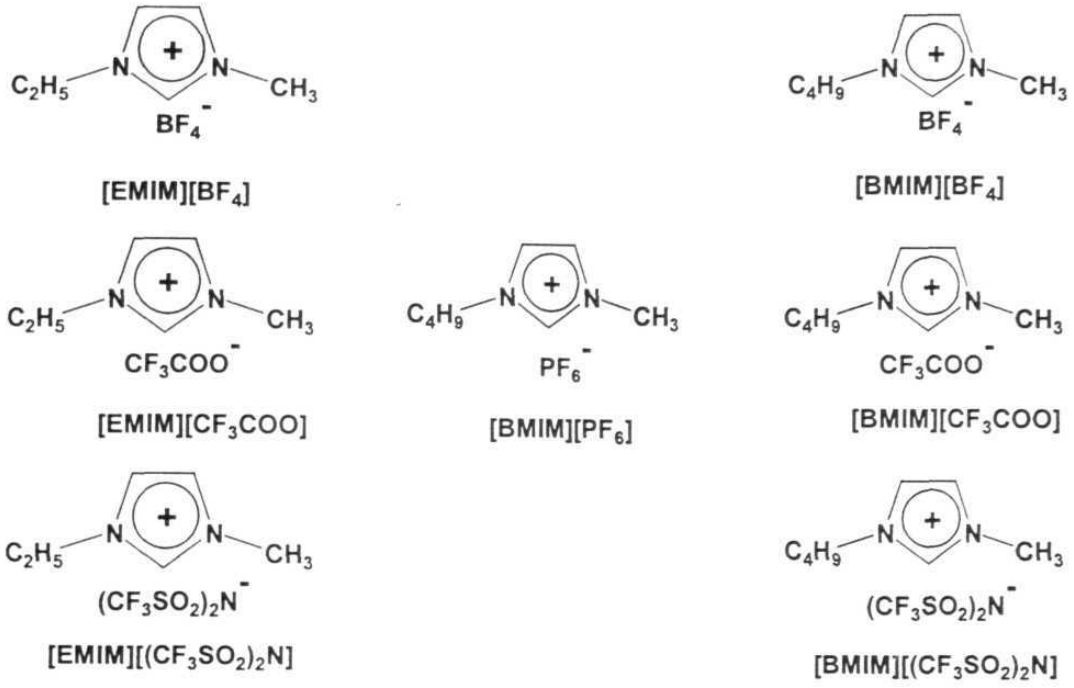

Fig. 4.1.

Table 4.1. *Physical properties of room temperature ionic liquids*

RTIL	Water content at saturation (% w/w)	mp (^{0}C)	Viscosity (cp)	Density (g.cm^{-3})
[BMIM][BF_4][a, c]	2.5	-81	154	1.2
[EMIM][BF_4][a]	s	6	66.5	1.3
[BMIM][CF_3COO][b]	s	-	73	1.2
[EMIM][CF_3COO][b]	s	-14	35	1.3
[BMIM][$(CF_3SO_2)_2N$][b]	1.4	-4	52	1.4
[EMIM][$(CF_3SO_2)_2N$][b]	1.4	-3	34	1.5
[BMIM][PF_6][a, c]	1.0	10	371	1.4
[BMIM]Cl[a]	s	65	142000	1.1

all data are at ~20 ^{0}C, s. water soluble, [a] from ref. 48, [b] from ref. 47, [c] from ref. 49

The inherent structures of the RTILs can be better viewed as a supramolecular three-dimensional network of cation and anion stabilized by different weak interactions.[49] Especially, the viscosity of these salts is largely controlled by van der Waals interaction and hydrogen-bonding ability of the ions.[47,48] Fluorination in the anion helps the delocalization of negative charges that reduces hydrogen-bonding capability and lowers the viscosity of the liquid. The effect is remarkable when one replaces the chloride ion, for which the hydrogen bonding is much more pronounced, by fluorinated anion (vide Table 4.1). On the other hand, a longer alkyl chain in the constituting cation increases the van der Waals interaction between the aliphatic alkyl chains, which leads to an enhanced viscosity of the salt.[47,48] This is why the viscosities of the [BMIM] salts are higher than that of the [EMIM] salts.

The polarity of the RTILs has already been examined by several research groups using different solvatochromic probe molecules.[43-46,52-54] The estimated polarity has been found to be dependent on the specific probe molecule used in that study. This indicates that the concept of polarity is much more complex in RTILs, where the constituting species are ions, rather than molecular dipoles present in conventional solvents. For precise determination of the polarity one should consider multiple interactions present in these liquids. Because of specific interaction between the probe molecule and the RTILs, the difference in polarity would be expected by altering the probes. However, all the previous results indicate that the polarity of RTILs are comparable to that of different lower alcohols and controlled by the nature of the cation present in it.

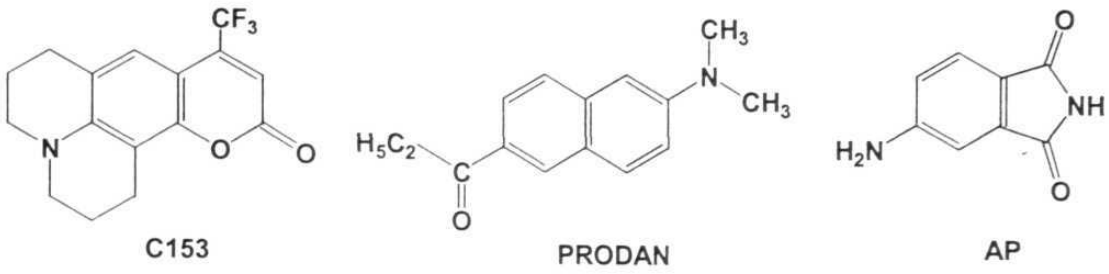

Fig. 4.2.

To explore further we have measured the polarity of the RTILs using three electron donor-acceptor (EDA) molecules, C153, PRODAN, AP (Fig. 4.2) and expressed the polarity values in two popular polarity scales, $E_T(30)$ and E_T^N, commonly used for the conventional solvents.[55] The time-dependent Stokes shift exhibited by these molecules, after excitation with an ultra-short laser pulse, has been used to find out the dynamical response of these new media around the photoexcited molecules. The idea behind using a number of probes for the study of solvation dynamics is to examine whether the solvation time is dependent on the nature of the probe molecule. In the coumarin dye series, C153 has been extensively used as a probe for the study of solvation dynamics in a variety of media.[56,57] The molecule has a rigid structure and the intramolecular charge transfer fluorescence band is highly sensitive to the polarity of the medium. Also, the $S_0 \leftrightarrow S_1$ transition of C153 is uncomplicated by other nearby transition or interfering reactions. A recent time-resolved dielectric loss measurement has indicated that the change in the dipole moment of the molecule on electronic excitation lies between 4.9 and 5.4 D.[58]

PRODAN is another extensively used probe molecule for the measurement of the microscopic polarity of various chemical and biological media.[22,59-68] That the location of the fluorescence maximum of PRODAN is extremely sensitive to the polarity of the medium is evident from the fact that the molecule shows a red shift of ~130 nm of λ_{max} when the medium is changed from cyclohexane to water.[59] Though the hypersensitivity of the fluorescence maximum of PRODAN was thought to be due to the twisted intra-molecular charge transfer (TICT) nature of the emitting state,[69-71] a recent study suggests that the change in the dipole moment on excitation of the system is rather low (around 4.4 – 5.0 D) and the molecule emits from a locally excited state. Hydrogen bonding interaction seems to play a major role in dictating the location of the emitting state in alcoholic or aqueous media.[72]

The photophysics of AP is also very well studied[73-87] This molecule also exhibits highly sensitive fluorescence properties. The fluorescence maximum shows a large Stokes shift on increase of the polarity of the medium. High quantum yield, long fluorescence lifetime, well separated ground and first excited electronic state and extreme sensitivity towards the polarity of the solvents makes it an attractive choice for studying the solvation dynamics for several years.[2,3,20,22,30,39,88-91]

4.2. Results and discussion

4.2.1. Steady state measurement

A broad structureless absorption and emission band, very similar to those observed in conventional polar solvents, has been observed for all three probe molecules in all RTILs. Typical fluorescence spectra of the three probe molecules in [BMIM][$(CF_3SO_2)_2N$] are shown in Fig. 4.3.

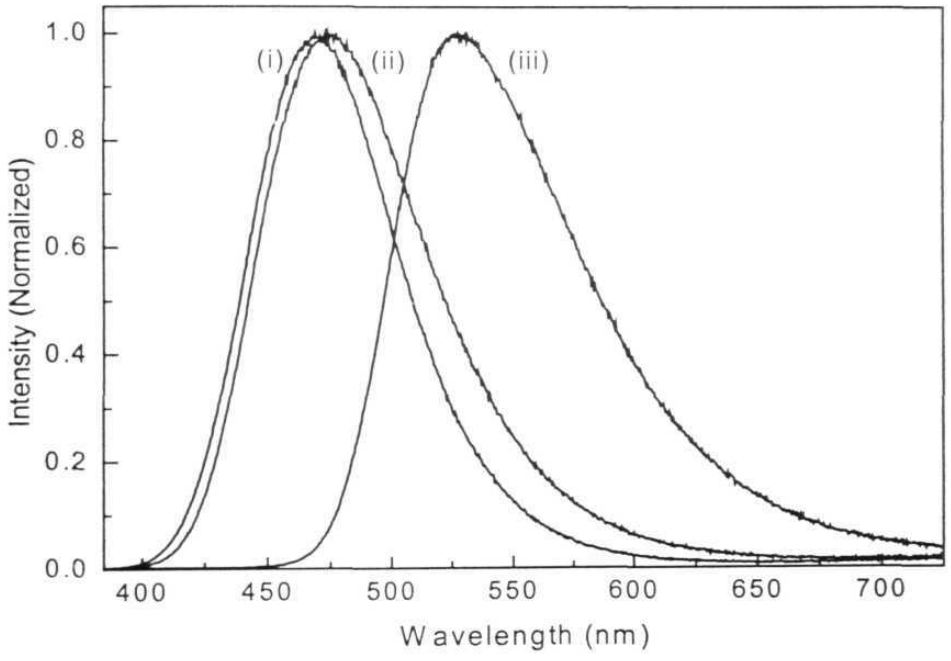

Fig. 4.3. *Steady state fluorescence spectra of (i) PRODAN, (ii) AP and (iii) C153 in [BMIM][$(CF_3SO_2)_2N$]. The excitation wavelength was 375 nm in all cases. All three spectra were corrected for the instrumental response.*

Table 4.2. *Fluorescence properties of the probe molecules in RTILs*[*]

RTIL	C153			PRODAN			AP		
	λ_{abs}^{max} (nm)	λ_{flu}^{max} (nm)	τ (ns)	λ_{abs}^{max} (nm)	λ_{flu}^{max} (nm)	τ (ns)	λ_{abs}^{max} (nm)	λ_{flu}^{max} (nm)	τ (ns)
[BMIM][BF_4]	435	537	6.8	378	475	4.2	371	483	24.8
[EMIM][BF_4]	433	538	5.7	366	477	4.1	370	486	15.1
[BMIM][CF_3COO]	427	531	6.0	351	472	3.9	376	499	24.7
[EMIM][CF_3COO]	428	535	5.0	349	476	3.6	372	499	11.8
[BMIM][$(CF_3SO_2)_2N$]	426	527	6.1	354	470	4.0	361	475	24.4
[EMIM][$(CF_3SO_2)_2N$]	424	530	6.1	349	472	3.9	361	476	23.5
[BMIM][PF_6]	424	531	6.0	358	470	3.9	353	471	22.4

[*]excitation wavelength was 375 nm in all cases and fluorescence lifetime (τ) was recorded by monitoring the decay at corresponding emission maximum at room temperature.

The absorption and emission wavelength maxima along with the measured fluorescence decay times of the various systems in different RTILs have been collected in Table 4.2. The steady state data indicates a slightly red-shifted absorption band of the molecules in hydrophilic [BF_4] and [CF_3COO] salts compared to that in hydrophobic [$(CF_3SO_2)_2N$] and [PF_6] RTILs. A similar solvatochromic shift has also been noticed in the fluorescence behavior of the molecules as well.

Polarity of these media has been estimated in terms of the microscopic polarity parameters $E_T(30)$ and E_T^N.[55] The $E_T(30)$ values have been estimated from the measured $\bar{\nu}_{flu}^{max}$ (wavenumber corresponding to emission maximum) values in the ionic liquids, using parameters obtained from the linear relationship between $\bar{\nu}_{flu}^{max}$ values of the same probe and the $E_T(30)$ values in several conventional solvents. Normalized E_T^N value of each liquid salt has been calculated from the $E_T(30)$ value of the corresponding RTIL using equation 2.6. The results are collected in Table 4.3.

Table 4.3. *Estimated polarity of the ionic liquids in the $E_T(30)$ and E_T^N scale*

RTIL	Solvent parameters estimated from					
	C153		PRODAN		AP	
	$E_T(30)$ kcal mol^{-1}	E_T^N	$E_T(30)$ kcal mol^{-1}	E_T^N	$E_T(30)$ kcal mol^{-1}	E_T^N
[BMIM][BF_4]	48.9	0.56	47.1	0.51	50.1	0.60
[EMIM][BF_4]	49.1	0.57	47.5	0.52	50.8	0.62
[BMIM][CF_3COO]	47.9	0.53	46.5	0.49	53.7	0.71
[EMIM][CF_3COO]	48.6	0.55	47.3	0.51	53.7	0.71
[BMIM][$(CF_3SO_2)_2N$]	47.2	0.51	46.1	0.47	48.2	0.54
[EMIM][$(CF_3SO_2)_2N$]	47.7	0.53	46.5	0.49	48.5	0.55
[BMIM][PF_6]	47.9	0.53	46.1	0.48	47.2	0.51

Table 4.4. *Comparative polarity of the RTILs and conventional solvents*

RTIL	Average $E_T(30)$ kcal mol^{-1}	E_T^N	Conventional solvent[d]	$E_T(30)$ kcal mol^{-1}	E_T^N
[BMIM][BF_4]	48.7	0.56	Acetonitrile	45.6	0.46
[EMIM][BF_4]	49.1	0.57	2-Butanol	47.1	0.51
[BMIM][CF_3COO]	49.4	0.58	2-Propanol	48.4	0.55
[EMIM][CF_3COO]	49.9	0.59	1-Pentanol	49.1	0.57
[BMIM][$(CF_3SO_2)_2N$]	47.2	0.51	1-Butanol	50.2	0.60
[EMIM][$(CF_3SO_2)_2N$]	47.6	0.52	Ethanol	51.9	0.65
[BMIM][PF_6]	47.1	0.51	Methanol	55.4	0.76

[d] from ref. 55

As expected, the polarity of a given medium as estimated by different probes is slightly different. This is why an average value of the polarity of each liquid has been calculated from these data and these results are presented in Table 4.4. Even though the minimum value of polarity has been observed with PRODAN and the maximum value with AP (except [BMIM][PF_6]), the data suggest that all the liquid salts are more polar than acetonitrile ($E_T(30)$ of 45.6; $E_T^N = 0.46$), but much less polar than methanol ($E_T(30)$ of 55.4; $E_T^N = 0.76$). This is illustrated in Fig. 4.4 with the help of the fluorescence spectra of PRODAN in four RTILs. Clearly the spectra of PRODAN in RTILs lie between those in acetonitrile and methanol. The polarity of the RTILs resembles more like that of the lower alcohols. More specifically, [BMIM][$(CF_3SO_2)_2N$] and [BMIM][PF_6] are as polar as 2-butanol ($E_T(30) = 47.1$; $E_T^N = 0.51$), whereas [BMIM][BF_4] and

[EMIM][BF_4] are in between 2-propanol ($E_T(30)$ = 48.4; E_T^N = 0.55) and 1-pentanol ($E_T(30)$ = 49.1; E_T^N = 0.57). Our result suggests a higher polarity (in between 1-pentanol and 1-butanol) for both [BMIM][CF_3COO] and [EMIM][CF_3COO]. This could be due to slightly hygroscopic nature of these salts.

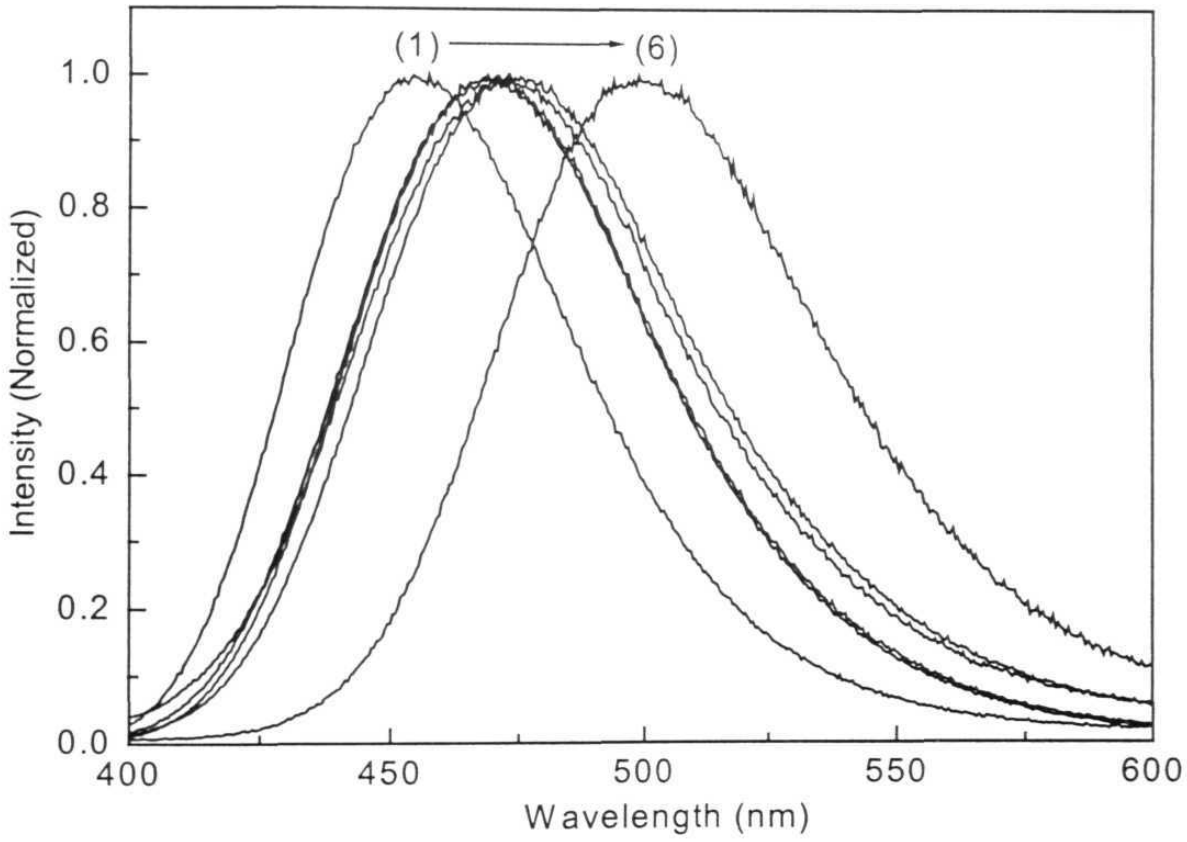

Fig. 4.4. *Steady state fluorescence spectra of PRODAN, in (1) acetonitrile, (2) [BMIM][$(CF_3SO_2)_2N$], (3) [BMIM][PF_6], (4) [BMIM][CF_3COO], (5) [BMIM][BF_4] and (6) methanol respectively. The excitation wavelength was 375 nm in all cases. All spectra were corrected for the instrumental response.*

All three probe molecules report that the butyl salts are marginally less polar than ethyl salts. This is in agreement with the presence of a relatively longer alkyl chain in [BMIM] salts. It is worth mentioning here that our estimated polarities of the ionic liquids are in fairly good agreement with those measured by several other groups[43-46,52-54] and the observed fluorescence band shapes in RTILs are quite similar to that in polar protic and aprotic solvents.

4.2.2. Time resolved studies

The time-resolved fluorescence decay profiles of the probe molecules are found to be dependent on the monitoring wavelengths. A clear growth followed by usual decay has been observed in the fluorescence time profile (irrespective of probe molecules used) monitored at the longer wavelength of the steady state emission spectrum. However, the rise component is absent when the fluorescence is monitored at the shorter wavelength region. This indicates a continuous relaxation process of the solvent molecules around the photoexcited probe molecule in the experimental time scale. Fig. 4.5 illustrates the wavelength-dependent fluorescence decay behavior of the PRODAN and C153 in [EMIM][BF_4] and [BMIM][BF_4] respectively. Typical quality of the fit to the decay profiles of C153 in [EMIM][$(CF_3SO_2)_2N$] has been shown in Fig. 4.6.

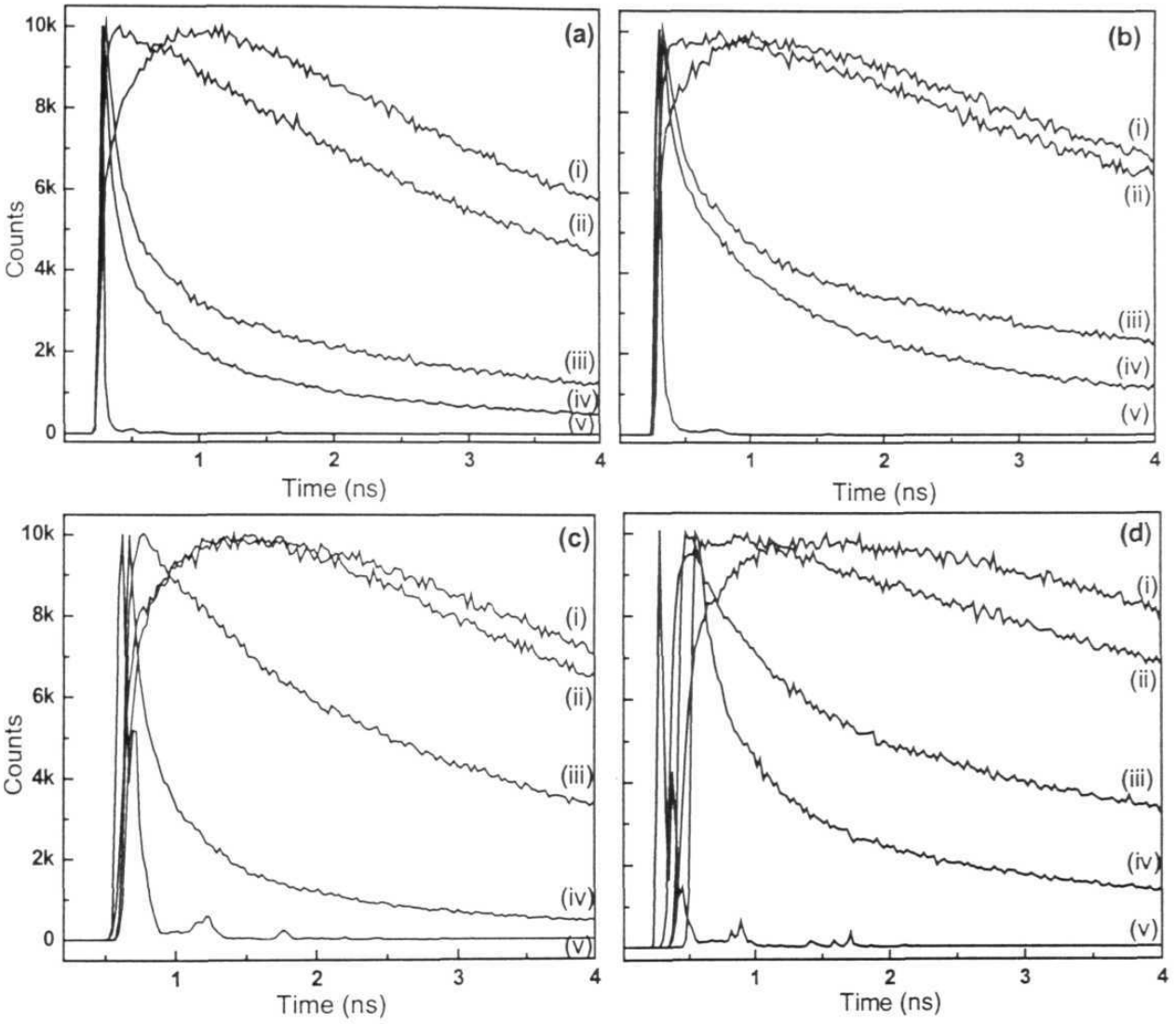

Fig. 4.5. *Time-resolved fluorescence decay behavior of PRODAN (a), C153 (b) in [EMIM][BF_4] and PRODAN (c), C153 (d) in [BMIM][BF_4] when the emission was monitored from higher wavelength to a lower one [(i) → (iv)] respectively. The excitation lamp profile (λ_{exc} = 375 nm) is shown in (v) in all cases.*

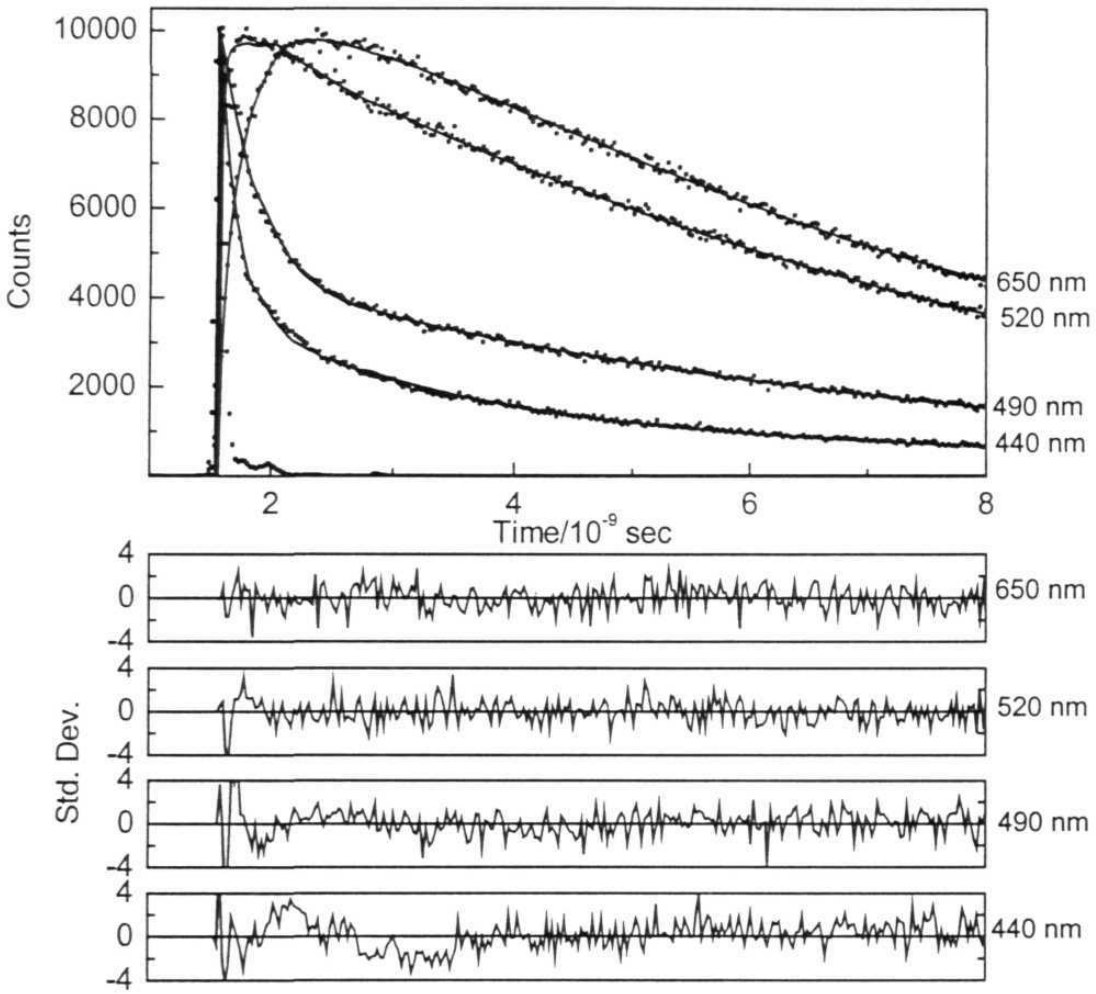

Fig. 4.6. *Fluorescence decay profiles of C153 in [EMIM][$(CF_3SO_2)_2N$] at various wavelengths along with the best fits. The excitation wavelength was 375 nm.*

The time-resolved emission spectra (TRES) of the molecules, constructed from the decay profiles by following the procedure stated in chapter 2 (*vide* Sec. 2.3), are shown in Fig. 4.7 and 4.8 as points. The solid lines represent the best-fitted curve obtained from lognormal line shape function known for its excellent representation of the fluorescence band shape in polar media.[19,92] The peak frequency of each spectrum has been extracted to construct the solvent spectral shift correlation function, C(t), which is defined as[93,94]

$$C(t) = \frac{\bar{\nu}(t) - \bar{\nu}(\infty)}{\bar{\nu}(0) - \bar{\nu}(\infty)}$$

The time dependence of C(t) is shown in Fig. 4.9 along with the best fit to the data points. In all cases, a biexponential decay function gives a reasonably good fit throughout the time window. Even though Barbara[95] and Huppert[34-37] preferred to use a stretched factor, β to improve their biexponential fitting parameters, we did not find any significant improvement to the quality of the fit by varying the β value from 0.4 to 0.9 in our cases. The relaxation times obtained from the fittings to the data are collected in Table 4.5. The salient features of our observation can be summarized as follows:

Although the overall relaxation in RTILs is slow, there appears to be an initial part of the solvation that occurs within 25 ps, the effective time resolution of our instrumental setup. This is evident from the fact that we have observed a typical time-dependent spectral shift of ~900 cm^{-1} for C153 in [BMIM][BF_4]. As

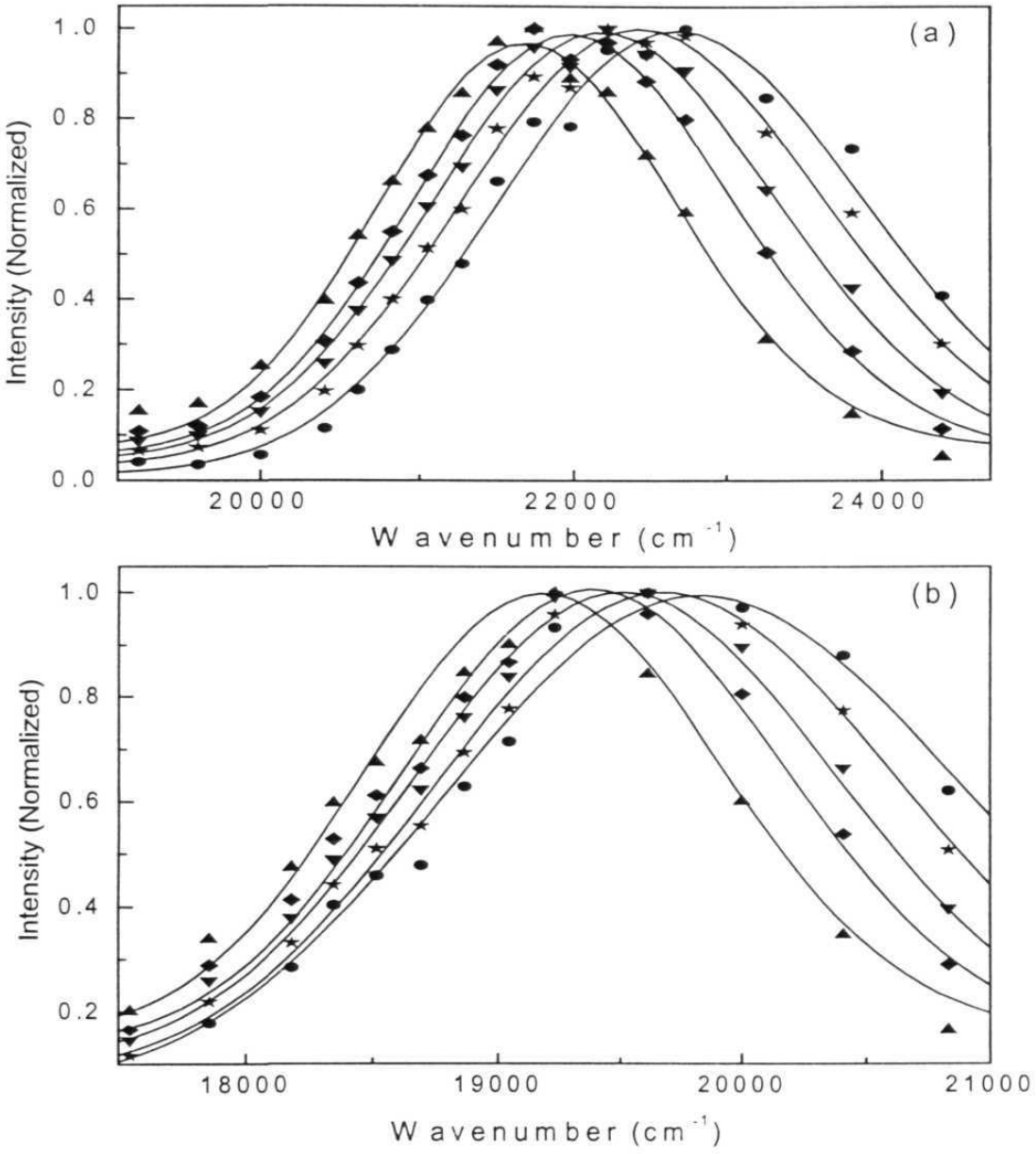

Fig. 4.7. *Time-resolved emission spectra (normalized at the peak) of (a) PRODAN and (b) C153 in [BMIM][BF_4] at 0 ps (●), 100 ps (★), 250 ps (▼), 500 ps (♦) and 2000 ps (▲) respectively.*

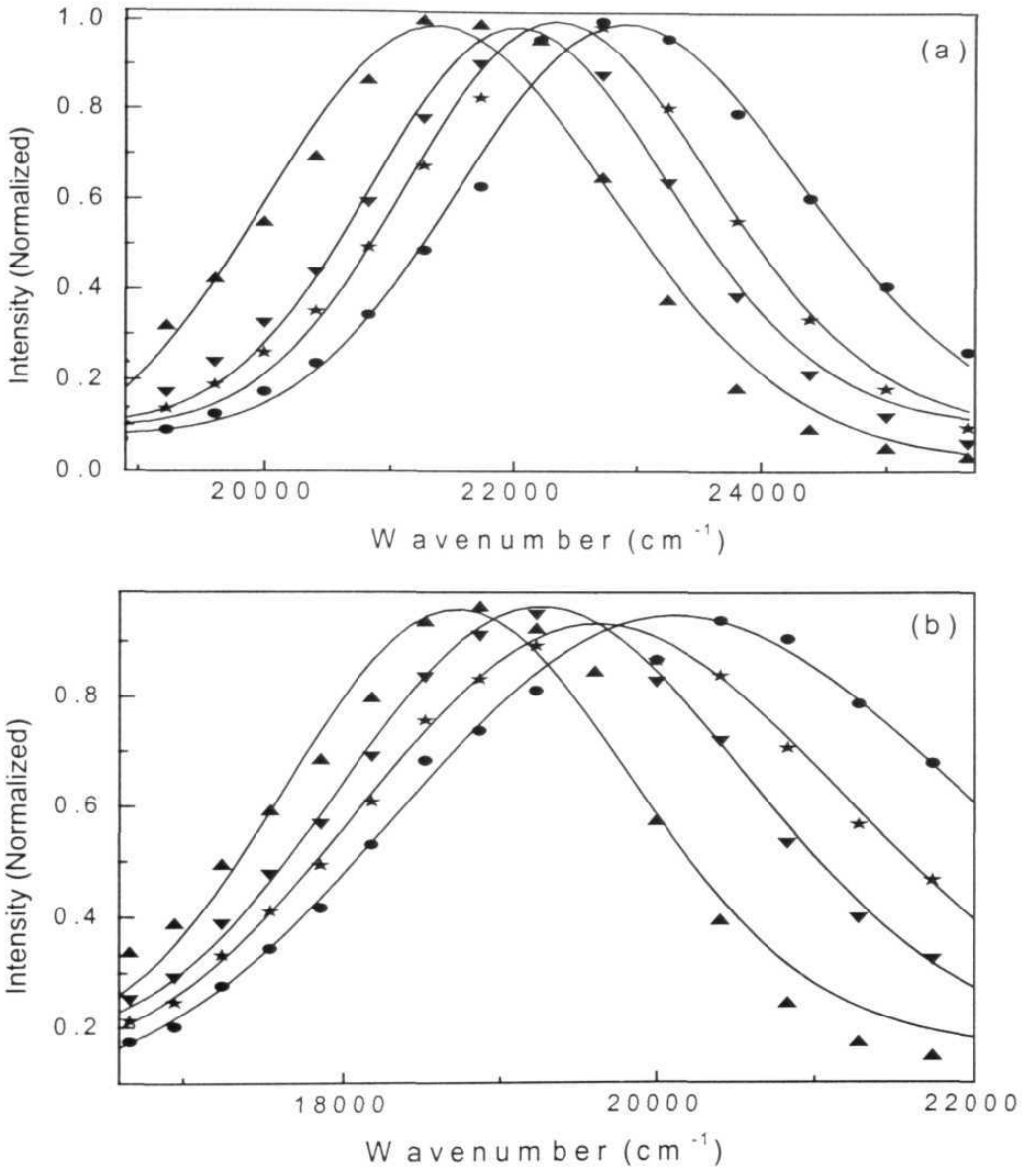

Fig. 4.8. *Time-resolved emission spectra (normalized at the peak) of (a) PRODAN and (b) C153 in [BMIM][CF_3COO] at 0 ps (●), 100 ps (★), 250 ps (▼), and 2000 ps (▲) respectively.*

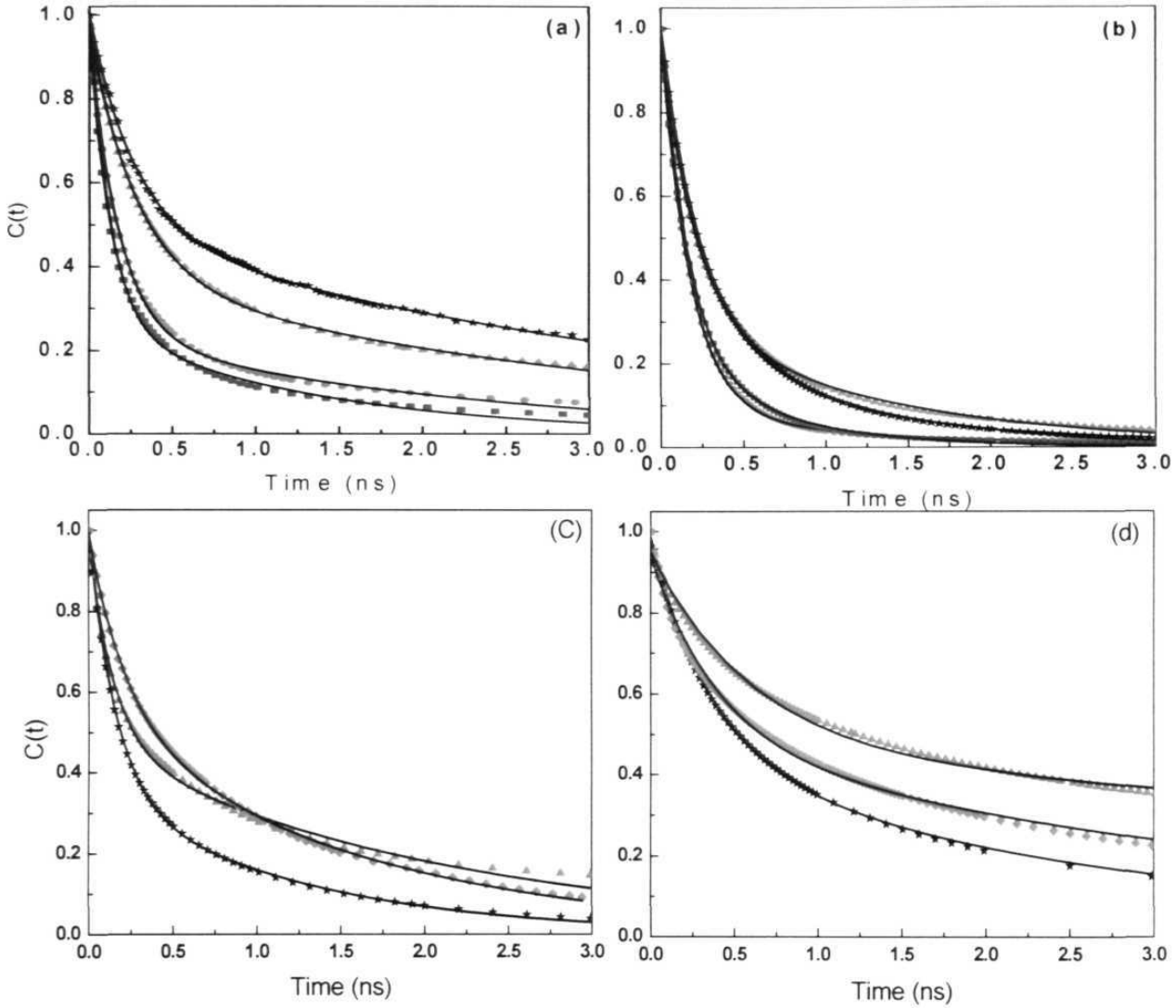

Fig. 4.9. *The time dependence of C(t) in various RTILs. The points denote the actual values of C(t), while the solid lines represent the biexponential fits.*
(a) C153 in [BMIM][BF_4] (★) and [EMIM][BF_4] (■), PRODAN in [BMIM][BF_4] (▲) and [EMIM][BF_4] (●).
(b) C153 in [BMIM][$(CF_3SO_2)_2N$] (★) and [EMIM][$(CF_3SO_2)_2N$] (■), PRODAN in [BMIM][$(CF_3SO_2)_2N$] (▲) and [EMIM][$(CF_3SO_2)_2N$] (●)
(c) C153 (★), PRODAN(▲) and AP(♦) in [BMIM][CF_3COO]
(d) C153 (★), PRODAN(▲) and AP(♦) in [BMIM][PF_6]

the polarity of this liquid salt is close to the polarity of 2-propanol, one should have observed, according to Maroncelli and coworkers, a shift of ~1900 cm^{-1} between exact t(0) and t(∞).[19,96] The fact that we are missing nearly 1000 cm^{-1} of shift at early times (and hence, the early part of the dynamics) is due to the low time resolution of the instrumental setup. This clearly indicates that the missing part of the solvation dynamics was much faster than 25 ps.

The solvation dynamics in RTILs, as observed by us, are bi-phasic in nature comprising a faster component in picosecond time scale and slower one in the nanosecond scale. Both the relaxation times depend on the bulk viscosity of the medium and the fluorescence probe molecules.

The average relaxation process is slower in butyl salts when compared with that in ethyl salts. The only exception is [EMIM][CF_3COO]. This particular salt could not be made free from parent halide because of its complete miscibility with water even at low temperature. We avoided using silver halide, as in our experience trace amount of silver salt was sufficient to destroy the fluorescence, presumably because of some photochemical reaction. The presence of unreacted halide enhances the solvent viscosity thereby slowing down the relaxation process in this medium. Interestingly, the amplitude of the slow component decreases with decrease in the size of the cation for salts with a common anion (except CF_3COO salts). This behavior is quite anomalous if one considers the individual motion of ions is responsible for the solvation dynamics in RTILs.

Table 4.5. *Relaxation time as measured by different probe molecules in RTILs at 20^0C*

Medium	Probe	$\bar{\nu}_{obs}$ [a] /cm^{-1}	Relaxation Time/ps τ_1	τ_2	Amplitude a_1	a_2	$<\tau>$[b] /ps
[BMIM][BF_4]	C153	900	278	3980	0.50	0.50	2130
	PRODAN	1270	280	3330	0.62	0.38	1440
	AP	1763	360	4830	0.50	0.50	2595
[EMIM][BF_4]	C153	1420	125	1290	0.73	0.27	440
	PRODAN	1172	175	2130	0.74	0.26	680
	AP	2147	230	3470	0.67	0.33	1299
[BMIM][CF_3COO]	C153	1606	154	1200	0.63	0.37	541
	PRODAN	1852	150	2100	0.52	0.48	1086
	AP	3110	220	1580	0.45	0.55	968
[EMIM][CF_3COO]	C153	1090	240	1980	0.47	0.53	1162
	PRODAN	1740	220	2310	0.51	0.49	1244
	AP	1185	400	2710	0.47	0.53	1624
[BMIM][$(CF_3SO_2)_2N$]	C153	1562	225	980	0.67	0.33	474
	PRODAN	1300	205	1320	0.68	0.32	562
	AP	1376	145	760	0.63	0.37	373
[EMIM][$(CF_3SO_2)_2N$]	C153	1018	165	650	0.78	0.22	273
	PRODAN	830	180	1300	0.92	0.08	270
	AP	680	240	1500	0.90	0.10	366
[BMIM][PF_6]	C153	1160	355	2550	0.54	0.45	1339
	PRODAN	1940	610	12000	0.50	0.50	6305
	AP	1585	400	4075	0.50	0.50	2238

[a] $\bar{\nu}_{obs} = \bar{\nu}_0 - \bar{\nu}_\infty$ calculated from TRES ; [b]average relaxation time $<\tau>$ is defined as, $<\tau> = a_1\tau_1 + a_2\tau_2$, where $(a_1 + a_2 = 1)$.

4.2.3. Mechanism of solvation dynamics in RTILs

The first theoretical treatment on solvation dynamics was proposed by Bakshiev[97] and Mazurenko,[98] commonly referred to as 'simple continuum' model, in which the microscopic structure of the solvent is disregarded and instead, the solvent is considered as a continuous, homogeneous fluid and is characterized by bulk, frequency-dependent dielectric response function.[15,93,94,99,100] The continuum model predicts exponential solvation kinetics with a lifetime equal to the longitudinal relaxation time, τ_L of the solvent. This bulk dielectric property is related to much slower Debye relaxation time, τ_D according to the equation $\tau_L = (\varepsilon_\infty / \varepsilon_0)\ \tau_D$, where ε_∞ and ε_0 are the optical and static dielectric constants of the solvent. The other approach initially proposed by Wolynes[101] and later developed by Rips,[11,102] and Nichols and Calef,[103] recognizes the molecular nature of the solvent. In this mean spherical approximation (MSA) model, the solvent molecules are considered as dipolar hard spheres. The dynamical MSA model predicts a more complex dynamics and a range of relaxation times between τ_L and τ_D instead of a single relaxation time τ_L predicted by the continuum theory.

To elucidate different physical properties associated with RTILs, theoretical investigation started through molecular dynamical study.[104-107] Using Monte Carlo simulation Hanke and his group[104] found a preferential orientation of the chloride ion around the central region of the di-alkylimidazolium cation but the localization was less strong in the case of larger PF_6^- ion. Another recent computer simulation study in [BMIM][PF_6] has revealed

a complex and slow solvation process in RTILs on two different time scales.[108] The short time behavior has been attributed to the sampling of the local basin and the long time for the diffusion. These simulation results are quite similar to our observations. The main features of the solvation dynamics in the room temperature ionic liquids, such as the bi-phasic nature and the probe dependence of the dynamics are similar to what was observed in the case of the molten salts by Huppert and coworkers.[34-36] Hence, we attempt to interpret our results in terms of the model suggested by Huppert et al rather than using the continuum models or the MSA model, which are applicable to dynamics in molecular solvents. According to Huppert and coworkers, the bi-phasic nature of the dynamics is due to the difference in the transport properties of the cations and the anions that differ in their sizes. If Huppert's model were followed, then the short component of the dynamics has to be assigned to the motion of the smaller species i.e. the anions, while the long component is due to the motion of the relatively larger species, the cations. As the ionic solvation involves a cooperative movement of the ions, the absolute values of the two components, as pointed out by Huppert et al, are dependent on the size of the larger species, the cation. This is why the relaxation time obtained for the short and the long component in the ionic liquids are different. However, if the slow component were exclusively due to the cations, as proposed by Huppert, then one would have expected a smaller amplitude of this component with an increase in the size of the cations. The present results (*vide* Table 4.5) show exactly opposite behavior. Interestingly, even though Huppert also observed a similar behavior, no explanation was offered to account for the change of the amplitude of the two components. The amplitude

of the two components can only be accounted for if it is assumed that the fast component is solely due to the initial response of the smaller species i.e. the anions, while the long component arises due to a collective diffusion involving both the cations and the anions. The close proximity of the ions makes this mechanism more realistic than the one involving separate contribution of the ions.

4.3. Conclusion

Steady state and time-resolved fluorescence behavior of C153, PRODAN and AP in seven different room temperature ionic liquids have been studied. The steady state fluorescence behavior of three probe molecules suggests that all the ionic liquids are more polar than acetonitrile but less polar than methanol. Very little difference in the polarity of the butyl and ethyl salts could be observed even though the cationic components of the ionic liquids contain alkyl chains of different length. The probe molecules exhibit wavelength-dependent decay profiles and time-dependent Stokes shift of the fluorescence spectrum. The solvation dynamics of the probe molecules in these media, as characterized by the time-correlated spectral shift function, C(t), are biexponential in all cases consisting of a short and a long component. The average solvation time, which is found to depend on the probe molecule used, lies in the nanosecond time scale (except $[(CF_3SO_2)_2N]$ salts). Based on the observed results, the fast initial response of the bi-phasic dynamics is attributed to the motion of the relatively smaller species, the anions, while the slow component originates from the collective motion of the cations and the anions. The relatively slower relaxation time observed in [EMIM][CF_3COO] compared to the corresponding butyl salt is

most likely due to an enhanced viscosity of the solvent due to the presence of unreacted parent halide in the medium.

4.4. References

(1) Nandi, N.; Bhattacharyya, K.; Bagchi, B. *Chem. Rev.* **2000**, *100*, 2013.

(2) Bhattacharyya, K. *Acc. Chem. Res.* **2003**, *36*, 95.

(3) Bhattacharyya, K.; Bagchi, B. *J. Phys. Chem. A* **2000**, *104*, 10603.

(4) Maroncelli, M. *J. Mol. Liq.* **1993**, *57*, 1.

(5) Barbara, P. F.; Jarzeba, W. *Adv. Photochem.* **1990**, *15*, 1.

(6) Bagchi, B. *Annu. Rev. Phys. Chem.* **1989**, *40*, 115.

(7) Maroncelli, M.; Macinnis, J.; Fleming, G. R. *Science* **1989**, *243*, 1674.

(8) Simon, J. D. *Acc. Chem. Res.* **1988**, *21*, 128.

(9) Su, S. G.; Simon, J. D. *J. Phys. Chem.* **1987**, *91*, 2693.

(10) Wetzler, D. E.; Chesta, C.; Prini, R. F.; Aramendia, P. F. *J. Phys. Chem. A.* **2002**, *106*, 2390.

(11) Rips, I.; Klafter, J.; Jortner, J. *J. Chem. Phys.* **1988**, *88*, 3246.

(12) Rau, J.; Ferrante, C.; Kneuper, E.; Deeg, F. W.; Brauchle, C. *J. Phys. Chem. A.* **2001**, *105*, 5734.

(13) Pant, D.; Levinger, N. E. *J. Phys. Chem. B.* **1999**, *103*, 7846.

(14) Molotsky, T.; Koifman, N.; Huppert, D. *J. Phys. Chem. A.* **2002**, *106*, 12185.

(15) Maroncelli, M., Fleming, G. R. *J. Chem. Phys.* **1988**, *89*, 875.

(16) Maroncelli, M.; Fleming, G. R. *J. Chem. Phys.* **1988**, *89*, 5044.

(17) Krishnaji; Manish, A. *J. Chem. Phys.* **1964**, *41*, 827.

(18) Ito, N.; Kajimoto, O.; Hara, K. *J. Phys. Chem. A.* **2002**, *106*, 6024.

(19) Horng, M. L.; Gardecki, J. A.; Papazyan, A.; Maroncelli, M. *J. Phys. Chem.* **1995**, *99*, 17311.

(20) Fee, R. S.; Milsom, J. A.; Maroncelli, M. *J. Phys. Chem.* **1991**, *95*, 5170.

(21) Cichos, F.; Willert, A.; Rempel, U.; von Borczyskowski, C. *J. Phys. Chem. A.* **1997**, *101*, 8179.

(22) Chapman, C. F.; Fee, R. S.; Maroncelli, M. *J. Phys. Chem.* **1995**, *99*, 4811.

(23) Chapman, C. F.; Fee, R. S.; Maroncelli, M. *J. Phys. Chem.* **1990**, *94*, 4929.

(24) Castner, E. W., Jr.; Maroncelli, M.; Fleming, G. R. *J. Chem. Phys.* **1987**, *86*, 1090.

(25) Biswas, R.; Bagchi, B. *J. Phys. Chem. A.* **1999**, *103*, 2495.

(26) Brauns, E. B.; Madaras, M. L.; Coleman, R. S.; Murphy, C. J.; Berg, M. A. *Phys. Rev. Lett.* **2002**, *88*, 158101-1.

(27) Balasubramanian, S.; Bagchi, B. *J. Phys. Chem. B.* **2001**, *105*, 12529.

(28) Sarkar, N.; Datta, A.; Das, S.; Bhattacharyya, K. *J. Phys. Chem.* **1996**, *100*, 15483.

(29) Sarkar, N.; Das, K.; Datta, A.; Das, S.; Bhattacharyya, K. *J. Phys. Chem.* **1996**, *100*, 10523.

(30) Sen, S.; Sukul, D.; Dutta, P.; Bhattacharyya, K. *J. Phys. Chem. A.* **2001**, *105*, 10635.

(31) Sen, S.; Dutta, P.; Sukul, D.; Bhattacharyya, K. *J. Phys. Chem. A.* **2002**, *106*, 6017.

(32) Sen, S.; Sukul, D.; Dutta, P.; Bhattacharyya, K. *J. Phys. Chem. B.* **2002**, *106*, 3763.

(33) Pal, S. K.; Sukul, D.; Mandal, D.; Sen, S.; Bhattacharyya, K. *Chem. Phys. Lett.* **2000**, *327*, 91.

(34) Bart, E.; Meltsin, A.; Huppert, D. *Chem. Phys. Lett.* **1992**, *200*, 592.

(35) Bart, E.; Meltsin, A.; Huppert, D. *J. Phys. Chem.* **1994**, *98*, 3295.

(36) Bart, E.; Meltsin, A.; Huppert, D. *J. Phys. Chem.* **1994**, *98*, 10819.

(37) Bart, E.; Meltsin, A.; Huppert, D. *J. Phys. Chem.* **1995**, *99*, 9253.

(38) Argaman, R.; Molotsky, T.; Huppert, D. *J. Phys. Chem. A.* **2000**, *104*, 7934.

(39) Chapman, C. F.; Maroncelli, M. *J. Phys. Chem.* **1991**, *95*, 9095.

(40) Karmakar, R.; Samanta, A. *J. Phys. Chem. A* **2002**, *106*, 4447.

(41) Karmakar, R.; Samanta, A. *J. Phys. Chem. A.* **2002**, *106*, 6670.

(42) Karmakar, R.; Samanta, A. *Communicated for publication* **2003**.

(43) Aki, S. N. V. K.; Brennecke, J. F.; Samanta, A. *Chem. Commun.* **2001**, 413.

(44) Muldoon, M. J.; Gordon, C. M.; Dunkin, I. R. *J. Chem. Soc., Perkin Trans. 2* **2001**, *2001*, 433.

(45) Carmichael, A. J.; Seddon, K. R. *J. Phys. Org. Chem.* **2000**, *13*, 591.

(46) Fletcher, K. A.; Storey, I. A.; Hendricks, A. E.; Pandey, S.; Pandey, S. *Green Chemistry* **2001**, *3*, 210.

(47) Bonhote, P.; Dias, A. P.; Papageorgiou, N.; Kalyanasundaram, K.; Gratzel, M. *Inorg. Chem.* **1996**, *35*, 1168.

(48) Seddon, K. R.; Stark, A.; Torres, M.-J. *Personal Communication* **2001**.

(49) Dupont, J.; de Souza, R. F.; Suarez, P. A. Z. *Chem. Rev.* **2002**, *102*, 3667.

(50) Seddon, K. R.; Stark, A.; Torres, M.-J. *Pure Appl. Chem.* **2000**, *72*, 2275.

(51) Holbrey, J. D.; Seddon, K. R. *J. Chem. Soc., Dalton Trans.* **1999**, 2133.

(52) Baker, S. N.; Baker, G. A.; Kane, M. A.; Bright, F. V. *J. Phys. Chem. B.* **2001**, *105*, 9663.

(53) Baker, S. N.; Baker, G. A.; Bright, F. V. *Green Chem.* **2002**, *4*, 165.

(54) Fletcher, K. A.; Pandey, S.; Storey, I. K.; Hendricks, A. E.; Pandey, S. *Anal. Chim. Acta.* **2002**, *453*, 89.

(55) Reichardt, C. *Solvents and Solvent Effects in Organic Chemistry*; VCH: Weinheim, 1988.

(56) Becker, R. S.; Chakravorti, S.; Gartner, C. A.; Miguel, M. *J. Chem. Soc., Faraday Trans.* **1993**, *89*, 1007.

(57) Kuznetsova, N. A.; Kaliya, O. L. *Russ. Chem. Rev.* **1992**, *61*, 683.

(58) Samanta, A.; Fessenden, R. W. *J. Phys. Chem. A* **2000**, *104*, 8577.

(59) Weber, G.; Farris, J. F. *Biochemistry* **1979**, *18*, 3075.

(60) Parusel, A. *J. Chem. Soc. Faraday Trans.* **1998**, *94*, 2923.

(61) Macgregor, R. B.; Weber, G. *Nature* **1986**, *319*, 70.

(62) Lakowicz, J. R.; Balter, A. *Biophys. Chem.* **1982**, *16*, 223.

(63) Narang, U.; Jordan, J. D.; Bright, F. V.; Prasad, P. N. *J. Phys. Chem.* **1994**, *98*, 8101.

(64) Lissi, E. A.; Abuin, E. B.; Rubio, M. A.; Ceron, A. *Langmuir* **2000**, *16*, 178.

(65) Parasassi, T.; Krasnowska, E. K.; Bagatolli, L.; Gratton, E. *J. Fluoresc.* **1998**, *8*, 365.

(66) Bonder, O. P.; Rowe, E. S. *Biophys. J.* **1999**, *76*, 956.

(67) Sheffield, M. J.; Baker, B. L.; Li, D.; Owen, N. L.; Baker, M. L.; Bell, J. D. *Biochemistry* **1995**, *34*, 7796.

(68) Karukstis, K. K.; Frazier, A. A.; Loftus, C. T.; Tuan, A. S. *J. Phys. Chem. B.* **1998**, *102*, 8163.

(69) Rettig, W. *Angew. Chem. Int. Ed. Engl.* **1986**, *25*, 971.

(70) Rotkiewicz, K.; Grellmann, K. H.; Grabowski, Z. R. *Chem. Phys. Lett.* **1973**, *19*, 315.

(71) Rotkiewicz, K.; Grabowski, Z. R.; Krowczynski, A.; Kühnle, W. *J. Lumin.* **1976**, *12-13*, 877.

(72) Samanta, A.; Fessenden, R. W. *J. Phys. Chem. A* **2000**, *104*, 8972.

(73) Noukakis, N.; Suppan, P. *J. Lumin.* **1991**, *47*, 285.

(74) Karmakar, R.; Samanta, A. *J. Am. Chem. Soc.* **2001**, *123*, 3809.

(75) Laitinen, E.; Salonen, K.; Harju, T. *J. Chem. Phys.* **1996**, *104*, 6138.

(76) Ware, W. R.; Lee, S. K.; Brant, G. J.; Chow, P. P. *J. Chem. Phys.* **1971**, *54*, 4729.

(77) Aich, S.; Raha, C.; Basu, S. *J. Chem. Soc., Faraday Trans.* **1997**, *93*, 2991.

(78) Ramachandram, B.; Sankaran, N. B.; Samanta, A. *Res. Chem. Interm.* **1999**, *25*, 843.

(79) Ramachandram, B.; Samanta, A. *J. Chem. Soc., Chem. Commun.* **1997**, 1037.

(80) Saroja, G.; Ramachandram, B.; Saha, S.; Samanta, A. *J. Phys. Chem. B.* **1999**, *103*, 2906.

(81) Saroja, G.; Samanta, A. *J. Chem. Soc., Faraday Trans.* **1998**, *94*, 3141.

(82) Saroja, G.; Soujanya, T.; Ramachandram, B.; Samanta, A. *J. Fluores.* **1998**, *8*, 405.

(83) Saroja, G.; Samanta, A. *J. Chem. Soc., Faraday Trans.* **1996**, *92*, 2697.

(84) Saroja, G.; Samanta, A. *Chem. Phys. Lett.* **1995**, *246*, 506.

(85) Soujanya, T.; Krishna, T. S. R.; Samanta, A. *J. Phys. Chem.* **1992**, *96*, 8544.

(86) Soujanya, T.; Krishna, T. S. R.; Samanta, A. *J. Photochem. Photobiol. A.* **1992**, *66*, 185.

(87) Soujanya, T.; Fessenden, R. W.; Samanta, A. *J. Phys. Chem.* **1996**, *100*, 3507.

(88) Nagarajan, V.; Brearley, A. M.; Kang, T.-J.; Barbara, P. F. *J. Chem. Phys.* **1987**, *86*, 3183.

(89) Reid, P. J.; Silva, C.; Barbara, P. F. *J. Phys. Chem.* **1995**, *99*, 3554.

(90) Das, S.; Datta, A.; Bhattacharyya, K. *J. Phys. Chem. A.* **1997**, *101*, 3299.

(91) Mandal, D.; Datta, A.; Pal, S. K.; Bhattacharyya, K. *J. Phys. Chem. B.* **1998**, *102*, 9070.

(92) Maroncelli, M.; Fleming, G. R. *J. Chem. Phys.* **1990**, *92*, 3251.

(93) Bagchi, B.; Oxtoby, D. W.; Flemming, G. R. *Chem. Phys.* **1984**, *86*, 257.

(94) van der Zwan, G.; Hynes, J. T. *J. Phys. Chem.* **1985**, *89*, 4181.

(95) Kahlow, M. A.; Jarzeba, W.; Kang, T. J.; Barbara, P. F. *J. Chem. Phys.* **1989**, *90*, 151.

(96) Fee, R.; Maroncelli, M. *Chem. Phys.* **1994**, *183*, 235.

(97) Bakhshiev, N. G. *Opt. Spectrosc. (USSR)* **1964**, *16*, 446.

(98) Mazurenko, Y. T. *Opt. Spectrosc. (USSR)* **1974**, *36*, 283.

(99) Castner, E. W., Jr.; Fleming, G. R.; Bagchi, B. *Chem. Phys. Lett.* **1988**, *143*, 270.

(100) Castner, E. W., Jr.; Fleming, G. R.; Bagchi, B. *Chem. Phys. Lett.* **1988**, *148*, 269.

(101) Wolynes, P. G. *J. Chem. Phys.* **1987**, *86*, 5133.

(102) Rips, I.; Klafter, J.; Jortner, J. *J. Chem. Phys.* **1988**, *89*, 4288.

(103) Nichols, A. L., III; Calef, D. F. *J. Chem. Phys.* **1988**, *89*, 3783.

(104) Hanke, C. G.; Price, S. L.; Lynden-Bell, R. M. *Mol. Phys.* **2001**, *99*, 801.

(105) Morrow, T. I.; Maginn, E. J. *J. Phys. Chem. B.* **2002**, *106*, 12807.

(106) Andrade, J. D.; Boes, E. S.; Stassen, H. *J. Phys. Chem. B.* **2002**, *106*, 3546.

(107) Andrade, J. D.; Boes, E. S.; Stassen, H. *J. Phys. Chem. B.* **2002**, *106*, 13344.

(108) Margulis, C. J.; Stern, H. A.; Berne, B. J. *J. Phys. Chem. B.* **2002**, *106*, 12017.

Chapter 5

Intramolecular excimer formation kinetics of 1,3-bis(1-pyrenyl)propane in ionic liquids

In this chapter steady state and time-resolved fluorescence behavior of 1,3-bis(1-pyrenyl)propane (py(3)py) has been described in four different room temperature ionic liquids. A detailed analysis of the fluorescence decay profiles of the monomer and excimer has been performed in order to understand the mechanism of the formation of intramolecular excimer in room temperature ionic liquids.

5.1. Introduction

The photophysics of pyrene and py(3)py has been studied extensively in conventional solvents.[1-20] The ratio of the emission intensity of the third to the first vibronic peak of pyrene is known to be sensitive to the medium and this ratio serves as a measure of the polarity of various microheterogeneous media.[1,2] On the other hand, py(3)py (Fig. 5.1) has been an attractive model system for the study of intramolecular excimer formation.[4,6-9] The various models so far proposed to account for the excimer formation kinetics assume two kinetically different monomeric species in the ground state simultaneously forming an excimer or a single monomer forming two kinetically distinguishable excimers. It has been further indicated that the fluorescence decay parameters and steady state

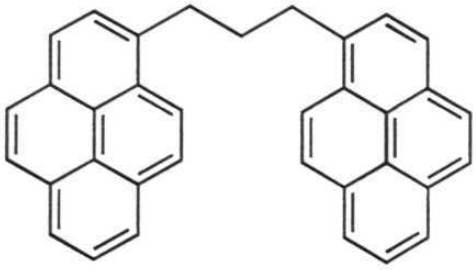

py(3)py

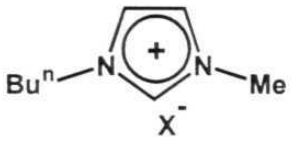

$X^- = PF_6,\ BF_4,\ (CF_3SO_2)_2N]$

[BMIM]X

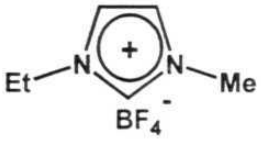

[EMIM][BF_4]

Fig. 5.1

excimer to monomer emission intensity ratio of py(3)py are strongly influenced by solvent viscosity.[4,9] As the ionic liquids are sufficiently polar and viscous at room temperature, these could be suitable media for fine-tuning the excimer formation kinetics in this probe molecule. With this in mind, we have chosen four ionic liquids with different cation-anion combinations (Fig. 5.1) such that the influence of viscosity or other factors in the excimer decay kinetics can be determined.

5.2. Results and discussion

5.2.1. Steady state studies

The absorption behavior of py(3)py in RTILs is very similar to that observed in conventional polar solvents. Fig. 5.2 shows the absorption spectra of py(3)py in [BMIM][PF_6] and acetonitrile at room temperature.

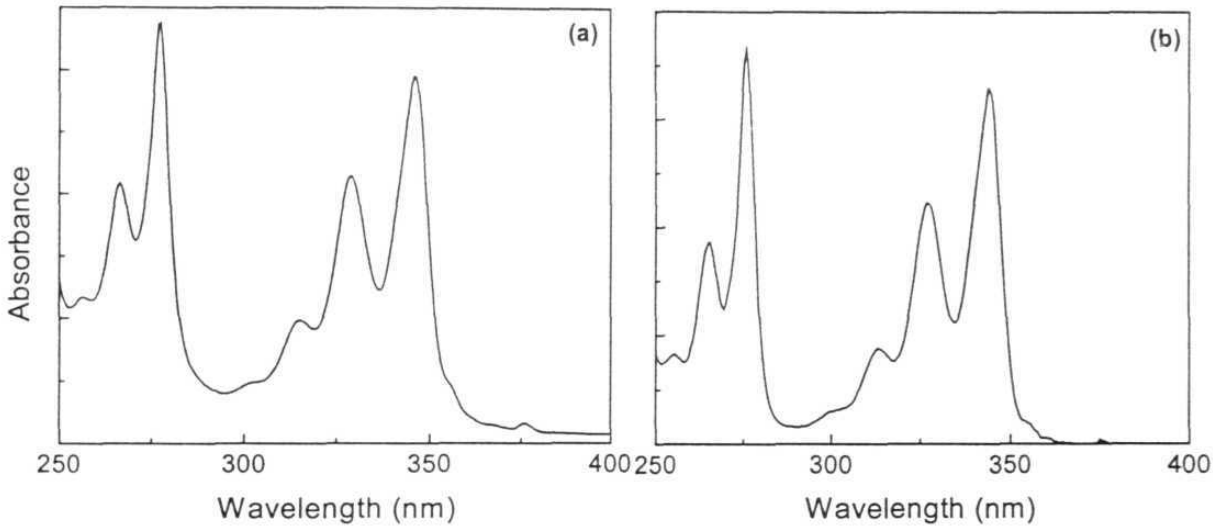

Fig. 5.2. *Absorption spectra of py(3)py in (a) [BMIM][PF_6] and (b) acetonitrile*

The fluorescence spectrum of py(3)py in RTILs consists of two well-separated emission bands (Fig. 5.3). While the structured fluorescence is due to the monomer, the broad emission band that appears at a longer wavelength must be due to the formation of intramolecular excimer resulting from the interaction between the two terminal pyrenyl moieties of the molecule. This is because the concentration of py(3)py chosen for the absorption and fluorescence studies is

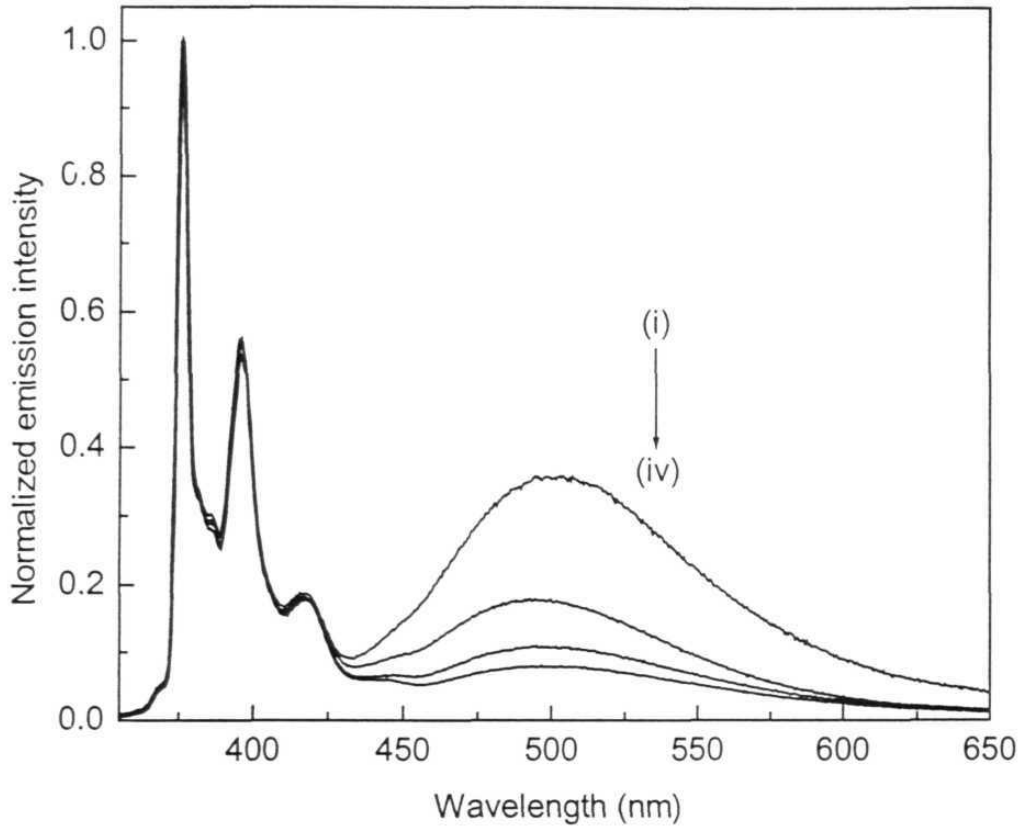

Fig. 5.3 *Fluorescence spectra of py(3)py in degassed (i) [EMIM][BF_4], (ii) [BMIM][$(CF_3SO_2)_2N$], (iii) [BMIM][BF_4] and (iv) [BMIM][PF_6] respectively. Sample concentration was 20 μM and the excitation wavelength was 345 nm in all cases. All spectra were corrected for the instrumental response and normalized at the monomer emission maxima.*

sufficiently small (~20 μM) to ensure that intermolecular interaction does not give rise to the formation of the excimer. While the wavelengths corresponding to the monomer and excimer emission peaks of py(3)py in RTILs have been found to be very similar to those observed in conventional solvents, the relative intensities of the excimer band compared to monomer emission (I_D / I_M) are rather low in all

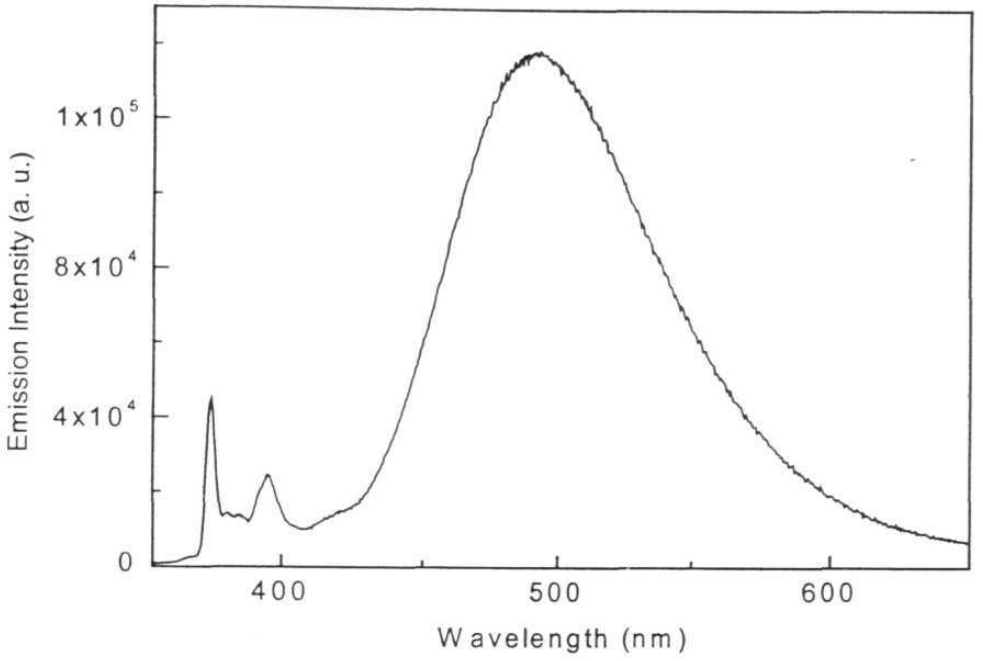

Fig. 5.4. *Fluorescence spectrum of py(3)py in degassed acetonitrile. The excitation wavelength was 345 nm. The spectrum was corrected for the instrumental response.*

Table 5.1. *Photophysical data of py(3)py in room temperature ionic liquids.*

Ionic liquid	Viscosity[a] (cp)	λ_{abs}^{max} (nm)	λ_{flu}^{max} (nm)	I_D/I_M[d]
[BMIM][PF_6]	371[b]	346.5	376	0.08
[BMIM][BF_4]	154[b]	346.5	376	0.11
[EMIM][BF_4]	66.5[b]	347	376	0.36
[BMIM][$(CF_3SO_2)_2N$]	52[c]	346	376	0.18

[a]at 20 ^{0}C; [b]ref[21] ; [c]ref [22]; [d] ratio of the excimer to monomer emission intensity measured at 500 and 376 nm respectively.

four room temperature ionic liquids. This is also evident from the data presented in Table 5.1. The reported value of (I_D/I_M) in conventional polar media is greater than unity (indicating that excimer emission is stronger than the monomer emission).[4,9] Our own measurement yielded a value of 3.1 for (I_D / I_M) in acetonitrile (Fig. 5.4). However, this value is far lower than unity in all four RTILs studied.

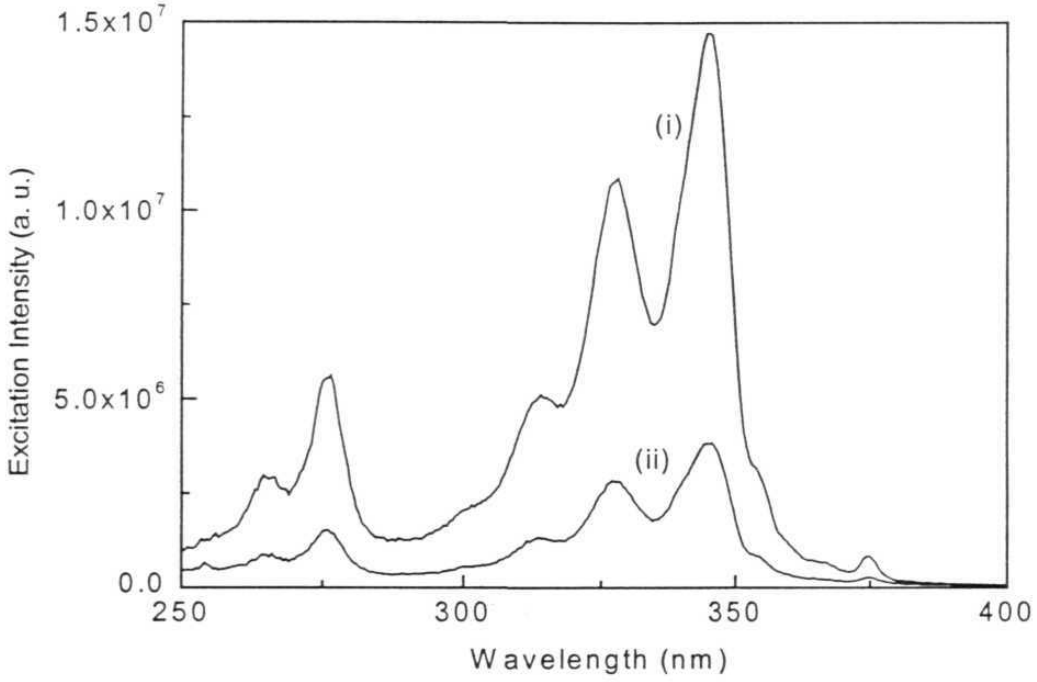

Fig. 5.5. *Fluorescence excitation spectra of py(3)py in degassed [BMIM][PF_6]. The monitoring wavelengths were (i) 420 nm and (ii) 510 nm respectively. Both the spectra were corrected for the instrumental response.*

Fig. 5.5 depicts the fluorescence excitation spectra of py(3)py in [BMIM][PF_6] obtained on monitoring the monomer and excimer emission. Since excimer

formation and dissociation dynamics are not very sensitive to the polarity of the media,[3,9] it is obviously the high viscosity of the RTILs that is responsible for relatively low fluorescence intensity of the excimer band in these media. Since a closer approach of the terminal pyrenyl moieties is essential for the formation of the excimer, the viscosity of the medium is expected to play a crucial role. However, a highly viscous medium not only slows down the formation kinetics but also can slow down its dissociation. If both the processes are affected to the same extent, one should not observe a reduction of the intensity of the excimer band. Since only time-resolved measurements can suggest to what extent the various rate constants are affected, we have studied the fluorescence decay profiles of py(3)py in RTILs monitoring the monomer and excimer bands.

5.2.2. Time resolved studies

The fluorescence decay profiles of py(3)py in each ionic liquid have been measured monitoring the monomer emission at 375 nm and the excimer emission at 510 nm. A biexponential fit to the decay profiles corresponding to the monomer emission is found to be quite satisfactory [Fig. 5.6 (a)]. No further improvement in the fit could be observed when the data is fitted to a triexponential decay function. This is evident from the plot of the residuals shown in Fig. 5.6 (b). On the other hand, a triexponential fit to the excimer decay profiles is found to be the most satisfactory one [Fig. 5.7. (a)]. A relatively larger error can be seen, especially around the peak position, when one attempts to fit the excimer data using a biexponential decay equation [Fig. 5.7. (b)]. The fluorescence decay parameters associated with the excimer emission suggest that out of three decay

times, two relatively short lifetime components are associated with negative preexponential factors (vide Table 5.2) irrespective of the nature of ionic liquid used. Another point worth mentioning is that the mismatch between the slower decay time of monomer and the rise time of excimer could not be overcome even when we used a triexponential fit to both monomer and excimer data. The decay parameters obtained from the analysis of the kinetic data are collected in Table 5.2 for all the ionic liquids.

Table 5.2. *Fluorescence decay parameters associated with monomer and excimer of py(3)py in RTILs*

Solvent	Monomer lifetime[a,b] (ns)		Excimer lifetime[a,c] (ns)		
	τ_1	τ_2	τ_1	τ_2	τ_3
[BMIM][PF_6]	10.2 (0.16)	107.9 (0.53)	18.4 (-0.35)	58.4 (-0.51)	141.1 (1.05)
[BMIM][BF_4]	8.8 (0.10)	94.4 (0.49)	8.9 (-0.08)	57.2 (-0.70)	132.2 (0.99)
[EMIM][BF_4]	6.3 (0.27)	52.7 (0.43)	8.4 (-0.07)	34.8 (-0.69)	109.9 (1.11)
[MIM][$(CF_3SO_2)_2N$]	8.3 (0.13)	84.5 (0.70)	8.5 (-0.003)	57.0 (-1.76)	127.9 (2.01)

[a]The quantity indicated within the bracket represents the preexponential factor associated with each decay component. [b]The monomer emission is monitored at 375 nm. [c]The excimer emission is monitored at 510 nm.

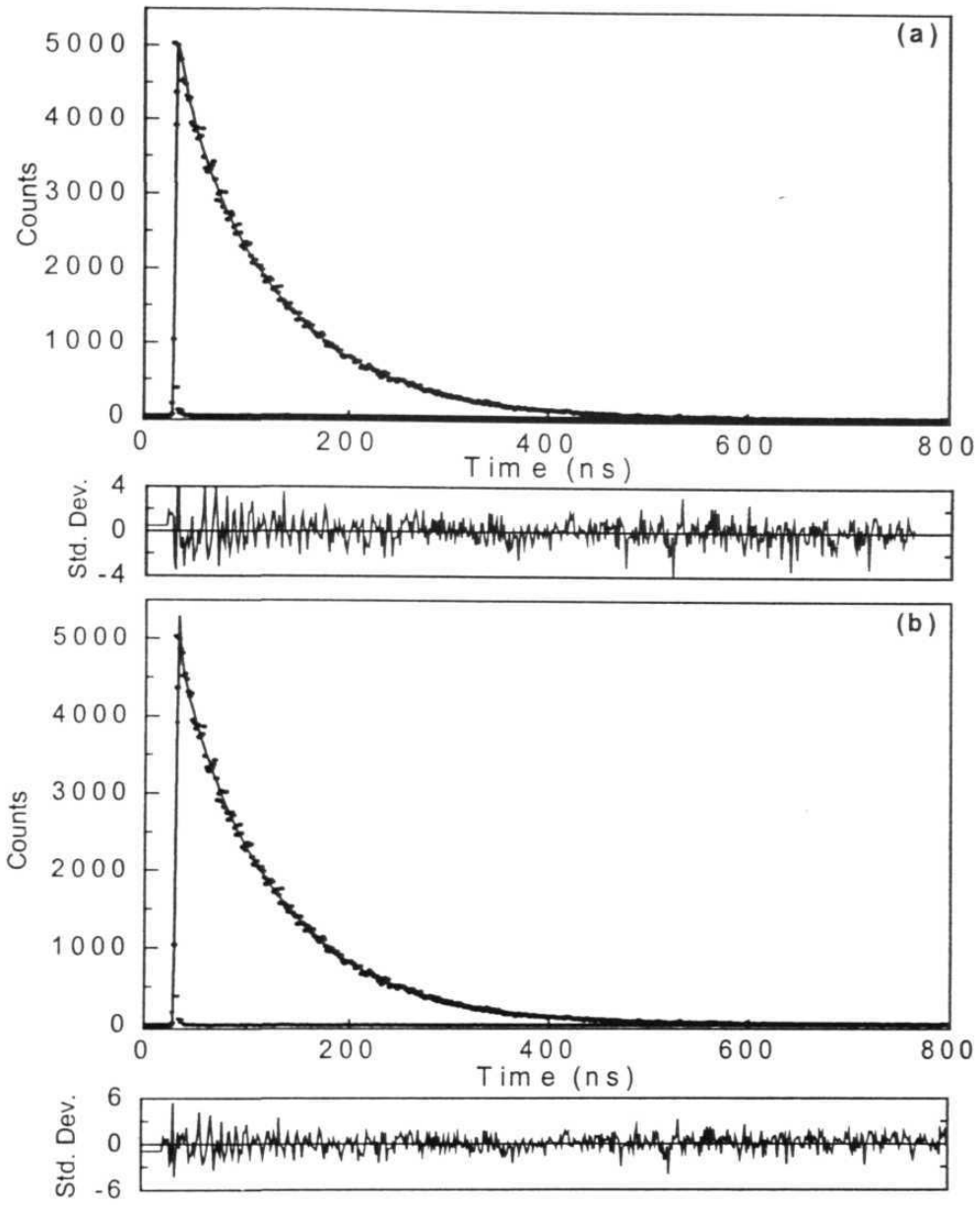

Fig. 5.6. *Typical monomer fluorescence decay profiles of py(3)py in[BMIM][BF_4] at room temperature. The decay curve was fitted to (a) biexponential and (b) triexponential decay function along with the weighted deviation. The monitoring wavelength was 375 nm in both cases. The excitation wavelength was 345 nm.*

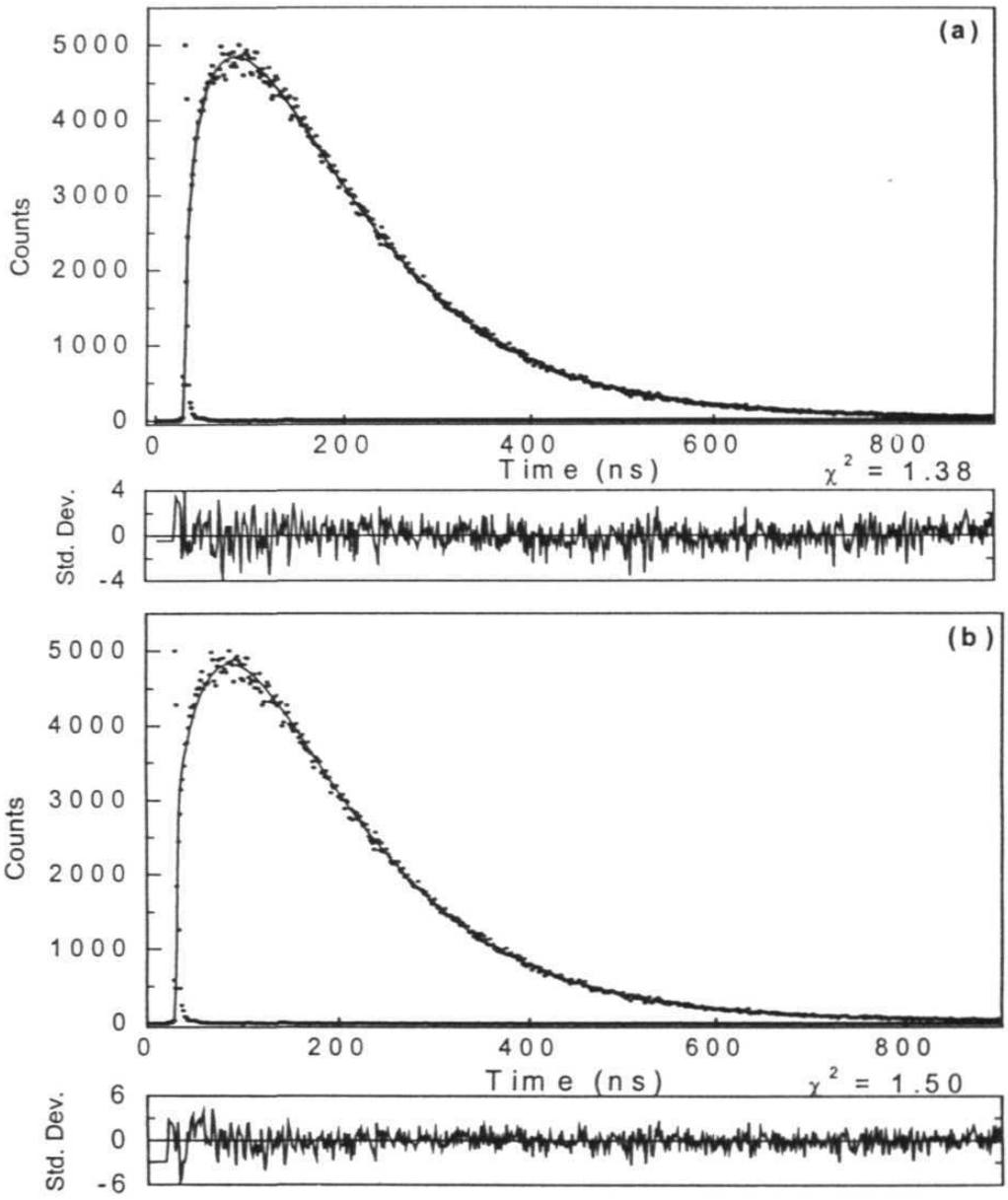

Fig. 5.7. *Typical excimer fluorescence decay profiles of py(3)py in [BMIM][BF_4] at room temperature. The decay curve was fitted to (a) triexponential and (b) biexponential decay function along with the weighted deviation. The monitoring wavelength was 510 nm in both cases. The excitation wavelength was 345 nm.*

We first attempt to determine the mechanism of the formation of the excimer in RTILs based on the measured decay parameters and then try to understand why the steady state intensity of the excimer emission is low in these media. If the formation and decay of the excimer were governed by Scheme 1, which is the most commonly used model for the analysis of the kinetic data for the formation of excimer,[8,23-25] then one would have expected a biexponential decay kinetics for both the monomer and excimer with the two lifetimes identical.

Scheme 1.

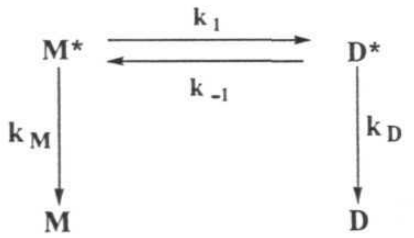

The time evolution of the emission from the locally excited state, $I_M(t)$, and from the excimer, $I_D(t)$ is then described by,

$$I_M(t) = k_{FM}\frac{\lambda_2 - X}{\lambda_2 - \lambda_1}[\exp(-\lambda_1 t) + A\exp(-\lambda_2 t)] \quad (1)$$

$$I_D(t) = \frac{k_{FD}k_1}{\lambda_2 - \lambda_1}[\exp(-\lambda_1 t) - \exp(-\lambda_2 t)] \quad (2)$$

where, $\lambda_{1,2} = \frac{1}{2}\left[X + Y \mp \sqrt{(Y-X)^2 + 4k_1k_{-1}}\right]$ and $A = \frac{X - \lambda_1}{\lambda_2 - X}$

$X = k_M + k_1 \qquad Y = k_D + k_{-1}$

However, the observed triexponential kinetics for the excimer emission clearly suggests that intramolecular excimer formation in RTILs is governed by a different mechanism.

Apart from Scheme 1, a few other models have been invoked previously. In order to account for the mismatch between the decay time of the monomer and the rise time of the excimer, Mataga et al invoked Scheme 2, according to which the excimer formation is preceded by the formation of a non-fluorescent species, (represented by B).[26]

Scheme 2.

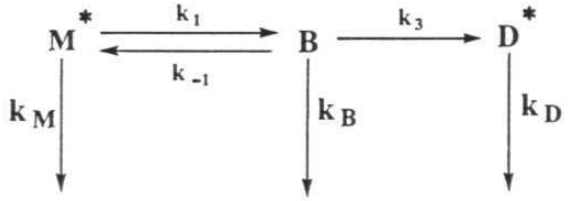

According to scheme 2, the time evolution of the monomer emission will be biexponential, similar to that obtained in scheme 1, but the excimer emission response function is expressed as a triple exponential form,

$$I_D(t) = k_{FD}k_3k_1\left[\frac{\exp(-\lambda_1 t)}{(\lambda_2-\lambda_1)(k_D-\lambda_1)} - \frac{\exp(-\lambda_2 t)}{(\lambda_2-\lambda_1)(k_D-\lambda_2)} + \frac{\exp(-k_D t)}{(k_D-\lambda_1)(k_D-\lambda_2)}\right] \quad (3)$$

where, $\lambda_{1,2} = \frac{1}{2}\left[X + Y \mp \sqrt{(Y-X)^2 + 4k_1k_{-1}}\right]$ and

$X = k_M + k_1 \qquad Y = k_B + k_3 + k_{-1}$

However, since a single rise time for the excimer emission is expected according to this model, our kinetic data could not be interpreted in terms of this scheme.

As stated earlier, excimer formation kinetics of py(3)py in conventional solvents has been previously studied by Snare et al[9] and in more detail by Zachariasse and coworkers.[4,6] While Zachariasse and coworkers considered two possibilities, two excited monomers producing a single excimer and one excited monomer giving rise to two excimers, Snare et al interpreted their kinetic data assuming the presence of two dominant conformations of the molecule (M(1) and M(2) in Scheme 3) in the ground state, which on electronic excitation gave the same excimer (D*) with two different rate constants (k_1 and k_2 respectively). Snare et al did not consider the back reaction (the dissociation of the excimer into the monomer) for the analysis of their data, though Zachariasse et al pointed out the importance of the back reaction in less viscous media. In the case of viscous solvents (or in solvents at low temperature), it was, however, found that the back reaction could be neglected.[4,27] Interestingly, Van der Auweraer et al invoked a very similar scheme earlier to account for intramolecular exciplex formation in ω-phenyl-α-*N,N*-dimethylaminoalkanes[27,28] and Todesco et al. in intramolecular excimer formation in bis(α-naphthylmethyl)ether.[29]

Scheme 3.

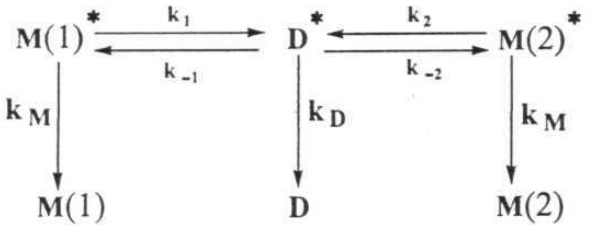

Based on the above discussion, we now examine whether our kinetic data of py(3)py in RTILs is consistent with Scheme 3. While doing so we neglect the back reactions taking into consideration the existing literature and the high viscosity (vide Table 5.1) of the RTILs.[4,27] Neglecting the back reaction and assuming an identical value of k_M for both the monomers, the time dependence of the monomer $I_M(t)$ and excimer $I_D(t)$ emission, according to this model*, is given by

$$I_M(t) = k_{FM}\left[f_1 \exp-(k_1 + k_M)t + f_2 \exp-(k_2 + k_M)t\right] \quad (4)$$

$$I_D(t) = \frac{k_{FD}\, k_1 f_1}{(k_D - k_1 - k_M)} \exp-(k_1 + k_M)t + \frac{k_{FD}\, k_2 f_2}{(k_D - k_2 - k_M)} \exp-(k_2 + k_M)t - \left[\frac{k_{FD}\, k_1 f_1}{(k_D - k_1 - k_M)} + \frac{k_{FD}\, k_2 f_2}{(k_D - k_2 - k_M)}\right] \exp-(k_D t) \quad (5)$$

where, f_1 and f_2 are the fractions of the molecule originally present in M(1) and M(2) form respectively, k_M is the sum of the radiative (k_{FM}) and nonradiative (k_{IM}) rate constants of the monomer, k_{FD} is the radiative rate constant for the excimer and the other notations are as indicated in Scheme 3. Therefore, a biexponential decay kinetics for the monomer and a triexponential decay kinetics for the excimer (with two components having negative preexponential factors), as observed here, can be accounted for in terms of Scheme 3 when the back reaction from the excimer to the monomer is neglected. It should be noted here that consideration of the back reaction would have resulted in a more complex kinetics

* Derivation of equation (4) and (5) from scheme 3 has been given in appendix 2.

(with four decay times each for the monomer and the excimer when the excimers are non-degenerate and for degenerate excimer three decay times in each case) than what we have observed here.

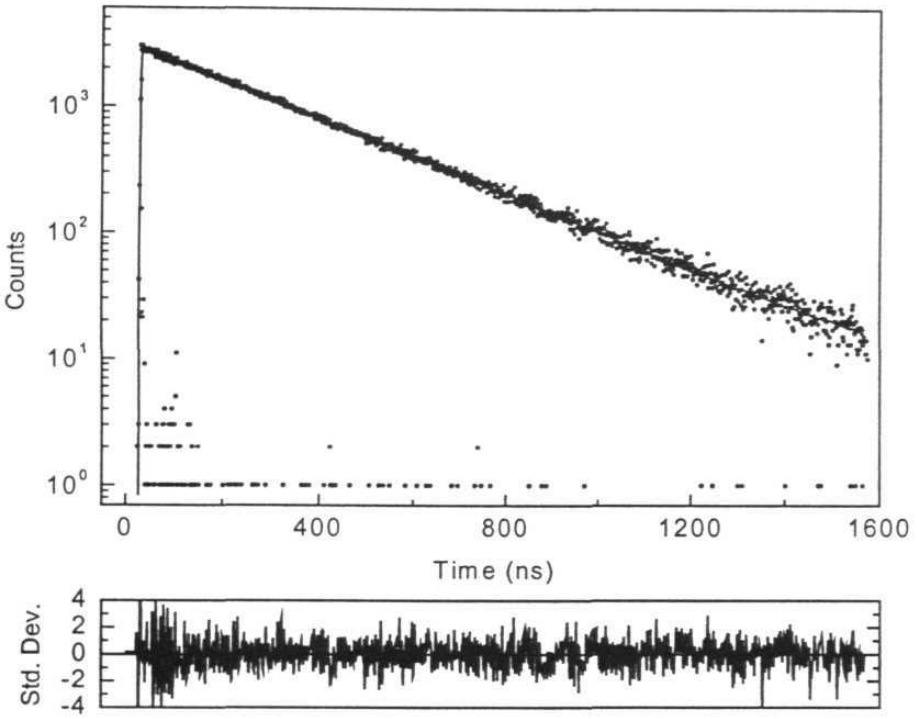

Fig. 5.8. *Fluorescence decay profile of pyrene in [BMIM][PF_6] at room temperature. The decay curve was fitted to single exponential decay equation along with the weighted deviation. The monitoring wavelength was 390 nm and the excitation wavelength was 335 nm.*

We have estimated the fractions f_1 and f_2 from the preexponential factors associated with the monomer decay parameters. One can evaluate the two rate constants, k_1 and k_2, either from the two lifetimes (τ_1, τ_2) associated with the monomer or from the two growing components of the excimer. However, since the τ_1 (or τ_2) values, as obtained from the monomer and excimer kinetics, are

slightly different, we have taken the average of the two τ_1 values (or τ_2 values) for the estimation of the rate constants k_1 and k_2. The averaged τ_1 and τ_2 gave us (k_1 + k_M) and (k_2 + k_M), respectively. The individual excimer formation rate constants, k_1 and k_2 have been evaluated by separately measuring the k_M values in each liquid using pyrene (~6 μM) as the reference compound. A typical decay profile of pyrene in [BMIM][PF_6] has been shown in Fig. 5.8. The other rate constant, k_D has been evaluated from the τ_3 value associated with the excimer kinetics. The estimated rate constants in various RTILs are collected in Table 5.3. It is evident that the rate of formation of the excimer from M(1) is faster than that from M(2). While in less viscous conventional solvents, the fast component is the dominant one,[4,9] it is the slower component that dominates in highly viscous RTILs. The overall rate constants for the formation of the intramolecular excimer (k_{eff}) in RTILs, which have been estimated taking into consideration the weightages of both the forms (f_1 and f_2 values), are also collected in Table 5.3.

Table 5.3. *Rate constants associated with excimer formation and deactivation of py(3)py in RTILs*

Solvent	k_1 ($10^6 s^{-1}$)	k_2 ($10^6 s^{-1}$)	k_D ($10^6 s^{-1}$)	f_1 %	f_2 %	k_{eff} ($10^6 s^{-1}$)
[BMIM][PF_6]	66.4	8.5	7.1	23	77	21.8
[BMIM][BF_4]	109.3	9.5	7.6	17	83	26.5
[EMIM][BF_4]	130.9	18.6	9.1	39	61	62.4
[IM][$(CF_3SO_2)_2N$]	115.4	10.4	7.8	16	84	27.2

As can be seen, the k_{eff} values of py(3)py in RTILs are lower than those in less viscous conventional solvents by a factor of 2 – 5.[4] Interestingly, we find that the deactivation rate of the excimer in RTILs is slightly faster by a factor of ~ 1.5 compared to that in less viscous conventional solvents.[4] Therefore, a slower rate of formation of the excimer as well as its slightly faster rate of deactivation is responsible for a low I_D/I_M value in RTILs. However, of the two factors, the former influences the I_D/I_M value more than the latter.

We take note of the fact that with the exception of [EMIM][BF_4], the k_{eff} values of py(3)py in RTILs vary within a narrow range (between 21.8 – 27.2 x 10^6 s^{-1}). Since all the RTILs used here are highly viscous compared to the conventional liquids, this near constancy of the k_{eff} value or lack of variation of the k_{eff} value with the viscosity of the RTILs is not unexpected. We have also noticed that the effective rate of formation of the excimer (k_{eff}) is surprisingly higher in [EMIM][BF_4] compared to that in a less viscous medium, [BMIM][Tf_2N]. Even though this behavior is consistent with a higher steady state (I_D/I_M) value in the former, we do not understand why this data is not consistent with the viscosity data of the RTILs.

5.3. Conclusion

Steady state and time-resolved fluorescence behavior of 1,3-bis(1-pyrenyl)propane has been investigated in four different room temperature ionic liquids. It is found that the excimer to monomer fluorescence intensity ratio of the system in the room temperature ionic liquids is significantly lower than that observed in conventional solvents. A detailed analysis of the fluorescence decay

profiles of the monomer and excimer reveals that even though the mechanism of intramolecular excimer formation in room temperature ionic liquids is similar to that in conventional solvents, the kinetics of the formation of the excimer is considerably slower in the former media whereas the deactivation of the excimer is slightly faster than that in conventional solvents. This slow formation kinetics is attributed to high viscous nature of the ionic liquids at room temperature. Among the various possible mechanisms of the formation and deactivation of the intramolecular excimer, our kinetic data can be explained considering the presence of two kinetically different monomers in the ground state, which on excitation produce a common excimer with different rate constants. The back dissociation process of the excimer is found to be unimportant in these viscous liquids.

5.4. References

(1) Kalyanasundaram, K. *Photochemistry in Microheterogeneous Systems*; Academic Press: New York, 1987.

(2) Kalyanasundaram, K.; Thomas, J. K. *J. Am. Chem. Soc.* **1977**, *99*, 2039.

(3) Birks, J. B. In *"Photophysics of Aromatic Molecules"*; Wiley: New York, 1970.

(4) Zachariasse, K. A.; Duveneck, G.; Busse, R. *J. Am. Chem. Soc.* **1984**, *106*, 1045.

(5) Avnir, D.; Busse, R.; Ottolenghi, M.; Wellner, E.; Zachariasse, K. A. *J. Phys. Chem.* **1985**, *89*, 3521.

(6) Zachariasse, K. A.; Striker, G. *Chem. Phys. Lett.* **1988**, *145*, 251.

(7) Zachariasse, K. A. *Chem. Phys. Lett.* **1978**, *57*, 429.

(8) Zachariasse, K. A.; Duveneck, G.; Kuhnle, W. *Chem. Phys. Lett.* **1985**, *113*, 337.

(9) Snare, M. J.; Thistlethwaite, P. J.; Ghiggino, K. P. *J. Am. Chem. Soc.* **1983**, *105*, 3328.

(10) Yang, J. S.; Lin, C. S.; Hwang, C. Y. *Org. Lett.* **2001**, *3*, 889.

(11) Mmereki, B. T.; Donaldson, D. J. *Phys. Chem. Chem. Phys.* **2002**, *4*, 4186.

(12) Matsui, J.; Mitsuishi, M.; Miyashita, T. *J. Phys. Chem. B.* **2002**, *106*, 2468.

(13) Michalec, J. F.; Bejune, S. A.; McMillin, D. R. *Inorg. Chem.* **2000**, *39*, 2708.

(14) Kim, J. S.; Shon, O. J.; Rim, J. A.; Kim, S. K.; Yoon, J. *J. Org. Chem.* **2002**, *67*, 2348.

(15) Maeda, H.; Sugimoto, A.; Mizuno, K. *Org. Lett.* **2000**, *2*, 3305.

(16) Juris, A.; Prodi, L. *New J. Chem.* **2001**, *25*, 1132.

(17) Jones II, G.; Vullev, V. I. *Org. Lett.* **2001**, *3*, 2457.

(18) Imahori, H.; Nishimura, Y.; Norieda, H.; Karita, H.; Yamazaki, I.; Sakata, Y.; Fukuzumi, S. *Chem. Commun.* **2000**, 661.

(19) Gridin, V. G.; Korol, A.; Bulatov, V.; Schechter, I. *Anal. Chem.* **1996**, *68*, 3359.

(20) Fletcher, K. A.; Storey, I. A.; Hendricks, A. E.; Pandey, S.; Pandey, S. *Green. Chem.* **2001**, *3*, 210.

(21) Seddon, K. R.; Stark, A.; Torres, M.-J. *Personal Communication* **2001**.

(22) Bonhote, P.; Dias, A. P.; Papageorgiou, N.; Kalyanasundaram, K.; Gratzel, M. *Inorg. Chem.* **1996**, *35*, 1168.

(23) Birks, J. B. *Rep. Prog. Phys.* **1975**, *38*, 903.

(24) Hirayama, F. *J. Chem. Phys.* **1965**, *42*, 3163.

(25) Hui, M. H.; Ware, W. R. *J. Am. Chem. Soc.* **1976**, *98*, 4718.

(26) Mataga, N.; Migita, M.; Nishimura, T. *J. Mol. Struct.* **1978**, *47*, 199.

(27) Van der Auweraer, M.; Gilbert, A.; De Schryver, F. C. *J. Am. Chem. Soc.* **1980**, *102*, 4008.

(28) Van der Auweraer, M.; Gilbert, A.; De Schryver, F. C. *J. Phys. Chem.* **1981**, *85*, 3198.

(29) Todesco, R.; Gelan, J.; Martens, H.; Put, J.; De Schryver, F. C. *J. Am. Chem. Soc.* **1981**, *103*, 7304.

Concluding remarks

A summary of the results obtained in the thesis and the conclusions drawn from the current investigation are presented in this chapter. The scope of further work that can be carried out based on the present observation is also outlined at the end of this chapter.

6.1. Summary of the results and conclusion

The work embodied in this thesis describes the steady state and time-resolved fluorescence behavior of several molecules in media containing the phase transfer catalysts (PTCs) and in room temperature ionic liquids (RTILs). The present investigation has been undertaken with a view to obtaining a better understanding of the mechanism of *phase transfer catalysis*, a phenomenon extensively used in various synthetic applications, and to examine the fluorescence response of various systems in *room temperature ionic liquids*, currently being considered as 'green' substitute of the conventional solvents. Synthesis and purification of the ionic liquids comprise a necessary and integral part of the thesis work. Conversion of the fluorescence decay profiles, recorded across the whole range of the steady state emission spectra, to appropriately normalized time-resolved emission spectra (TRES) and extracting the correlation function, C(t) using the peak frequency of each TRES to quantitatively estimate

the solvation dynamics in room temperature ionic liquids form another major part of this thesis.

Quaternary ammonium salts with four identical alkyl chains are known to be the most commonly used PTCs. In order to understand how the PTCs interact with the dipolar systems in nonpolar media, we have used several quaternary ammonium salts and a series of EDA molecules and examined the UV-visible absorption and fluorescence behavior of the latter in the presence of the former. The results show that the PTCs interact with the EDA molecules and in the process modify both the absorption and fluorescence properties of these systems. A gradual red shift of the absorption maximum with the formation of isosbestic point is observed in the presence of quaternary salts in nonpolar solvents. The effect is much more prominent in emission studies. For AP and ANP, the original fluorescence gets quenched and a new low intense band is formed on the longer wavelength region on addition of PTC. For multi-component systems, the intensity of the largely Stokes-shifted new band is considerably higher. A clear isosbestic point is observed in all cases. The spectral changes of the EDA molecules induced by the tetraalkylammonium salts suggest the formation of a 1:1 complex between the two in nonpolar media. The complex formation process is found to be rather weak when the polarities of the solvents are gradually increased and it is completely absent in highly polar solvents like acetonitrile or alcohols.

An electrostatic interaction between the phase transfer catalysts and the dipolar molecules is shown to be the driving force for the formation of the complex. The dependence of the formation constant of the complex on the

polarity of the media suggests a charge transfer nature of the complex. It has been shown that the anionic component of the salts serves as a source of electron to the positive end (4-amino group) of the dipolar molecules, while the tetraalkylammonium cation, besides helping solubilization of its anionic counterpart in the nonpolar media, serve neutralizing the negative charge at the acceptor end of the EDA molecules. In effect, a cooperative influence of the cationic and anionic components of the PTC enhances the charge separation within the dipolar fluorophore. Among the various salts employed in the study we noticed that PTCs containing the chloride ion as the anionic counterpart are the most effective in inducing the spectral changes. This can be understood in terms of a higher charge to volume ratio of this ion compared to others. Both steady state and time-resolved data indicate that the interaction is a ground state phenomenon rather that an excited state one. Based on the PTC induced changes in the photophysical behavior of the EDA molecules we have proposed a possible structure for the 1:1 complex in ground state. It has been concluded that a phase transfer catalyst should not be treated as an innocuous substance that merely helps transfer of a polar substance from a polar to a nonpolar environment. Instead, we have demonstrated that the association of a PTC with a dipolar species can significantly change various properties of the latter.

In the second part of the thesis, we have studied solvation dynamics in different room temperature ionic liquids using some commonly used fluorescence probe molecules, C153, PRODAN and AP. We have synthesized seven RTILs comprising 1-ethyl-3-methylimidazolium [EMIM], and 1-butyl-3-

methylimidazolium [BMIM], cations with a combination of different fluorinated anions that show a range of viscosities. Before undertaking time-resolved measurements on these air and water stable liquids, we have estimated the polarity of these 'green' liquids in terms of the microscopic solvent polarity parameters, $E_T(30)$ and E_T^N from the steady state emission spectra. These results suggest that the present ionic liquids are more polar than acetonitrile but less polar than methanol. The polarity of the [EMIM] salts has been found to be slightly higher than that of the [BMIM] salts. A higher polarity for the $[CF_3COO]$ salt compared to the $[PF_6]$ or $[(CF_3SO_2)_2N]$ salt has been observed, while for the $[BF_4]$ salt the polarity is in between.

We have studied the fluorescence decay behavior of the probe molecules using picosecond time-correlated single photon (TCSPC) counting technique. While the time-dependence of fluorescence in the blue region of the spectrum is represented by a multi-component decay, that in the red region of the spectrum consists of a clear growth followed by normal decay for all the probe molecules. This wavelength dependent decay behavior of the EDA molecules is shown to be a reflection of slow solvation of the fluorescent state of the molecules. The time constant for the solvation process has been estimated from the time-dependence of the Stokes shift correlation function, C(t). Time-dependence of C(t) has been found to be biexponential in all cases suggesting that the solvation process in RTILs occur in two different time scales. The average solvation time has been found to lie between hundreds of picosecond to thousands of picosecond. This implies that the process of solvation is rather slow in these high viscous media when compared with that in conventional low viscous solvents. Taking into

consideration the amplitudes of the slow and fast components we have attributed the fast component to the initial response of the anion to the newly created charge separation and the long component to the collective motion of the cation and anion. We have also observed that the solvation dynamics in RTILs depends on the probe molecule used but no clear trend can be identified.

Lastly, we have investigated the intramolecular excimer formation process in 1,3-bis(1-pyrenyl)propane (py(3)py) by steady state and time-resolved fluorescence techniques in four different room temperature ionic liquids. In conventional solvents, the mechanism of intramolecular excimer formation of this molecule has been well studied. The results show that the excimer formation is controlled by the viscosity of the medium. Although the absorption behavior of this molecule in the present RTILs is not very different from that in conventional polar solvent like acetonitrile, the excimer to monomer fluorescence intensity ratio of the system in these liquid salts is found to be significantly lower than that in acetonitrile at room temperature. In order to find out in what respect the excimer formation and dissociation kinetics in RTILs differ from that in less viscous media we have studied the time-resolved behavior of the system monitoring the monomer and excimer fluorescence. In all the ionic liquids, the monomer emission can be fitted to a biexponential decay function whereas a triexponential decay function is necessary for the excimer fluorescence. The excimer emission kinetics reveals two growth components and a single decay. The results have been analyzed in terms of various kinetic models proposed by previous researchers for the interpretation of the kinetic data of excimer/exciplex formation in conventional solvents. It is shown that the kinetic data of py(3)py in

RTILs can be interpreted considering the presence of two dominant conformers of the molecule (in the ground state), which on electronic excitation give rise to the formation of a common excimer at two different rates. A comparatively lower formation rate constant of the excimer and slightly faster rate of its deactivation compared to those observed in conventional solvents have been attributed to relatively low steady state concentration of the excimer in room temperature ionic liquids.

6.2. Scope of further work

With the help of the spectroscopic data we have shown that the phase transfer catalysts and EDA molecules form 1:1 complex in nonpolar solvents. However, we could not succeed in obtaining single crystals of the charge transfer complex and in determining the structural details of the complex by single crystal X-ray diffraction studies. It would be worthwhile to make further attempts to achieve this objective. We have synthesized RTILs based on imidazolium cation, which are optically transparent above ~300 nm. Because of the absorption due to the imidazole moiety, these liquids have a strong absorption maximum at ~275 nm and the tail extend upto 300 nm and sometimes little beyond this wavelength. It is indeed a problem for using these RTILs as a solvent in spectroscopic studies on molecules that absorb in the wavelength region below 300 nm. If one can replace the imidazolium cation by some other cation such as quaternary ammonium cation, then one can enhance the wavelength range for the optical studies. The problem however is the fact that the currently available quaternary

ammonium salts have comparatively higher melting point. Therefore, one should look for newer RTILs that can offer transparency below 300 nm.

We have studied only a couple of photophysical processes in RTILs. There are a variety of other photophysical processes that can be examined in these media. As the RTILs are highly polar and moderate to highly viscous liquids at ambient temperature it will be quite interesting to find out how photophysical processes such as twisted intramolecular charge transfer (TICT) process in 4-N,N-dimethylaminobenzonitrile (DMABN) or 4-(1H-pyrrol-1-yl)ethyl benzoate in these media are affected. We have already noted that some systems show red edge excitation shift (REES) in RTILs. A systematic investigation of this phenomenon with this probe as well as few other molecules could be attempted as a future work. Intramolecular proton transfer process and photoinduced conformation change of molecules can also be studied in this new generation liquids.

Appendix 1

A1. Estimation of binding constant from the absorption spectra

When a fluorophore (represented as A) and phase transfer catalyst (represented as B) interact to form a complex (denoted as C), the complexation process can be written as

$$A + B <=> C \quad (1)$$

The equilibrium concentration (indicated by the subscript, e) and the total concentration (indicated by the subscript, t) of a species are related as

$[A]_e = [A]_t - [C]_e$ and $[B]_e = [B]_t - [C]_e$

In the experimental condition, when $[B]_t >> [A]_t$; $[B]_e$ can be equated to $[B]_t$.

The formation constant (K) of the complex, $K = \dfrac{[C]_e}{[A]_e[B]_e}$ (2)

Replacing $[B]_e$ by $[B]_t$ and $[A]_e$ as $[A]_t - [C]_e$

We can write $\dfrac{[A]_t[B]_t}{[C]_e} = \dfrac{1}{K} + [B]_t$ (3)

Taking into consideration the fact that the phase transfer catalyst, B does not contribute to the absorption in the spectral range studied, the total absorbance (OD_t) at any given wavelength is the sum of that due to the complex and the probe. The total OD at any specific wavelength (OD_t) can be expressed as, $OD_t = \varepsilon_A[A]_e + \varepsilon_C[C]_e$, where ε is the molar extinction coefficient.

This can be transformed as, $OD_t = \varepsilon_A[A]_t + (\varepsilon_C - \varepsilon_A)[C]_e = OD_A + OD_C$

Where, OD_A stands for the initial OD due to A at any given wavelength (= $\varepsilon_A[A]_t$) and OD_C represents the OD at the same wavelength (at equilibrium) due to the complex (= $\varepsilon_C[C]_e$).

We can write, $[C]_e = \frac{\varepsilon_A OD_C [A]_t}{\varepsilon_k OD_A}$ (4)

Where, ε_k stands for (ε_C - ε_A)

Substituting the expression for $[C]_e$ from equation (4) into equation (3), we obtain

$$\frac{OD_A}{OD_t - OD_A} = \frac{1}{[B]_t}\left(\frac{1}{K}\frac{\varepsilon_A}{\varepsilon_k}\right) + \frac{\varepsilon_A}{\varepsilon_k} \quad (5)$$

A2. Estimation of binding constant from the emission spectra

Assuming a similar equilibrium between A and B (equation 1), we can rewrite the expression of the formation constant (K) as obtained in equation (2)

$$K = \frac{[C]_e}{[A]_e[B]_e}$$

replacing $[B]_e$ by $[B]_t$;

$$K = \frac{[C]_e}{[A]_e[B]_t}$$

If I_A and I_C represent the intensity of the light absorbed by fluorophore, A and complex, C respectively, then we can write

$$\frac{I_C}{I_A} = \frac{\varepsilon_C[C]_e}{\varepsilon_A[A]_e} = \frac{K\,\varepsilon_C[B]_t}{\varepsilon_A}$$

Assuming an identical molar extinction coeffecient of the fluorophore (ε_A) and complex (ε_C), we can write

$$\frac{I_C}{I_A} = K[B]_t \qquad (6)$$

We can express the overall fluorescence intensity (or quantum yield), ϕ of the system (where both the fluorophore and the complex are emitting species) as,

$$\phi = \frac{\phi_A I_A + \phi_C I_C}{I_A + I_C} \qquad (7)$$

where, ϕ_A and ϕ_C correspond to the individual emission intensity at a particular wavelength due to uncomplexed fluorophore and the complex, respectively.

Substituting the expression for $\frac{I_C}{I_A}$ (from equation 6) in equation (7),

we obtain,

$$\phi = \frac{\phi_A + \phi_C\ k[B]_t}{1 + k[B]_t}$$

Subtracting ϕ_A from both sides we obtain

$$\phi - \phi_A = \frac{k[B]_t(\phi_C - \phi_A)}{1 + k[B]_t} \qquad (8)$$

Dividing equation (8) by ϕ_A and then rearranging the same we get

$$\frac{\phi_A}{\phi - \phi_A} = \left[\left(\frac{\phi_A}{\phi_C - \phi_A}\right)\frac{1}{K}\right]\frac{1}{[B]_t} + \frac{\phi_A}{\phi_C - \phi_A} \qquad (9)$$

Appendix 2

A1. Derivation of fluorescence response function of monomer and excimer

According to scheme 3, the time-dependence of $M(1)*$ can be written as,

$$\frac{d}{dt}[M(1)^*] = -(k_1 + k_M)t$$

On integration we get,

$$\frac{[M(1)^*]}{[M^*]_0} = f_1 \exp-(k_1 + k_M)t \qquad (1)$$

where, f_1 is the fraction of molecule originally present in $M(1)$ form and $[M^*]_0$ is the initial concentration of $[M(1)^*]$ at time, t = 0 after excitation with a δ-function light flash.

Similarly, for the other species $M(2)*$ we can write,

$$\frac{[M(2)^*]}{[M^*]_0} = f_2 \exp-(k_2 + k_M)t \qquad (2)$$

The overall monomer response function, $I_M(t)$ will be the sum of the contributions from $M(1)*$ and $M(2)*$.

$$I_M(t) = k_{FM} \frac{[M(1)^*] + [M(2)^*]}{[M^*]_0}$$

$$= k_{FM}\left[f_1 \exp-(k_1 + k_M)t + f_2 \exp-(k_2 + k_M)t\right] \qquad (3)$$

For the excimer (D^*), the rate equation takes the form,

$$\frac{d[D^*]}{dt} = k_1[M(1)^*] + k_2[M(2)^*] - k_D[D^*] \qquad (4)$$

Substituting the value of $[M(1)^*]$ and $[M(2)^*]$ in equation (4)

$$\frac{d[D^*]}{dt} + k_D[D^*] = [M^*]_0\left[k_1 f_1 \exp-(k_1 + k_M)t + k_2 f_2 \exp-(k_2 + k_M)\right]$$

Multiplying both sides by $\exp(k_D t)$ and on integration we get

$$\begin{aligned}\frac{[D^*]}{[M^*]_0} &= \frac{k_1 f_1}{(k_D - k_1 - k_M)} \exp-(k_1 + k_M)t + \frac{k_2 f_2}{(k_D - k_2 - k_M)} \exp-(k_2 + k_M)t \\ &\quad - \left[\frac{k_1 f_1}{(k_D - k_1 - k_M)} + \frac{k_2 f_2}{(k_D - k_2 - k_M)}\right] \exp-(k_D t)\end{aligned} \tag{5}$$

Using equation (5), we obtain the following time-dependent response function of the excimer,

$$\begin{aligned}I_D(t) &= k_{FD} \frac{[D^*]}{[M^*]_0} \\ &= \frac{k_{FD}\, k_1 f_1}{(k_D - k_1 - k_M)} \exp-(k_1 + k_M)t + \frac{k_{FD}\, k_2 f_2}{(k_D - k_2 - k_M)} \exp-(k_2 + k_M)t \\ &\quad - \left[\frac{k_{FD}\, k_1 f_1}{(k_D - k_1 - k_M)} + \frac{k_{FD}\, k_2 f_2}{(k_D - k_2 - k_M)}\right] \exp-(k_D t)\end{aligned} \tag{6}$$